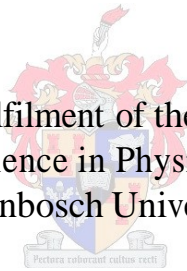


The effect of MKP-1 inhibition on the cytotoxicity of chemotherapeutic drugs in breast cancer

By Heloïse Le Roux

Thesis presented in fulfilment of the requirements for the degree Master of Science in Physiological Sciences at Stellenbosch University



Promoter: Dr AM Engelbrecht
Faculty of Science
Department of Physiological Sciences

December 2012

Declaration

By submitting this thesis, I declare that the entirety of the work contained therein is my own, original work, that I am the owner of the copyright thereof (unless to the extent explicitly otherwise stated) and that I have not previously in its entirety or in part submitted it for obtaining any qualification.

Signature _____

Date _____

Abstract

Introduction: Cancer is an emerging health problem in South Africa, with breast cancer being one of the leading cancers affecting women globally. Therefore, there is a need to find novel targets to improve the therapeutic options for these patients. A recently proposed target is the mitogen-activated protein kinase phosphatase-1 (MKP-1). Studies have suggested that mitogen-activated protein kinase phosphatases are involved in the development of cancer and play an important role in the response of cancer cells to chemotherapy. Additionally, numerous studies have indicated that there is increased expression of MKP-1 in breast cancers where its over-expression is proposed to be a significant mediator in chemo-resistance. We propose that inhibition of MKP-1 will increase the cytotoxic effect of doxorubicin in breast cancer cells, thus making the cells more responsive to treatment leading to increased cell death through autophagy and apoptosis.

Methods: In MDA-MB231 cells, MKP-1 was inhibited using sanguinarine or MKP-1 siRNA and this was compared to a known inducer of MKP-1, dexamethasone. MDA-MB231 cells were treated with doxorubicin alone or in combination with MKP-1 inhibitors or an inducer. Following treatment, cell death was determined by trypan blue and a caspase glo assay as well as with western blotting. Autophagy was determined by western blotting and flow cytometry. LC3 and p62 were used as markers of autophagy and caspase 3 and PARP as apoptosis markers. Likewise, the level of MKP-1 expression under conditions of MKP-1 induction, inhibition or silencing was evaluated by means of western blotting. C57BL6 tumour bearing mice was used to analyse apoptosis and autophagy *in vivo* under conditions of MKP-1 inhibition, using sanguinarine, together with doxorubicin treatment. Western blotting was used to determine levels of caspase 3, LC3, p62 and MKP-1 expression.

Results and discussion: A concentration and time curve indicated that 5 μ M doxorubicin reduced cell viability in the MDA-MB231 cells significantly after 24 hours of treatment. MKP-1 expression was significantly reduced with sanguinarine and MKP-1 siRNA. Furthermore, our results indicate a significant increase in apoptosis in MDA-MB231 cells when treated with doxorubicin, under conditions of MKP-1 inhibition or MKP-1 silencing. Also, an increase in autophagic activity was observed following treatment with doxorubicin in combination with sanguinarine. Whole excised tumours of C57BL6 mice also showed an increase in apoptosis and autophagy following treatment with sanguinarine in combination with doxorubicin. This indicates that the inhibition of MKP-1 with sanguinarine sensitized the MDA-MB231 cells and E0771 cell tumours to doxorubicin-induced-apoptosis through a mechanism involving autophagy.

Conclusion: This is an encouraging finding that could hopefully be used in future studies to overcome doxorubicin-resistance in breast cancer cells overexpressing MKP-1. Targeting MKP-1 can have potential therapeutic benefits for breast cancer patients by making chemotherapy more effective. Sanguinarine thus has potential to be developed as a clinically relevant inhibitor of MKP-1 which could provide a novel avenue for therapeutic intervention in combination with chemotherapy in breast cancer patients.

Opsomming

Inleiding: Kanker is 'n vinnig groeiende gesondheidsprobleem in Suid-Afrika, met borskanker as een van die vernaamste kankers wat vroue wêreldwyd raak. Daar is dus 'n behoefte aan nuwe terapeutiese opsies vir hierdie pasiënte en mitogeen-geaktiveerde proteïenkinase fosfatase-1 (MKP-1) is onlangs voorgestel as 'n moontlike teiken. Verskeie studies toon dat mitogeen-geaktiveerde proteïenkinase fosfatasas betrokke is by die ontwikkeling van kanker en ook belangrike rolspelers is in die reaksie van kanker op chemoterapie. Daarbenewens toon talle studies dat daar verhoogde MKP-1 uitdrukking in borskanker is, asook dat dit 'n belangrike bemiddelaar is vir die weerstand wat borskanker teen chemoterapie bied. Ons het dus voorgestel dat die inhibisie van MKP-1 die sitotoksiese effek van doxorubicin op borskanker selle sal verhoog; sodoende sal die kanker selle beter reageer op behandeling en dit sal dus lei tot verhoogde seldood deur autofagie en apoptose.

Metodes: MKP-1 is geïnhibeer met behulp van sanguinarine of MKP-1 siRNA in MDA-MB231 selle en dit is vergelyk met 'n bekende MKP-1 induseerder, dexamethasone. MDA-MB231 selle is met doxorubicin alleen behandel of in kombinasie met MKP-1 inhibeerders of 'n induseerder. Seldood is bepaal deur middel van 'n trypan blou en kaspase toetsingsmetode, asook met die westelike kladtegniek. Autofagie is bepaal deur westelike kladtegniek en vloeisitometrie. LC3 en p62 is gebruik as merkers van autofagie en kaspase 3 en PARP is as apoptose merkers gebruik. MKP-1 uitdrukking is geëvalueer deur middel van westelike kladtegniek. C57BL6 muise met kankeragtige gewasse is gebruik om apoptose en autofagie *in vivo* te ondersoek. MKP-1 is geïnhibeer met sanguinarine en die muise is behandel met 'n kombinasie van sanguinarine en doxorubicin. Kaspase 3, LC3, p62 en MKP-1 uitdrukking is bepaal deur middel van die westelike kladtegniek.

Resultate en bespreking: 'n Konsentrasie en tyd kurwe het aangedui dat 5 μ M doxorubicin die MDA-MB231 selle se lewensvatbaarheid aansienlik verminder het na 24 uur. MKP-1 uitdrukking is ook aansienlik verminder met sanguinarine en MKP-1 siRNA. Verder dui die resultate op 'n beduidende toename in apoptose in MDA-MB231 selle na behandeling met doxorubicin onder toestande van MKP-1 inhibisie. 'n Toename in autofagiese aktiwiteit is waargeneem na behandeling met doxorubicin en sanguinarine. Die kankeragtige gewasse van die C57BL6 muis toon ook 'n toename in apoptose en autofagie na behandeling met sanguinarine en doxorubicin. Hierdie resultate dui daarop dat die inhibisie van MKP-1 met sanguinarine die MDA-MB231 selle en E0771 sel gewasse gesensitiseer het tot doxorubicin-geïnduseerde apoptose deur middel van 'n meganisme wat autofagie insluit.

Gevolgtrekking: Hierdie bevinding kan hopelik in toekomstige studies gebruik word om doxorubicin weerstand te voorkom in borskanker selle waar MKP-1 verhoog is. Deur MKP-1 te teiken, kan dit lei tot potensiële terapeutiese voordele vir borskanker pasiënte en sodoende kan dit chemoterapie meer effektief maak. Sanguinarine het dus die potensiaal om ontwikkel te word as 'n klinies relevante inhibeerder van MKP-1 wat sodoende kan dien as terapeutiese intervensie in kombinasie met chemoterapie vir borskanker pasiënte.

Hiermee erken ek met dank die finansiële hulp (beurs) wat ek van die Struwig-Germeshuysen Kankernavorsingstrust ontvang het, vir die voltooiing van my studies. Menings wat in die publikasie uitgespreek word of gevolgtrekkings waartoe geraak is, is dié van die navorser alleen en strook nie noodwendig met dié van die SGKN-Trust nie.

Acknowledgements

I would like to thank the following people:

Firstly, Johan, for your love and the fact that you listened to my explanations of what I did in the lab every single day even though you had no idea what was going on.

My supervisor, Prof Engelbrecht, thank you for giving me the opportunity to do this study and for all your help through the years.

My sister, also for listening and for understanding me and keeping up with my emotions during the year.

Mark Thomas, for teaching me animal handling techniques.

My family at home thanks for your support and understanding.

My friends, Anna, Clare and Justin thank you for your wonderful friendship in and out of the lab.

DSG for all the interesting talks we had and especially the Hons students of 2012.

Theo Nell for editing my thesis.

Finally, CANSA, NRF, Struwig-Germeshuysen Kankernavorsingstrust and the Ethel and Ericksen Trust for providing funds.

Table of contents

| | |
|--|------|
| List of Figures | v |
| List of abbreviations | viii |
| Chapter 1: | 1 |
| Introduction | 1 |
| 1.1 Motivation for study..... | 1 |
| 1.2 Problem statement..... | 2 |
| 1.3 Hypothesis | 2 |
| 1.4 General aims..... | 3 |
| 1.5 Specific aims | 3 |
| 1.6 Structure of the thesis | 4 |
| Chapter 2: | 5 |
| Literature review | 5 |
| 2.1 Introduction..... | 5 |
| 2.2 Mitogen-activated protein kinase signalling | 7 |
| 2.2.1 MKP-1 inhibition..... | 10 |
| 2.2.2 MKP-1 induction..... | 12 |
| 2.3 Apoptosis..... | 13 |
| 2.3.1 The role of MKP-1 signalling in apoptosis | 19 |
| 2.4 Autophagy | 21 |
| 2.4.1 Autophagy and MKP-1..... | 25 |
| 2.5 Crosstalk between autophagy and apoptosis | 25 |
| 2.6 Treatment options for breast cancer | 27 |
| 2.7 Sensitizing breast cancer cells to cell death..... | 27 |
| 2.8 Hypothesis..... | 28 |
| 2.9 Aims..... | 29 |
| Chapter 3: | 30 |
| Materials and Methods | 30 |
| 3.1 Study design | 30 |
| 3.2 Cell culture..... | 31 |
| 3.3 Experimental protocol..... | 31 |
| 3.3.1 Treatment preparations | 32 |
| 3.3.2 MKP-1 siRNA Transfection..... | 33 |
| 3.4 Determination of cell death | 35 |

| | | |
|---------|--|----|
| 3.4.1 | Morphological analysis..... | 35 |
| 3.4.2 | Trypan blue assay | 36 |
| 3.4.3 | Caspase 3/7 activity assay | 37 |
| 3.4.4 | Western blot analysis of Caspase 3 and Cleaved PARP | 37 |
| 3.4.4.1 | Protein extraction and quantification | 38 |
| 3.4.4.2 | Sample preparation..... | 38 |
| 3.4.4.3 | SDS-PAGE and Western blot analysis | 39 |
| 3.5 | Determination of MKP-1 expression | 40 |
| 3.6 | Determination of autophagic induction..... | 42 |
| 3.6.1 | Flow cytometry..... | 42 |
| 3.6.2 | LysoTracker™ Stain..... | 43 |
| 3.6.3 | Western blot analysis of LC3 and p62 | 44 |
| 3.7 | In-vivo mouse model | 45 |
| 3.7.1 | Study design | 45 |
| 3.7.2 | Experimental protocol..... | 46 |
| 3.7.3 | Treatment..... | 47 |
| 3.7.4 | Western blot analyses of autophagy, apoptosis and MKP-1 | 48 |
| 3.7.4.1 | Protein extraction and quantification | 48 |
| 3.7.4.2 | Sample preparation..... | 48 |
| 3.7.4.3 | SDS-PAGE and Western blot analysis | 48 |
| 3.8 | Statistical analysis..... | 49 |
| | Chapter 4: | 50 |
| | Results | 50 |
| 4.1 | Determination of cell death | 50 |
| 4.1.1 | Trypan blue assay | 50 |
| 4.1.2 | Caspase 3/7 activity assay | 54 |
| 4.1.3 | Western blot analysis | 57 |
| 4.1.3.1 | Total caspase 3 | 57 |
| 4.1.3.2 | Cleaved PARP..... | 59 |
| 4.2 | LysoTracker™ and Hoechst 33342 stain | 61 |
| 4.3 | MKP-1 expression in MDA-MB231 cells | 63 |
| 4.4 | Determination of autophagic induction in MDA-MB231 cells | 64 |
| 4.4.1 | Flow cytometry..... | 64 |
| 4.4.2 | Western blot analysis | 67 |
| 4.4.2.1 | LC3 | 67 |

| | | |
|---------------------|---|-----------|
| 4.4.2.2 | p62..... | 68 |
| 4.5 | <i>In-vivo</i> Study | 70 |
| 4.5.1 | Tumour growth..... | 70 |
| 4.5.2 | Western blot analysis | 71 |
| 4.5.2.1 | Total Caspase 3..... | 71 |
| 4.5.2.2 | MKP-1 | 72 |
| 4.5.2.3 | LC3 II | 73 |
| 4.5.2.4 | p62..... | 74 |
| Chapter 5: | | 75 |
| Discussion | | 75 |
| 5.1 | <i>In vitro</i> study..... | 75 |
| 5.1.1 | Role of MKP-1 inhibition on cell viability | 75 |
| 5.1.2 | The role of MKP-1 on apoptosis in MDA-MB231 cells | 76 |
| 5.1.3 | MKP-1 expression in MDA-MB231 cells..... | 79 |
| 5.1.4 | The relation of MKP-1 with autophagy in MDA-MB231 cells | 80 |
| 5.2 | <i>In vivo</i> study..... | 82 |
| 5.2.1 | The effect of MKP-1 inhibition on autophagy and apoptosis in tumour bearing mice..... | 82 |
| 5.3 | Conclusions..... | 83 |
| 5.4 | Limitations and future studies | 85 |
| Bibliography | | 86 |
| Appendix A | | 102 |

List of Figures

| | |
|--|---------|
| Figure 2.1: Incidence of Breast cancer compared to other cancers in women of all ages in South Africa..... | page 5 |
| Figure 2.2: The molecular structure of sanguinarine..... | page 11 |
| Figure 2.3: Apoptosis signalling pathway..... | page 17 |
| Figure 2.4: Autophagy..... | page 23 |
| Figure 3.1: Study design..... | page 30 |
| Figure 3.2: The human metastatic mammary carcinoma cell line, MDA-MB231, was obtained from a patient in 1973 at M.D Anderson Cancer Center..... | page 31 |
| Figure 3.3: Experimental plan for treatment of MDA-MB231 breast cancer cells.... | page 34 |
| Figure 3.4: Study design..... | page 45 |
| Figure 3.5: Experimental plan for <i>In-vivo</i> study..... | page 46 |
| Figure 3.6: The injection of a cell suspension into a mammary pad..... | page 47 |
| Figure 4.1: The effect of treatment with doxorubicin on cell death induction in MDA-MB231 cells..... | page 50 |
| Figure 4.2: The effect of treatment with dexamethasone in conjunction with doxorubicin on cell death induction in MDA-MB231 cells..... | page 51 |
| Figure 4.3: The effect of treatment with sanguinarine in conjunction with doxorubicin on cell death induction in MDA-MB231 cells..... | page 52 |
| Figure 4.4: The effect of MKP-1 siRNA in conjunction with doxorubicin on cell death induction in MDA-MB231 cells..... | page 53 |
| Figure 4.5: The effect of treatment with dexamethasone in conjunction with doxorubicin on caspase 3/7 activity in MDA-MB231 cells..... | page 54 |
| Figure 4.6: The effect of sanguinarine in conjunction with doxorubicin on caspase 3/7 activity in MDA-MB231 cells..... | page 55 |

| | |
|--|---------|
| Figure 4.7: The effect of MKP-1 siRNA in conjunction with doxorubicin on the caspase 3/7 activity in MDA-MB231 cells..... | page 56 |
| Figure 4.8: The effect of 24 hour doxorubicin treatment together with MKP-1 inhibitors and inducers on caspase 3 expression in MDA-MB231 cells..... | page 58 |
| Figure 4.9: The effect of 24 hour doxorubicin treatment together with MKP-1 inhibitors and inducers on cleaved PARP expression in MDA-MB231 cells..... | page 60 |
| Figure 4.10: The effect of 24 hour doxorubicin treatment together with MKP-1 inhibitors and inducers on autophagy and apoptosis in MDA-MB231 cells..... | page 62 |
| Figure 4.11: The effect of 24 hour doxorubicin treatment together with MKP-1 inhibitors and inducers on MKP-1 expression in MDA-MB231 cells..... | page 63 |
| Figure 4.12: The effect of treatment with dexamethasone in conjunction with doxorubicin on the degree of autophagic induction in MDA-MB231 cells..... | page 64 |
| Figure 4.13: The effect of sanguinarine in conjunction with doxorubicin on the degree of autophagic induction in MDA-MB231 cells..... | page 65 |
| Figure 4.14: The effect MKP-1 siRNA in conjunction with doxorubicin on the degree of autophagic induction in MDA-MB231 cells..... | page 66 |
| Figure 4.15: The effect of 24 hour doxorubicin treatment together with MKP-1 inhibitors and inducers on LC3 II expression in MDA-MB231 cells..... | page 67 |
| Figure 4.16: The effect of 24 hour doxorubicin treatment together with MKP-1 inhibitors and inducers on p62 expression in MDA-MB231 cells..... | page 69 |
| Figure 4.17: Change in tumour volume of C57BL6 mice injected with E0771 murine mammary cancer cells..... | page 70 |
| Figure 4.18: The effect of doxorubicin treatment together with a MKP-1 inhibitor, sanguinarine, on caspase 3 expression in tumour bearing mice..... | page 71 |
| Figure 4.19: The effect of doxorubicin treatment together with a MKP-1 inhibitor, sanguinarine, on MKP-1 expression in tumour bearing mice..... | page 72 |

Figure 4.20: The effect of doxorubicin treatment together with a MKP-1 inhibitor, sanguinarine, on LC3 II expression in tumour bearing mice.....page 73

Figure 4.21: The effect of doxorubicin treatment together with a MKP-1 inhibitor, sanguinarine, on p62 expression in tumour bearing mice..... page 74

List of abbreviations

Units of measurement

| | |
|-----------------|--------------------------|
| °C | degrees Celcius |
| µg | microgram |
| µg/ml | microgram per milliliter |
| µl | microliter |
| µM | micromolar |
| µm | micrometer |
| cm ² | centimeter square |
| kD | kilo Dalton |
| M | molar |
| mg/kg | milligram per kilogram |
| mg/ml | milligram per milliliter |
| min | minute |
| ml | milliliter |
| mM | millimolar |
| mm | millimeter |
| nM | nanomolar |
| nm | nanometer |
| nmol/L | nanomol per liter |
| pmol | picomol |
| rpm | revolutions per minute |
| w/v | weight per volume |
| V | Volt |
| mA | milli Ampere |

A

| | |
|--------|--|
| ADP | Adenosine diphosphate |
| AIF | Apoptosis inducing factor |
| AMPK | Adenosine monophosphate activated protein kinase |
| ANE | Areca nut extract |
| ANOVA | Analysis of variance |
| Apaf-1 | Apoptotic protease activating factor 1 |
| Atg | Autophagy regulated genes |
| ATP | Adenosine triphosphate |

B

| | |
|--------------------|--------------------------------------|
| Bad | BCL2 antagonist of cell death |
| Bak | BCL2 antagonist killer 1 |
| Bax | BCL2 associated X protein |
| Bcl-2 | B-cell lymphoma protein 2 |
| Bcl-w | BCL2 like 2 protein |
| Bcl-X _L | BCL2 related protein, long isoform |
| Bcl-X _s | BCL2 related protein, short isoform |
| Bid | BH3 interacting domain death agonist |
| Bik | BCL2 interacting killer |
| Bim | BCL2 interacting protein BIM |

C

| | |
|-----------------|---|
| C57BL6 | C57 Black 6 |
| CAD | Caspase-activated DNase |
| CIDE | Cell death-inducing DNA fragmentation factor- α -like effector |
| CO ₂ | Carbon dioxide |

D

| | |
|--------|--|
| Dex | Dexamethasone |
| DIABLO | Direct IAP binding protein with low PI |
| DMEM | Dulbecco's Modified Eagle's medium |

DNA Deoxyribonucleic acid

Dox Doxorubicin

DR Death receptor

E

ECL Enhanced chemiluminescence

EDTA Ethylene diamine tetra-acetic acid

ERK Extracellular signal-regulated kinase

F

FACS Fluorescence Activated Cell Sorting

FADD Fas associated death domain

Fas-L Fas ligand

FBS Fetal bovine serum

G

GR Glucocorticoid receptor

H

HCl Hydrochloric acid

I

IAP Inhibitor of apoptosis

ICAD Inhibitor of caspase activated deoxyribonuclease

J

JNK c-Jun NH₂-terminal protein kinase

L

LC3 Microtubule-associated protein 1 light chain 3

M

MAPK Mitogen activated protein kinase

MAPKKK MAPK kinase kinase

MEF Mouse embryonic fibroblast

MEKKK MAPK kinase kinase

| | |
|-------|--|
| MKK | MAP kinase kinase |
| MKKK | MAPK kinase kinase |
| MKP-1 | Mitogen activated protein kinase phosphatase-1 |
| mRNA | messenger RNA |
| mTOR | Mammalian target of rapamycin |

N

| | |
|-------|-----------------------------------|
| NAD | Nicotinamide adenine dinucleotide |
| NAM | Nitric acid monohydrate |
| NF-κB | Nuclear factor kappa B |

P

| | |
|------|-------------------------------|
| PARP | Poly (ADP-ribose) polymerase |
| PBS | Phosphate buffered saline |
| PI3K | Phosphoinositide 3-kinase |
| PMSF | Phenylmethylsulfonyl fluoride |
| PVDF | Polyvinylidene difluoride |

R

| | |
|------|--------------------------------|
| RIPA | Radioimmunoprecipitation assay |
|------|--------------------------------|

S

| | |
|----------|--|
| Sang | Sanguinarine |
| SDS-PAGE | Sodium Dodecyl Sulphate polyacrylamide gel electrophoresis |
| SEM | Standard error of the mean |
| SiRNA | small interfering Ribonucleic Acid |
| Smac | Second mitochondrial activator of caspase |

T

| | |
|--------|---------------------------------------|
| T75 | 75 cm ² culture flask |
| TBST-T | Tris buffered saline-Tween 20 |
| TNF | Tumour necrosis factor |
| TRAIL | TNF related apoptosis inducing ligand |

Tris 2-Amino-2-(hydroxymethyl)-1,3-propandiol

U

UV Ultra violet

UVC ultra violet light C

Chapter 1: Introduction

1.1 Motivation for study

Cancer is an emerging health problem in South Africa, with breast cancer being one of the leading causes of death in women globally (Vorobiof *et al.* 2001). Although major progress has been made in reducing mortality rates due to increased screening, digital mammography, specialized care and widespread use of therapeutic agents, defining the genetic architecture of breast cancer still remains an important long-term goal for the development of more effective therapeutic strategies and early interventions (Hicks *et al.* 2011).

Furthermore, cancer cells are becoming increasingly more resistant to conventional chemotherapeutic agents; therefore there is a need to find novel targets to improve the therapeutic options for these patients. A recently proposed target is the mitogen-activated protein kinase phosphatase-1 (MKP-1). It was shown in a recent study that MKPs are involved in the development of cancer and play an important role in the response of cancer cells to chemotherapy (Wu. 2007). In human breast cancer, MKP-1 was found to be increased in malignant samples compared to non-malignant samples (Wu. 2007). This might implicate MKP-1 as a critical role player in cancer development and may be a useful marker for predicting the survival of patients with cancer. Additionally, it has been indicated that there is increased expression of MKP-1 in ovarian, breast and prostate cancer (Rojo *et al.* 2009). Here, overexpression of MKP-1 is proposed to be a significant mediator of chemoresistance in these cancers.

It has been shown that MKP-1 inhibits events associated with apoptosis, including the activation of caspase-3 and proteolytic cleavage of the caspase-3 substrate, poly (ADP ribose) polymerase (PARP) (Franklin *et al.* 1998). These findings indicate the MKP-1 acts through upstream caspase activation within the apoptotic program (Franklin *et al.* 1998).

Another mechanism which is used by cancer cells to induce chemoresistance is to increase autophagy induction. Under normal conditions, basal autophagy is responsible for protein turnover and the elimination of damaged or aged organelles and cytoplasmic components to maintain homeostasis in the cells (Maiuri *et al.* 2007). Autophagic induction under pathological conditions is considered as a pro-survival mechanism; however inappropriate activation of autophagy can also result in cell death (Yang *et al.* 2008).

1.2 Problem statement

A major goal in the search for an effective chemotherapeutic agent is to increase the susceptibility of cancer cells to cell death without harming normal cells. Doxorubicin is a well-known chemotherapeutic agent, with high anti-tumour efficacy, for the treatment of breast cancer patients. However, its clinical effects are limited due to its dose-dependent side effects such as cardiotoxicity (Roninson *et al.* 2001). Furthermore, resistance to doxorubicin therapy has also become a major problem in the treatment of this disease (Smith *et al.* 2006).

1.3 Hypothesis

We hypothesize that the inhibition of MKP-1, using a chemical inhibitor or siRNA, will increase the cytotoxic effect of doxorubicin (chemotherapeutic drug) in breast cancer cells, thus making the cells more responsive to treatment which will lead to increased cell death through autophagy and apoptosis.

1.4 General aims

This study therefore aims to inhibit MKP-1 in breast cancer cells to sensitise it to doxorubicin treatment. This could eventually lead to the usage of lower doses of doxorubicin which will limit the harmful side-effects on normal cells and increase cell death to overcome resistance in cancer cells.

1.5 Specific aims

The aims of the research were:

- First, to determine a dose for doxorubicin to induce apoptosis in breast cancer cells (MDA-MB231).
- Secondly, to characterize the effect of doxorubicin treatment on apoptosis under conditions of MKP-1 induction and inhibition to determine the functional role of MKP-1 in apoptosis.
- Thirdly, to determine the level of MKP-1 expression in breast cancer cells treated with a MKP-1 inducer (dexamethasone), MKP-1 inhibitors (sanguinarine or MKP-1 siRNA) and doxorubicin.
- Fourthly, to inhibit (sanguinarine, MKP-1 siRNA) and induce (dexamethasone) MKP-1 to determine the role of MKP-1 in autophagy during doxorubicin treatment in breast cancer.
- Fifthly, to determine whether inhibiting MKP-1, with siRNA or sanguinarine, will improve the cytotoxic effect of doxorubicin in breast cancer cells.
- Finally, to determine the effect of MKP-1 inhibition, with sanguinarine, and combined doxorubicin treatment on autophagy and apoptosis *in vivo* in C57BL6 tumour bearing mice.

1.6 Structure of the thesis

The effect of MKP-1 inhibition on the cytotoxicity of chemotherapeutic drugs in breast cancer is explored in this dissertation. Chapter 1 is an introductory chapter to present the background of the study as well as the aims and hypothesis. Chapter 2 reviews the current knowledge on MKP-1 expression in cancer and the effect that it has on autophagy and apoptosis. Chapter 3 highlights the methods used to collect data and Chapter 4 presents the results. Chapter 5 discuss the results in context with the data, and ends with conclusions and recommendations for future research.

Chapter 2:

Literature review

2.1 Introduction

Cancer is a disease characterized by the unrestrained growth and spread of abnormal cells, which, if not ceased, can result in death (Garcia *et al.* 2007). It is caused, both by external factors (chemicals, radiation and infectious organisms) and internal factors (inherited mutations, hormones and mutations occurring from metabolism) that may act together or in sequence to promote carcinogenesis (Garcia *et al.* 2007). All cancers encompass errors in genes that control cell growth, division and death. Most of the genetic abnormalities that affect cancer risk are in fact not hereditary but result from gene mutations occurring throughout one's lifetime.

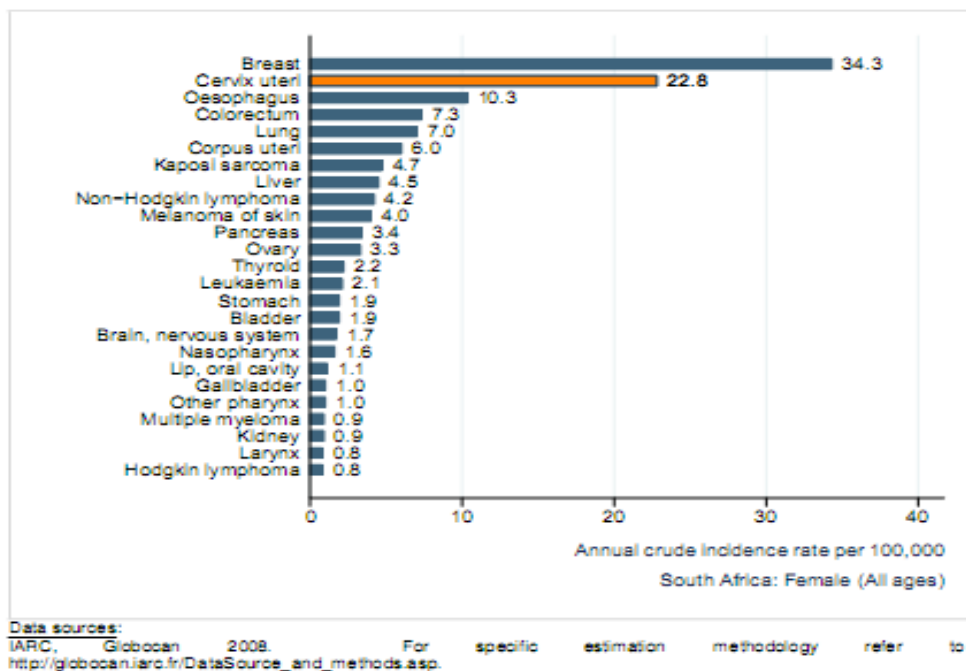


Figure 2.1: Incidence of Breast cancer compared to other cancers in women of all ages in South Africa (WHO, 2010).

Worldwide, public health data indicate that the burden of breast cancer in women, measured by incidence, mortality and economic costs, is extensive and on the increase (Jemal *et al.* 2011). Breast cancer is currently the most prevalent cancer and the primary cause of cancer related deaths in women worldwide, accounting for 23% (1.38 million) of total new cancer cases and 14% (458 400) of the total cancer deaths in 2008 (Jemal *et al.* 2011).

Worldwide, it is estimated that one million women are diagnosed every year and, of this one million, more than 410 000 will die from the disease (Coughlin and Ekwueme. 2009). In South Africa, breast cancer is now the most prevalent cancer in woman (Figure 2.1) (Vorobiof *et al.* 2001) and it is estimated that the incidence of breast cancer will increase with 15.8% by 2015 in this population (United Nations. 2008).

The statistics are alarming, and finding practical solutions to help improve breast cancer treatment is imperative. Major progress has been made to reduce the mortality rates; these include increased screening, digital mammography, specialized care and widespread use of therapeutic agents. However, an important long-term goal for the development of more effective therapeutic strategies would be to define the genetic architecture of breast cancer (Hicks *et al.* 2011).

In cancer, the normal mechanisms of cell cycle regulation are dysfunctional; oncogene and tumour-suppressor gene mutations drive the neoplastic process by increasing tumour cell number through over-proliferation of cells or inhibition of cell death or cell-cycle arrest (King and Cidlowski. 1998; Lowe *et al.* 2004; Vogelstein and Kinzler. 2004). These cells have complementary capabilities that enable tumour growth and metastasis. Hanahan and Weinberg (Hanahan and Weinberg. 2000) described these capabilities to be: self-sufficiency in growth signals, insensitivity towards anti-growth signals, the ability to evade apoptosis,

limitless replicative potential, sustained angiogenesis and the ability to invade other tissues and metastasize. More recently they added the ability to re-program energy metabolism and the ability to evade immune destruction to the already existing hallmarks of cancer (Hanahan and Weinberg. 2011).

Since cancer develops through many pathophysiological mechanisms and several signalling pathways play a role in disease progression, exploiting certain mediators of these pathways can potentially be therapeutic.

2.2 Mitogen-activated protein kinase signalling

Mitogen-activated protein kinases (MAPKs) are major signal transduction molecules that play a vital role in the regulation of a variety of cellular responses, including cell proliferation, differentiation and apoptosis (Wu. 2007). Mammalian MAPKs mainly consist of three sub-families: The c-Jun NH₂-terminal protein kinases (JNKs), the p38 MAP kinases, and the extracellular signal-regulated kinases (ERKs 1 & 2), can be activated by a variety of stimuli including growth factors and cellular/extracellular stresses (Wu. 2007).

MAPKs are activated in response to stimuli through the reversible phosphorylation of both threonine and tyrosine residues in the catalytic domain by upstream dual-specificity kinases namely MKK (MAP kinase kinase) (Wu. 2007). The MKKs are, in turn, activated by MAPK kinase kinases (MKKK or MEKKK) (Chang and Karin. 2001; Kennedy and Davis. 2003; Pearson *et al.* 2001). Upon activation, MAPKs phosphorylate a number of substrates which subsequently activate signalling pathways leading to diverse outcomes such as cell proliferation and apoptosis (Chang and Karin. 2001). The dephosphorylation and subsequent inactivation of MAPKs by members of the mitogen-activated protein kinase (MAPK)

phosphate (MKP) family has been shown to play a critical role in negatively regulating MAPK signal transduction pathways (Wu. 2007).

The MAPK phosphatases (MKPs) are a family of dual-specificity protein phosphatases that are responsible for the dephosphorylation of both phosphothreonine and phosphotyrosine residues in MAP kinases, including JNK, the p38 MAPK, ERK (Wu. 2007). Dephosphorylation of MAP kinases by MKPs inhibits MAPK activity, thereby negatively regulating MAPK signalling (Wu. 2007).

The MKPs encompass a family of ten enzymes, with each one having distinct properties in terms of transcriptional regulation, subcellular localization, and substrate specificity (Staples *et al.* 2010). The first member of this family of enzymes to be discovered was the nuclear phosphatase, MKP-1 (Chu *et al.* 1996). It was initially characterized as an ERK1 and -2 phosphatase but further research indicated that MKP-1 also had activity towards p38 and JNK MAPKs and it was capable of inactivating all three classes of MAPK *in vivo* (Groom *et al.* 1996).

The broad substrate selectivity is governed by the ability of MKP-1 to form physical complexes with ERK, p38 and JNK MAPKs. Hence, MAPK phosphatase-1 (MKP-1) is a mitogen and stress-inducible dual specificity protein phosphatase that has the ability to inactivate all three major classes of MAPK in mammalian cells (Staples *et al.* 2010). MKP-1 is believed to be involved in regulating the cell cycle (Wu. 2004; Yang and Wu. 2004) and apoptosis (Sanchez-Perez *et al.* 2000; Wang *et al.* 2006; Zhou *et al.* 2006), since JNK, p38, and ERK are capable of either inducing apoptosis or cell proliferation. MKP-1 can be induced by stresses (Wang *et al.* 2006; Zhou *et al.* 2006) and plays a role in cellular protection against a variety of genotoxic insults including hydrogen peroxide, ionizing radiation and cisplatin (chemotherapeutic drug) treatment, and also mediates breast cancer chemoresistance (Rojo

et al. 2009). However, its role in the interaction between different MAPK pathways in determining cell death and survival is not fully understood (Staples *et al.* 2010).

Recent studies have suggested that MKPs are involved in the development of cancer and play an important role in the response of cancer cells to chemotherapy. The role of MKPs in cancer stems from studies on MKP-1 expression in the different stages of various cancer types (Boutros *et al.* 2008; Wu. 2007). Numerous studies indicated that MKP-1 expression is altered in various cancer types including breast, lung, prostate, ovarian, pancreatic, gastric and liver cancer (Haagenson and Wu. 2010; Rojo *et al.* 2009). Furthermore, clinical studies have shown that MKP-1 expression correlates with cancer progression and can aid in prognosis. In human breast cancer, MKP-1 was found to be increased in malignant samples compared to non-malignant samples (Wang *et al.* 2003). MKP-1 expression was also increased in non-small cell lung cancer cells when compared to the normal lung (Vicent *et al.* 2004).

MKP-1 mRNA and protein levels were also found to be increased in pancreatic cancer; here MKP-1 down-regulation decreased pancreatic cancer cell growth and tumourigenicity in a nude mouse tumour model (Liao *et al.* 2003). To summarize: These findings indicate that MKP-1 plays a critical role in cancer development and may be a useful marker for predicting the survival of patients with cancer.

Evidence is growing to suggest a role of MKP-1 as a mediator of acquired breast cancer chemoresistance in human cell lines. Rojo *et al.* (Rojo *et al.* 2009) provided evidence on the role of MKP-1 in human breast cancer at three levels: Firstly, MKP-1 is overexpressed during the malignant transformation of the breast; secondly, MKP-1 overexpression is linked to poor patient outcome and lastly MKP-1 can be repressed by doxorubicin in many human breast cancers. The repression of MKP-1 is proposed to be associated with increasing levels

of phospho-extracellular signal-regulated kinase 1/2 (ERK) and c-Jun NH₂-terminal kinase (JNK) (Rojo *et al.* 2009). Their results add support to the concept that MKP-1 can act as a novel target for breast cancer therapy and also justify further studies on MKP-1 as promising prognostic marker.

2.2.1 MKP-1 inhibition

Evidence for the role of MKP-1 in cancer originates from a study by Liao *et al.* (Liao *et al.* 2003) who showed that PANC-1 human pancreatic cells were unable to form tumours in nude mice following transfection with a full-length MKP-1 antisense construct (Liao *et al.* 2003). The exact mechanism by which MKP-1 inhibition affects tumourigenicity remains unknown however.

There is a lack of optimal small-molecule inhibitors for MKP-1 (Ding *et al.* 2002). Such compounds will be beneficial for improving the efficacy of anticancer agents during conditions of MKP-1 overexpression. The availability of a selective inhibitor for MKP-1 would prove to be a valuable tool for understanding the intricate processes involved in ERK, JNK and p38 down-regulation, and to outline the contribution of MKP-1 and its cellular targets to cancer progression.

Since the three-dimensional structure for MKP-1 is still unknown, proper inhibitors are not available. However, several compounds have been found to block MKP-1 activity or protein function: Benzofuran blocks MKP-1 protein function (Lazo *et al.* 2006) and Ro 31-8220 inhibits kinase activity and prevents protein expression (Beltman *et al.* 1996). An alkaloid plant extract, sanguinarine, (Vogt *et al.* 2005) has also been shown to inhibit MKP-1 activity.

Sanguinarine is a bioactive quaternary benzophenanthridine alkaloid plant extract found in *Sanguinaria Canadensis*, (blood root), *Poppy fumaria*, *Bocconia frutescens*, *Chelidonium*

majus, and *Macleya cordata* and is a structural homologue of chelerythrine (Aburai *et al.* 2010; Adhami *et al.* 2004; Das *et al.* 2004; Jang *et al.* 2009; Mackraj *et al.* 2008; Park *et al.* 2010; Serafim *et al.* 2008; Vogt *et al.* 2005). A positive moiety is present in the aromatic ring of the sanguinarine molecule (Serafim *et al.* 2008) (Figure 2.2) and it is suggested that the core structure is a pharmacophore with rich potential for structural and functional modifications (Vogt *et al.* 2005).

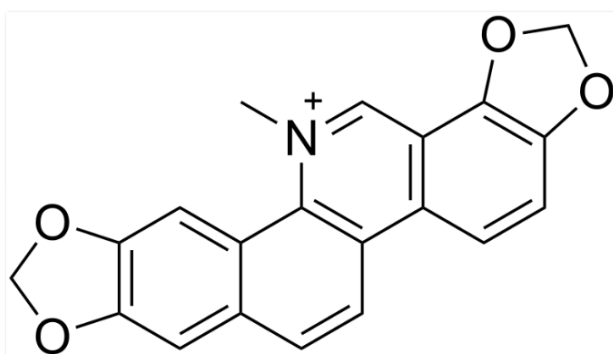


Figure 2.2: The molecular structure of Sanguinarine (Serafim *et al.* 2008)

Sanguinarine extracts have long been used in herbal medicine and documented properties include antiviral, antimicrobial, antibacterial, anti-oxidant, anti-inflammatory and pro-apoptotic activity (Jang *et al.* 2009; Vogt *et al.* 2005). Recent studies showed that sanguinarine can induce apoptosis in a variety of cancer cells through cell cycle arrest (Adhami *et al.* 2004), caspase activation (Kim *et al.* 2008), modulation of Bcl-2 (Ahsan *et al.* 2007) and down-regulation of ERKs (Han *et al.* 2007; Jang *et al.* 2009). Sanguinarine is used in traditional medicine as a pain reliever, sedative, expectorant and for infections (Das *et al.* 2004). It is also commonly used in toothpaste and various oral-hygiene products to combat gingivitis, inflammation and plaque formation (Adhami *et al.* 2004; Das *et al.* 2004).

Sanguinarine has been reported to possess multiple cellular activities which include inhibition of nuclear factor κ B (NF- κ B), suppression of vascular endothelial growth factor-induced angiogenesis and cell cycle arrest in G₁/S and G₂/M (Vogt *et al.* 2005). It

demonstrates activity in both the intrinsic and extrinsic apoptotic pathways in human promyelocytic leukaemia HL-60 cells (Vrba *et al.* 2009) and induces apoptosis in human squamous carcinoma (Ahmad *et al.* 2000). These effects and a more recent finding stating that sanguinarine sensitized human cervical cancer cells selected for cisplatin resistance to cell death, led Vogt *et al.* (2005) to discover that sanguinarine is an inhibitor of MKP-1. Sanguinarine treatment inhibited MKP-1 activity and consequently, increased phospho-ERK and phospho-JNK levels in a human pancreatic cell line, PANC1 (Vogt *et al.* 2005). This finding suggested a link between the sanguinarine-induced cell death and reduced MKP-1 activity; however this still has to be further elucidated.

2.2.2 MKP-1 induction

Glucocorticoids have the ability to inhibit tumour necrosis factor α -induced apoptosis in subcutaneous adipocytes (Zhang *et al.* 2001), mediate cell survival in primary cultures of human and rat hepatocytes (Bailly-Maitre *et al.* 2001), and protect against growth factor withdrawal-induced apoptosis in mammary epithelial cells (Wu *et al.* 2005). They observed that glucocorticoids have the ability to inhibit chemotherapy-induced apoptosis both *in vitro* (Wu *et al.* 2004) and *in vivo* (Herr *et al.* 2003).

It is possible that the activation of the glucocorticoid receptor regulates numerous complementary signalling pathways that lead to cell survival. In light of this, dexamethasone, an anti-inflammatory glucocorticoid, was shown to induce MKP-1 and subsequently inhibit p38 MAPK phosphorylation in HeLa cells (Lasa *et al.* 2002). Increased MKP-1 gene expression and the attenuation of proteosomal degradation were also observed (Kassel *et al.* 2002).

Dexamethasone has MKP-1 induction capabilities in several cell types including the RBL-2H3 mast cells and NIH 3T3 fibroblast (Kassel *et al.* 2002), HeLa cervical carcinoma (Lasa *et al.*

2002), MBA-15.4 bone marrow stromal, and the MG-63 pre-osteoblast cell lines (Engelbrecht *et al.* 2003). The rapid induction of MKP-1 by dexamethasone and the presence of three putative glucocorticoid response elements in the promoter region, suggested that MKP-1 is transcriptionally regulated by the glucocorticoid receptor (GR) (Kassel *et al.* 2002).

Research has shown that MKP-1 is one of the consistently up-regulated genes that contribute to the GR mediated inhibition of apoptosis which led to the discovery that induction of MKP-1 by dexamethasone in breast cancer cells, inhibited paclitaxel induced apoptosis (Wu *et al.* 2004; Fan *et al.* 2004). Hence, the up-regulation of MKP-1 following glucocorticoid receptor activation plays an important role in inhibiting chemotherapy-induced MAPK activation thus promoting cell survival and inhibiting apoptosis.

2.3 Apoptosis

The observation that cell death forms part of normal development was made more than a century ago. Only much later the term “programmed cell death” was used to describe the observation that some cells are intended to die as if driven by a cell-intrinsic program (Lockshin and Williams. 1965).

The term “apoptosis”, was first introduced in 1972 (Kerr *et al.* 1972), and is defined as an evolutionary conserved, active process that leads to cell death mediated by programmed signalling pathways associated with a set of morphological features (Hengartner. 2000). It is characterized by typical morphological and biochemical hallmarks. Apoptosis occurs in both physiological and pathological situations and activation can be initiated by a variety of extracellular or intracellular stimuli. It describes unique morphological changes that include cytoplasm shrinkage, membrane blebbing, nuclear chromatin condensation, chromosomal DNA fragmentation and formation of apoptotic bodies, which are eventually phagocytosed

by macrophages and other neighbouring epithelial cells, resulting from the activation of apoptotic signalling pathways (Arends and Wyllie. 1991).

A variety of cellular proteins are involved in the process of apoptosis. Among those, the proteolytic enzymes such as caspases are the well-established effector molecules and executioners of apoptosis (Cohen. 1997; Degterev *et al.* 2003).

Anticancer therapies lead to the activation of caspases, a family of cysteine proteases acting as death effector molecules in cell death (Degterev *et al.* 2003). They are synthesized as inactive proforms and when activated cleave next to aspartate residues (Degterev *et al.* 2003). The morphological features of cell death are mediated by caspases that cleave a variety of substrates in the cytoplasm or nucleus (Degterev *et al.* 2003). DNA fragmentation is mediated by ICAD (inhibitor of caspase-activated DNase) cleavage (Degterev *et al.* 2003). ICAD is an inhibitor of the endonuclease CAD (caspase-activated DNase) that cleaves DNA into the characteristic oligomeric fragments (Nagata. 2000). Proteolysis of cytoskeletal proteins leads to loss of cell shape and degradation of lamin results in nuclear shrinking (Degterev *et al.* 2003) (Figure 2.3, p17).

Cellular suicide can be initiated either through the activation of the extrinsic (receptor) pathway or at the mitochondria through stimulation of the intrinsic pathway (Fulda and Debatin. 2006) (Figure 2.3, p17). Apoptosis is regulated by the cytosolic signalling platform of cell death, the apoptosome (Riedl and Salvesen. 2007), and regulatory proteins such as the family of inhibitors of apoptosis (IAP) and Bcl-2 (Jang *et al.* 2009).

The first pathway – the extrinsic or cytoplasmic pathway – is triggered by the Fas death receptor, while the second pathway – the intrinsic or mitochondrial pathway – leads to the release of cytochrome c from the mitochondria and activation of the death signal (Ghobrial *et al.* 2005). The pathways finally converge to a common pathway that involves the

activation of a cascade of proteases that cleave regulatory and structural molecules culminating in cell death (Ghobrial *et al.* 2005).

The **extrinsic pathway** encompasses several protein members including the death receptors, membrane-bound Fas ligand (Fas-L), Fas complexes, Fas associated death domain (FADD) and caspase 8 and 10, which leads to the activation of downstream caspases and ultimately results in apoptosis. Activation is initiated with the ligation of the death receptors (DRs) of the tumour necrosis factor (TNF) receptor superfamily or TNF-related apoptosis inducing ligand (TRAIL) receptors (Walczak and Krammer. 2000).

Upon stimulation by a death signal, the membrane bound Fas-L interacts with the inactive Fas complexes and forms a death-inducing signalling complex. This complex consists of the adaptor protein Fas-associated death domain (FADD) protein and caspase 8 and 10 and leads to the activation of initiator caspase 8, which ultimately propagates apoptosis by cleavage of the effector caspase 3 (Ghobrial *et al.* 2005; Park *et al.* 2010). The activation of caspase 8 may be sufficient to execute death in some cell types; however, in other cell types, caspase 8 interacts with the intrinsic apoptotic pathway *via* Bid cleavage and the subsequent release of cytochrome-c (Ghobrial *et al.* 2005).

The Bcl-2 family of proteins are important regulators of the **intrinsic pathway**. Bcl-2 overexpression causes resistance to chemotherapeutic drugs and radiation *via* the accumulation of cells in the G₀ phase, while a decrease in Bcl-2 expression promotes the apoptotic response (Ghobrial *et al.* 2005). The Bcl-2 family includes both pro- and anti-apoptotic members. The anti-apoptotic Bcl-2 members - Bcl-2, Bcl-X_L, Bcl-W, Bfl-1, and Mcl-1 - repress apoptosis by hindering the release of cytochrome c.

The pro-apoptotic members act as promoters of apoptosis and they include: Bax, Bak, Bad, Bcl-Xs, Bid, Bik, Bim and Hrk (Ghobrial *et al.* 2005; Park *et al.* 2010). Proapoptotic proteins undergo posttranslational modifications following a death signal. These modifications include activation *via* dephosphorylation and cleavage which results in translocation to the mitochondria and finally apoptosis (Ghobrial *et al.* 2005).

The mitochondrial pathway is initiated by the release of cytochrome c, apoptosis inducing factor (AIF), Smac/DIABLO (second mitochondria derived activator of caspase/direct inhibitor of apoptosis protein (IAP)-binding protein with low PI) or endonuclease G from the mitochondrial intermembrane space (Fulda and Debatin. 2006; Park *et al.* 2010). Upon apoptotic stimuli, cytochrome c and Smac/DIABLO is released through the permeable outer mitochondrial membrane. Cytochrome c release into the cytosol triggers caspase 3 activation by the formation of the cytochrome c/Apaf-1/caspase-9-containing apoptosome complex (Fulda and Debatin. 2006), whilst Smac/DIABLO promotes caspase activation *via* the neutralization of the inhibitory effects to the IAPs (Fulda and Debatin. 2006; Gerl and Vaux. 2005). Caspase 9 then becomes proteolytically active and in turn activates caspase 3 which results in the activation of downstream caspases and subsequently leads to apoptosis (Ghobrial *et al.* 2005).

The two pathways converge at caspase 3, where cleavage of the inhibitor of the caspase-activated deoxyribonuclease (ICAD) activates the caspase-activated deoxyribonuclease (CAD), leading to nuclear apoptosis. The upstream caspases 9 and 8 converge on caspase 3 in the intrinsic and extrinsic pathways respectively. Cleavage of protein kinases, cytoskeletal proteins, DNA repair proteins, inhibitory sub-units of endonucleases (CIDE family) and the destruction of housekeeping cellular functions are all mediated by the downstream caspases. The effect of caspases on cytoskeletal structure, cell cycle regulation and signalling

pathways ultimately leads to the characteristic morphological changes associated with apoptosis such as DNA condensation and fragmentation, and membrane blebbing (Ghobrial *et al.* 2005) (Figure 2.3).

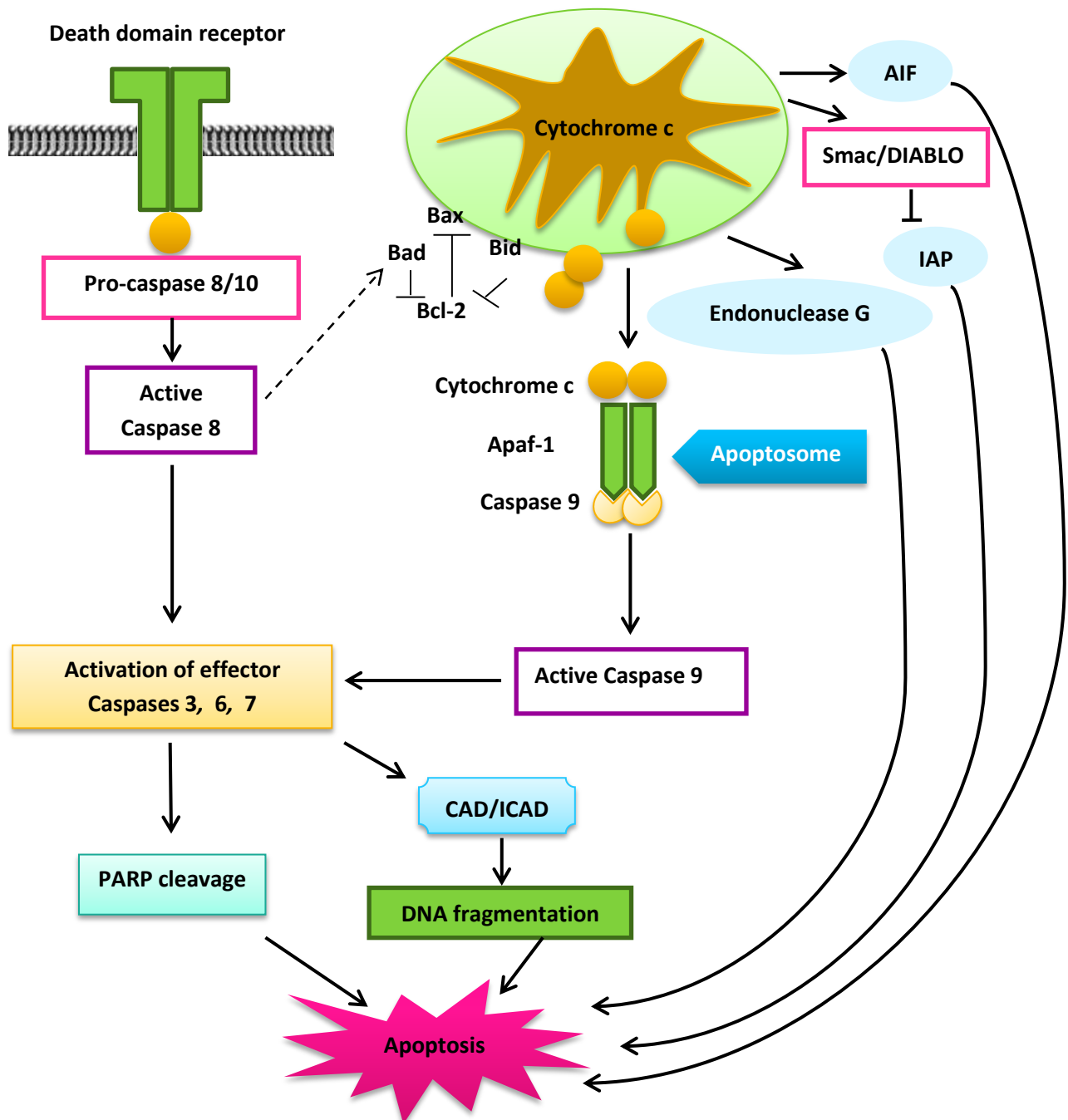


Figure 2.3: Apoptosis signalling pathway. Adapted from Ghobrial *et al.* 2005.

PARP cleavage is another hallmark of apoptosis. PARP binds to DNA fragments in response to DNA fragmentation and this catalyses the poly (ADP)-ribosylation of many proteins through converting nicotinamide adenine dinucleotide (NAD) to nitric acid monohydrate (NAM) and ADP-ribose (Zong and Thompson. 2006). PARP depletes cytosolic NAD during this process, as cytosolic and mitochondrial NAD do not exchange freely across the inner mitochondrial membrane (Zong and Thompson. 2006). If glucose breakdown is inhibited, the activation of PARP could induce necrosis, unless NAD pools are replenished (Zong and Thompson. 2006). Thus, PARP cleavage by caspases prevents energy depletion and the induction of necrosis; hence, caspases are not only important in the regulation of apoptosis but also in the inhibition of necrosis (Zong and Thompson. 2006).

Links between the receptor and mitochondrial pathway have been proposed at different levels. The activation of caspase 8 can result in cleavage of Bid, a protein from the Bcl-2 family, which translocates to the mitochondria to release cytochrome c and thereby initiate a mitochondrial amplification loop (Cory and Adams. 2002). Cleavage of caspase 6 downstream of the mitochondria may feed back to the receptor pathway by cleaving caspase 8 (Cowling and Downward. 2002).

Apoptosis is imperative in the maintenance of normal homeostasis and acts in concert with other processes like proliferation and differentiation. Dysregulation of the apoptotic machinery has disastrous consequences and is associated with many diseases such as cancer, auto-immunity and neuro-degeneration (Ghobrial *et al.* 2005).

It is well-known that anticancer agents such as chemotherapy, γ -irradiation or immunotherapy exert their antitumour effect by inducing apoptosis, and that the disruption of apoptotic processes can reduce the sensitivity of cancer to treatment (Fulda and Debatin.

2006). The underlying mechanism that initiates an apoptotic response following cytotoxic therapy depends on the individual stimulus and has often not yet been identified.

Nevertheless, a common initial event is considered to be damage to DNA which is then propagated by the cellular stress response (Fulda and Debatin. 2006). Stress inducible molecules such as JNK, ERK, NF- κ B or ceramide have been inferred to transmit the apoptotic signal in cancer therapy (Fulda and Debatin. 2006).

Apoptosis pathways have to be tightly controlled, and various anti-apoptotic mechanisms, such as mutations in apoptotic programs, have been associated with resistance to therapeutic agents in cancer cells. However, the notion that apoptosis is the major form of cell death by which cancer cells die should not be applied to all cancers as caspase independent apoptosis and other modes of cell death, including autophagy, have also been implicated in response to cancer therapy in certain instances (Brown and Wilson. 2003).

2.3.1 The role of MKP-1 signalling in apoptosis

Several studies have shown that MKP-1 inhibits cell death induced by a number of anti-cancer drugs in different cancer cells. It has been shown to inhibit biochemical events associated with apoptosis, such as the activation of caspase-3 and proteolytic cleavage of poly (ADP ribose) polymerase (PARP). These findings indicate the MKP-1 acts at a site upstream of caspase activation within the apoptotic program (Franklin *et al.* 1998).

It is proposed that caspase 3/7 is responsible for the activation of MAPKs, such as ERK1/2, p38 MAPK and JNK, *via* Mst1, an upstream kinase for MAPKKK, through an extrinsic apoptotic pathway-dependent mechanism (Song and Lee. 2008).

According to Song and Lee (2008), caspase 7 cleaves Mst1; thereby producing a 40 kD fragment which subsequently activates JNK and p38 MAPK, and caspase 3 produces a 36 kD

fragment of Mst1 responsible for the activation of ERK (Song and Lee. 2008). However, the functional significance of MAPK activation in this scenario still needs further investigation. If MKP-1 expression is upregulated in certain instances then its inhibitory effects on JNK, p38 MAPK and ERK demolishes the activation induced by caspase 3/7.

MKP-1 has been implicated in anti-apoptotic effects observed in mouse embryonic fibroblasts (MEFs) in the presence of anisomycin by suppressing caspase-3-mediated apoptosis (Wu and Bennett. 2005). Furthermore, Wang *et al.*, (2006) indicated that cisplatin treatment activates PARP and caspase 3 in MKP-1-null MEFs by inducing their cleavage which resulted in an increase in caspase 3 activity. This effect was, however, not seen in wild-type MEFs when treated similarly (Wang *et al.* 2006). Moreover, MKP-1 expression *via* transfection or adenoviral transduction reduced the increase in caspase 3/7 activity mediated by paclitaxel (Jordan and Wilson. 2004) and mechlorethamine in MDA-MB231 cells (Small *et al.* 2007).

A similar effect was seen in BT-474 and A1N4-myc cells where adenovirus-mediated expression of MKP-1 reduced DNA fragmentation following doxorubicin, paclitaxel or mechlorethamine treatment (Boutros *et al.* 2008). These results mirror those derived from treating wildtype MEFs and MKP-1 null MEFs with doxorubicin, paclitaxel, or mechlorethamine (Small *et al.* 2007).

To summarise, these findings indicated that in the presence of MKP-1, human mammary epithelial cells, breast carcinoma cells, and MEFs are protected from agents that induce DNA fragmentation through a JNK/c-Jun-mediated mechanism (Small *et al.* 2007). This suggests a role for MKP-1 in inhibiting apoptosis in these scenarios.

MKP-1 protein levels were found to be increased in human primary gastric tumours, when compared with normal gastric tissues (Bang *et al.* 1998). In these tumours ERK1/2 activity was elevated compared with patient matched normal gastric tissue and the authors believed that the increase in MKP-1 expression was a consequence of increased ERK1/2 activity and that it contributed to carcinogenesis (Bang *et al.* 1998). Liu *et al.* (1995) found that short-wavelength ultraviolet light (UVC) up-regulates ERK2 and JNK1 activity in HeLa cells, causing an increase in MKP-1 protein levels; this led to a subsequent down-regulation of JNK activity in these cells. Also, in U937 human leukaemia cells, a study on the effect of MKP-1 on UVC induced cell death indicated that MKP-1 overexpression reduced JNK-mediated apoptosis in these cells (Franklin *et al.* 1998). Low doses of UVC also decreased MKP-1 mRNA in transcription coupled repair-deficient human fibroblasts (Hamdi *et al.* 2005). These findings indicate that MKP-1 can protect cells from chemical- and radiation induced JNK activation. If one considers the protective effect MKP-1 has in certain tumour cell lines, it would make sense to investigate whether this effect is indeed demolished if MKP-1 is down-regulated or inhibited prior to the use of chemotherapeutic agents. Thus, understanding the role of MKP-1 in cancer development and its impact on chemotherapy can be exploited for therapeutic benefits for the treatment of cancer.

2.4 Autophagy

Many chemotherapy drugs, such as doxorubicin (Roninson *et al.* 2001), arsenic trioxide (Kanzawa *et al.* 2003) and cisplatin (Yang *et al.* 2008) are known to induce an autophagic response in cancer cells (de Bruin and Medema. 2008; Yousefi and Simon. 2009). Autophagy (Figure 2.4, p 23), first described in the 1960's, is a genetically regulated process that plays a critical role in the degradation of cytoplasmic proteins and other macromolecules

(Stromhaug and Klionsky. 2001). This occurs *via* their sequestration within autophagosomes which subsequently fuse with lysosomes in multicellular organisms (Yang *et al.* 2008).

Autophagy is initiated by the induction of several genes in the autophagy network including LC3, phosphatidylinositide 3-kinase and Beclin 1 (Yang *et al.* 2008). This occurs mainly in response to nutrient starvation, hypoxia, ATP depletion or signals prompting cellular remodelling and is controlled by the mTOR pathway (Meijer and Codogno. 2004). Autophagy is a highly regulated process that can be either generally involved in the turnover of long-lived proteins and organelles or can specifically target distinct organelles and thereby eliminate damaged cellular constituents (Maiuri *et al.* 2007).

During autophagy, parts of the cytoplasm and intracellular organelles are sequestered within the double-membraned autophagosomes before being delivered to lysosomes (Maiuri *et al.* 2007), a process regulated by the Atg genes (Hoyer-Hansen and Jaattela. 2008). Subsequently, the autophagosomes fuse with the lysosomes to form autophagolysosomes, where the sequestered material is digested (Maiuri *et al.* 2007). The initial step of autophagy can be regulated by class I and class III phosphoinositide 3 kinases (PI3K) (Hsieh *et al.* 2009). Activation of class I PI3K inhibits autophagy through successive phosphorylation of Akt and mTOR, while activation of class III PI3K in a complex with Beclin 1 promotes autophagy (Hsieh *et al.* 2009).

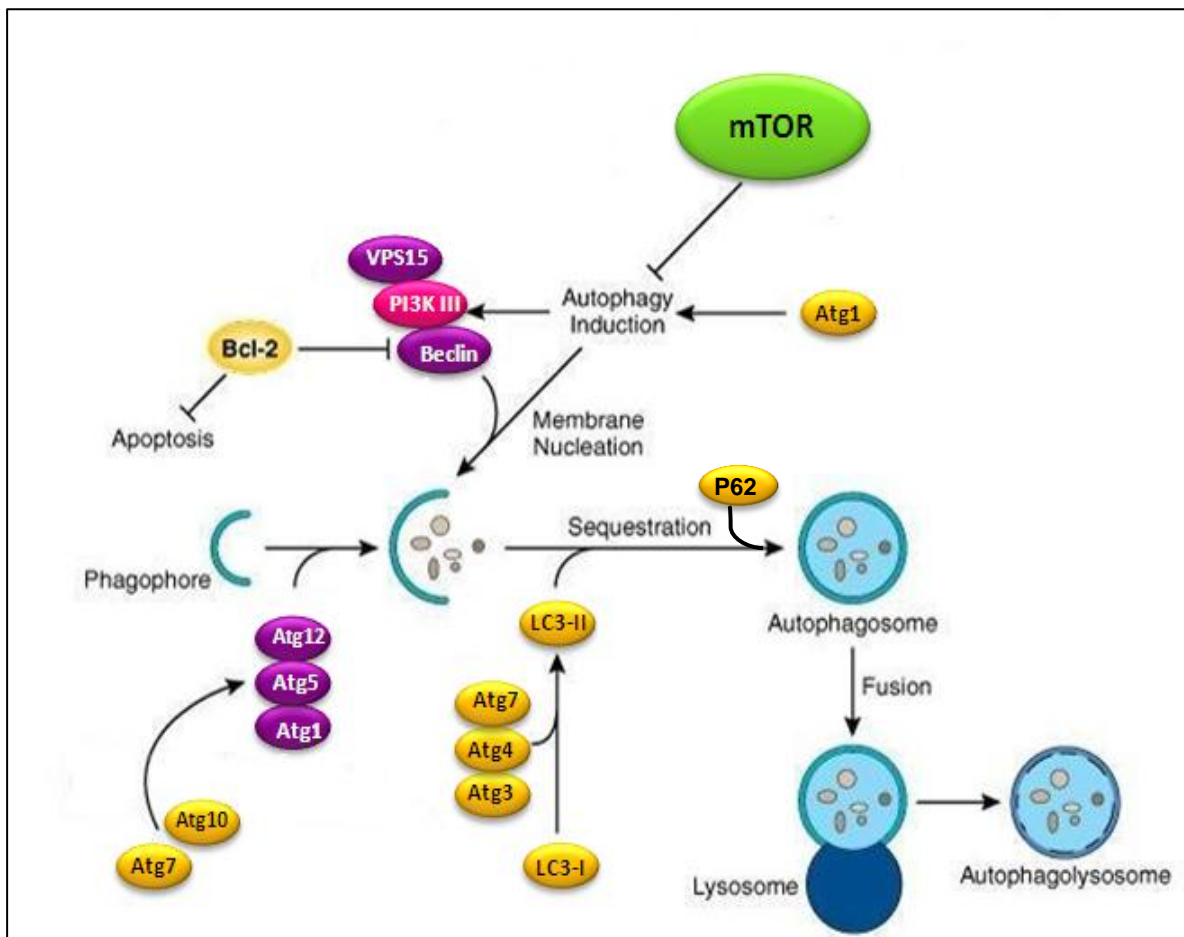


Figure 2.4: Induction of autophagy requires interaction between beclin 1 and class III phosphoinositide 3 kinase (PI3K III). Bcl-2 can bind to beclin 1 and inhibit autophagy. Autophagy is also negatively regulated by mTOR. Atg proteins are recruited to the membrane via nucleation and elongation of the membrane is initiated by the Atg12/Atg5/Atg16 complex. LC3 is cleaved by Atg 4 to generate LC3-I. LC3-I is then activated by the Atg7/Atg4/Atg3 complex. The resulting LC3-II then finalizes the formation of the autophagosome. P62 is responsible for the sequestration of the autophagy substrates into larger units or aggregates. Via the interaction with LC3-II through the LC3 interacting region (LIR), the phagophore is recruited and the autophagosome forms around the aggregated substrates (Moscat et al. 2009). Fusion to and incorporation of the lysosome creates the autophagolysosome which results in the degradation of the contents through hydrolase activities. Adapted from www.cellsignal.com/reference/pathway/Autophagy.html

Autophagy plays a role in regulating cell death in both physiological and pathophysiological conditions (Kundu and Thompson. 2008; Levine and Yuan. 2005). Under normal conditions, basal autophagy has been proposed as a mechanism for protein turnover and the elimination of damaged or aged organelles and cytoplasmic components to maintain homeostasis in the cell. Autophagic induction under pathological conditions is considered to be a pro-survival mechanism; however, extensive autophagy or inappropriate activation of autophagy results in cell death by bulk elimination of organelles (Yang and Wu. 2004).

Autophagic cell death is different from apoptosis in the sense that it is caspase-independent and can occur even if the apoptosis machinery of the cell is defective (Shimizu *et al.* 2004).

There is considerable controversy as to whether autophagy actually protects cells from death or causes cell death (Lockshin and Zakeri. 2004). Some researchers argue that the role of autophagy depends on the state of the cell, where initially, following a cellular stress, autophagy acts as a protective mechanism, but ultimately it results in the accumulation of cellular constituents in lysosomes and cell death (Cuervo. 2004).

Autophagy has been proposed as a mechanism for both tumour progression and tumour suppression, although the exact mechanism responsible for this dual action in cancer has not been fully elucidated (Salazar *et al.* 2009). Even though it is now widely accepted as a form of programmed cell death (Lockshin and Zakeri. 2004), many still believe that it might more accurately be described as a cell survival mechanism that acts alongside cell death but does not necessarily lead to it (Tsujiimoto and Shimizu. 2005).

During tumorigenesis normal cells are transformed into cancerous cells through the accumulation of gene mutations and epigenetic modifications (Folkman. 2006). These cells experience severe metabolic stress conditions since oxygen, growth factors and nutrients cannot diffuse efficiently to the cells at the centre of the tumour due to inadequate vascularisation (Folkman. 2006).

As a result, the cells at the centre of the tumour live in a metabolically stressed environment characterized by hypoxia, low pH and nutrient deprivation, all of which induces autophagy (Jin and White. 2008). Autophagy is thus localized to these metabolically stressed regions where it functions to support cell survival (Jin and White. 2008). This explains why some cancer cells have a high basal level of autophagy to begin with. Extensive activation of

autophagy in cancer cells lead to the disintegration of major cellular systems in such a way that the “point of no return” is crossed and cell recovery is unachievable (Eisenberg-Lerner and Kimchi. 2009). Therefore, autophagy can protect cells against death or mediate cell death depending on the autophagy stimuli and cellular context. It has been shown that a deficiency in autophagy can lead to cancer development.

Some breast cancer cell lines contain deletions in Beclin 1, which is required to induce autophagy (Liang *et al.* 1999). Introduction of Beclin 1 into these cell lines induced autophagy and inhibited tumorigenicity which has led to the conclusion that the deletion of Beclin 1 might contribute to the progression of breast cancer (Liang *et al.* 1999).

2.4.1 Autophagy and MKP-1

Little is known about the role of MKP-1 in autophagy. The only direct link found between MKP-1 and autophagy was discovered recently when it was observed that an areca nut extract (ANE), a carcinogen and addictive substance often used in Asia, causes induction of autophagy, which was mediated through p38 MAPK and MKP-1 activation, in oral cancer cells. ANE-induced autophagy inhibited apoptosis in this scenario (Lu *et al.* 2010).

2.5 Crosstalk between autophagy and apoptosis

When viewed dynamically, autophagy acts to delay cell death and only leads to it in a last desperate effort while attempting to keep the cell alive. We believe that this can only occur once autophagy has progressed and persisted beyond the so-called “point of no return”, resulting in apoptosis or possibly necrosis (Loos and Engelbrecht. 2009).

Crosstalk between autophagy and apoptosis is a dynamic physiological relationship. The relationship is complex in the sense that, in some scenarios, autophagy acts as a stress adaptation that helps to avoid cell death, whereas in other settings, it constitutes an

alternative pathway to cell death that is also referred to as autophagic cell death or type II cell death (de Bruin and Medema. 2008). In general terms it appears that autophagy and apoptosis can be induced by similar stimuli (Maiuri *et al.* 2007). This has been proved by the recent deciphering of pathways that link the autophagic and apoptotic machinery (Maiuri *et al.* 2007). Bcl-2 family proteins, consisting of pro- and anti-apoptotic proteins, are important regulators of apoptosis and autophagy (Igney and Krammer. 2002). Beclin-1 has a Bcl-2 binding domain and this domain serves as a point of crosstalk between autophagic and apoptotic pathways at the point of autophagic induction (Shimizu *et al.* 2004). The dissociation of Beclin 1 from anti-apoptotic Bcl-2 is essential for its autophagic activity; failure of dissociation results in autophagy being suppressed (Pattingre and Levine. 2006). The transcription factor, p53, is also linked to both autophagy and apoptosis. It is a well-known apoptosis inducer, but recent evidence has also linked it to autophagy through the inhibition of mTOR *via* AMPK (Tasdemir *et al.* 2008).

These pathways are thus regulated by certain common factors and share common components, each of which can possibly regulate and modify the activity of the other. Apoptosis and autophagy thus constitute the two processes through which damaged or aged cells and organelles are eliminated.

The availability of ATP is necessary for apoptosis as it is an energy dependent process (Leist *et al.* 1999). Lack of ATP would favour necrosis; therefore autophagy is required for tumour cells to undergo apoptosis as it provides ATP. Initially autophagy provides ATP and nutrients to tumour cells, but as the degree of autophagy increases it will eventually lead to cell death (Levine. 2007).

2.6 Treatment options for breast cancer

The anthracycline antibiotic, doxorubicin is one of the most important anticancer agents for a variety of solid tumours and leukaemias (Hortobagyi. 1997). It is generally accepted that the primary cytotoxic mechanism of doxorubicin can be attributed to its ability to intercalate with the cell's DNA and cause localized uncoiling of the double helix. It can also stabilize the complex between DNA and topoisomerase II which results in the subsequent induction of apoptosis (Cuvillier *et al.* 2001; Wang *et al.* 2004). It has the ability to generate reactive oxygen species from quinone-generated redox activity that also results in DNA degradation (Cuvillier *et al.* 2001; Wang *et al.* 2004). Interestingly, doxorubicin has also been shown to induce an autophagic response prior to the induction of apoptosis (Roninson *et al.* 2001).

One of the major goals in cancer research is to increase the susceptibility of cancer cells to apoptosis-based strategies. However, in some instances, the resistance to chemotherapy could not only be attributed to their inability to induce apoptosis, but also to the protection exerted by autophagy.

Furthermore, it has also been demonstrated that in some cases, breast cancers are highly resistant to doxorubicin treatment (Smith *et al.* 2006) which represents a major obstacle in successful treatment. The precise molecular sequences responsible for this resistance are unknown, but it is suggested that resistance occurs through the expression of a membrane transporter, P-glycoprotein/ MDR1 that pumps the drug out of the cell and generates reactive oxygen species and free radicals *via* Doxorubicin redox cycling (Finn *et al.* 2011).

2.7 Sensitizing breast cancer cells to cell death

It would be of great benefit to find adjuvant therapeutic targets that will be effective in inducing cell death in cancer cells without further harming normal cells. Evidence suggesting

that MKP-1 is overexpressed in breast cancer is accumulating; therefore targeting this protein can be a novel avenue for therapeutic intervention.

We, therefore, propose that by inhibiting MKP-1 with sanguinarine and inducing autophagy with doxorubicin, the already high basal level of autophagy in breast cancer cells will increase and move closer to the “point of no return.” Subsequently, as the “point of no return” is reached, apoptosis will be induced, thereby sensitizing the cells to chemotherapy.

Using combined doxorubicin and MKP-1 inhibition therapy to sensitize breast cancer cells to autophagy and bring them closer to the “point of no return” may prove to be a novel more effective treatment strategy for breast cancer patients. Recent studies have shown that autophagy can sensitize cancer cells to chemotherapeutic agents (Zhuang *et al.* 2009) as well as augment chemotherapy-induced apoptosis (Shingu *et al.* 2009). It has been confirmed that doxorubicin induces an autophagy response in cancer cells. However, the effect of doxorubicin treatment in conjunction with sanguinarine in MDA-MB231 cells as well as in an *in vivo* mouse model still needs to be elucidated.

2.8 Hypothesis

We hypothesize that the inhibition of MKP-1, using a chemical inhibitor or siRNA, will increase the cytotoxic effect of doxorubicin (chemotherapeutic drug) in breast cancer cells thus making the cells more responsive to treatment which will lead to increased cell death through autophagy and apoptosis.

2.9 Aims

- First, to determine a dose for doxorubicin to induce apoptosis in breast cancer cells (MDA-MB231).
- Secondly, to characterize the effect of doxorubicin treatment on apoptosis under conditions of MKP-1 induction and inhibition to determine the functional role of MKP-1 in apoptosis.
- Thirdly, to determine the level of MKP-1 expression in breast cancer cells treated with a MKP-1 inducer (dexamethasone), MKP-1 inhibitors (sanguinarine or MKP-1 siRNA) and doxorubicin.
- Fourthly, inhibit (sanguinarine, MKP-1 siRNA) and induce (dexamethasone) MKP-1 to determine the role of MKP-1 in autophagy during doxorubicin treatment in breast cancer.
- Fifthly, to determine whether inhibiting MKP-1, with siRNA or sanguinarine, will improve the cytotoxic effect of doxorubicin in breast cancer cells.
- Finally, to determine the effect of MKP-1 inhibition, with sanguinarine, and combined doxorubicin treatment on autophagy and apoptosis *in vivo* in C57BL6 tumour bearing mice.

Chapter 3: Materials and Methods

3.1 Study design

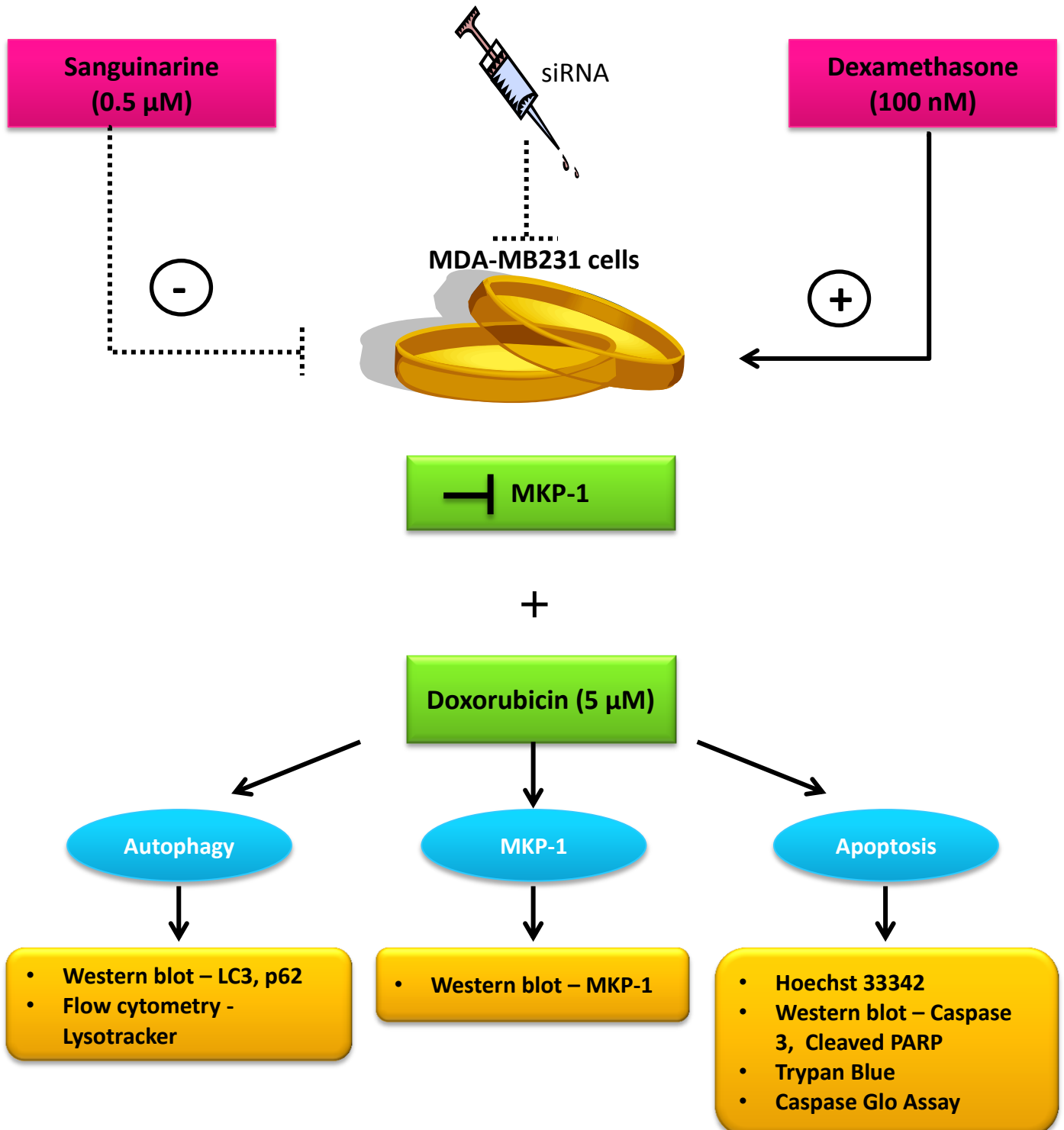


Figure 3.1: Study design: MKP-1 was inhibited or silenced in MDA-MB231 breast carcinoma cells by using either Sanguinarine or MKP-1 siRNA. After MKP-1 inhibition the cells were treated with doxorubicin and autophagy and apoptosis were detected by various methods. MKP-1 inhibition was compared to a known inducer of MKP-1 namely dexamethasone. MKP-1 induction and inhibition was detected by means of western blotting.

3.2 Cell culture

The human metastatic mammary carcinoma cell line, MDA-MB231, was used to perform experiments and was obtained from American Type Culture Collection (Rockville, MD, USA). The cells were cultured in Glutamax-Dulbecco's Modified Eagle's Medium (Glutamax-DMEM) (Celtic Molecular Diagnostics, Cape Town, South Africa) and supplemented with 10% Foetal



Figure 3.2: The human metastatic mammary carcinoma cell line, MDA-MB231, was obtained from a patient in 1973 at M.D Anderson Cancer Center

Bovine Serum (FBS) (Sigma Chemical Co., St Louis, MO, USA), hereafter collectively referred to as growth medium. The cells were cultured in T75 flasks (75 cm² flasks, Greiner Bio One, Germany) and maintained at 37°C in a humidified 5% CO₂ atmosphere and were routinely sub-cultured upon reaching 70 – 80% confluency. The MDA-MB231 cells were allowed to grow in the T75 flasks until they reached 80% confluency and were then split and seeded into appropriate plates or dishes with new growth medium for various experiments. Splitting was accomplished by washing the cell monolayer with warm sterile Phosphate Buffered Saline (PBS), followed by incubation with 4 ml 0.25% Trypsin EDTA (Sigma Chemical Co., St Louis, MO, USA) at 37°C until cells detached completely from the surface of the flask. All experiments were performed using exponentially growing cells. A complete step by step protocol of MDA-MB231 cell culture procedures is included in Appendix A.

3.3 Experimental protocol

MDA-MB231 cells were allowed to grow and become confluent before they were split and seeded accordingly for each experiment. Seeding densities were previously determined for each experiment so that equivalent sub-confluent cell populations were always present at the

time of treatment. The cells were randomly divided into treatment groups (see Table 1) and each group were treated as depicted in Figure 3.3 (p 34).

Table 1: MDA-MB231 cells were divided into ten groups and each group were treated accordingly.

| Group number | Group name | Treatment |
|--------------|----------------------------------|------------------------------|
| Group 1 | Control | No treatment |
| Group 2 | Dexamethasone Control | Dexamethasone |
| Group 3 | Dexamethasone and Doxorubicin | Dexamethasone Doxorubicin |
| Group 4 | Doxorubicin | Doxorubicin |
| Group 5 | Sanguinarine | Sanguinarine |
| Group 6 | Sanguinarine and Doxorubicin | Sanguinarine Doxorubicin |
| Group 7 | MKP-1 siRNA | MKP-1 siRNA |
| Group 8 | MKP-1 siRNA and Doxorubicin | MKP-1 siRNA Doxorubicin |
| Group 9 | Negative Control | Stealth RNAi |
| Group 10 | Vehicle | Methanol |

3.3.1 Treatment preparations

MDA-MB231 cells were treated with Doxorubicin hydrochloride (D1515, Sigma Chemical Co., St Louis, MO, USA) for 24 hours at a concentration of 5 μ M. The drug was dissolved in Glutamax-DMEM in ready to use aliquots to avoid freeze thaw cycles, and was stored at -20°C. Sanguinarine was used as a MKP-1 inhibitor. The cells were treated with Sanguinarine (Sigma Chemical Co., St Louis, MO, USA) at a concentration of 0.5 μ M for 24 hours before doxorubicin treatment started. The drug was dissolved in methanol and stored as a 0.01 M stock solution at 4°C. To determine the extent to which sanguinarine and MKP-1 siRNA inhibited MKP-1, it was compared to a known inducer of MKP-1, dexamethasone (Sigma Chemical Co., St Louis, MO, USA). MDA-MB231 cells were treated with dexamethasone at a

concentration of 100 nM for 24 hours. Dexamethasone was dissolved in distilled water and stored as a 0.1 M stock solution at 4°C. Methanol made up in the same concentration as Sanguinarine was used as vehicle. The growth medium of all groups was refreshed before treatment started. The concentrations of the various treatments were selected based on assessment by dose-response experiments.

3.3.2 MKP-1 siRNA Transfection

For groups 7, 8 and 9 the cells were transfected through a reverse transcription protocol (Appendix A). Twenty pmol of MKP-1 siRNA duplex was used per culture well. Twenty pmol of both MKP-1 siRNA duplexes (DUSP1VHS40581 and DUSP1VHS40583) (Invitrogen™, USA, MKP-1 siRNA #159527B10, #159527B11) was diluted into 250 µl of transfection medium (Glutamax-DMEM containing no antibiotics or serum). 2 µl of Lipofectamine™ RNAiMAX (13778075; Invitrogen™, USA) was added to this and the suspension was gently mixed. The RNAi duplex-Lipofectamine RNAiMAX complexes were allowed to incubate for 40 minutes and then made up to a final volume of 2 ml using Glutamax-DMEM (no antibiotics). MDA-MB231 cells were plated directly into the culture dishes containing the RNAi duplex-Lipofectamine RNAiMAX complexes. Stealth™ RNAi (STEALTH RNAi NEG CTL MED GC, 12935300; Invitrogen™, USA) was used as a negative control. Cells were incubated at 37°C and treated with doxorubicin 48 hours later.

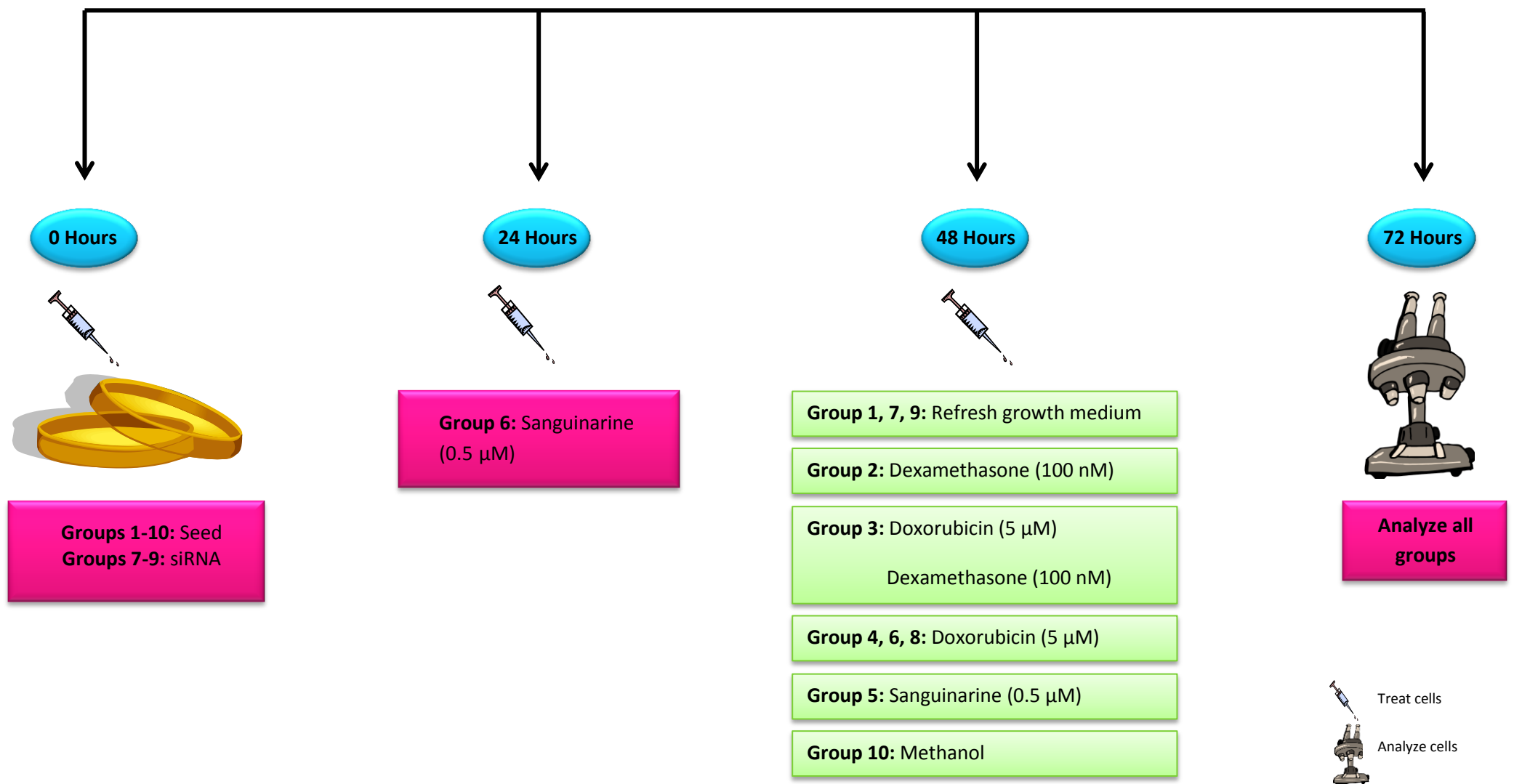


Figure 3.3: Experimental plan for treatment of MDA-MB231 breast cancer cells. A 72 hour treatment time was followed from seeding up to analysis. All groups were seeded at 0 hours and reverse transfection was done for groups 7-9. Twenty-four hours later Group 6 was treated with Sanguinarine. At 48 hours the remaining groups were treated and growth medium was refreshed for non-treatment groups. At 72 hours all treatment was stopped and data was analysed.

3.4 Determination of cell death

3.4.1 Morphological analysis

For morphological determination of cell death, MDA-MB231 cells were stained with Hoechst 33342 (10 mg/ml) in a 1:200 dilution. Hoechst 33342 is able to diffuse through cell membranes regardless of their condition. It is a DNA stain that detects early apoptosis and stains the nuclei blue. MDA-MB231 cells were randomly divided into groups and seeded in 8-well chambers (Greiner Bio One) at a seeding density of 3000 cells per well. For the groups that needed transfection, the cells were reverse transfected during plating (Section 3.3.2, p33). The cells were left to plate and grow in 200 µl growth medium per well and the experimental plan set out in Figure 3.3 was followed. Growth medium for all groups was changed and replaced with fresh growth medium before the indicated treatment (Section 3.3.1, p 32) (Figure 3.3, p 34) started. The treatment was administered straight into the medium at the correct concentration. After treatment of the groups as described in section 3.3.1, the medium was drained and the cell monolayer was washed with warm sterile PBS. Hoechst 33342 (1:200 dilution) was made up in growth medium and 200 µl growth medium/Hoechst solution was added to each well to cover the entire monolayer. The cells were left to incubate for 5 minutes. Images were acquired directly after the incubation period through an Olympus Cell[®] system attached to an IX-81 inverted fluorescence microscope equipped with an F-view-II cooled CCD camera (Soft Imaging Systems). By using a Xenon-Arc burner (Olympus Biosystems GMBH) as light source, images were excited with the 360 nm DAPI excitation filter. Emission was collected using a UBG triple band pass emission filter cube. Images were processed and background subtracted using the Cell[®] software. Images were taken of a minimum of three randomly chosen fields, of at least three independent experiments per treatment group. Morphological changes such as condensed

nuclear chromatin and apoptotic bodies were quantified using the Cell[®] system. A complete step by step protocol for Hoechst 33342 staining is reproduced in Appendix A (p 109).

3.4.2 Trypan blue assay

To determine the viability of MDA-MB231 cells after treatment, the Trypan blue exclusion technique (Kitakaze *et al.*, 1997) was used. Due to an intact, functional cellular membrane viable cells are able to exclude the blue dye, whilst non-viable cells are unable to prevent its entrance into the cytoplasm as a result of membrane leakage. MDA-MB231 cells were randomly divided into groups and seeded in 6-well cell culture plates (Greiner Bio One) at a seeding density of 100 000 cells per well. For the groups that needed transfection, the cells were reverse transfected during plating (Section 3.3.2, p 33). The cells were left to plate and grow in 2 ml growth medium per well and the experimental plan set out in Figure 3.3 (p 34) was followed. Growth medium for all groups were changed and replaced with fresh growth medium before the indicated treatment (Section 3.3.1, p 32) (Figure 3.3) started. The treatment was administered straight into the medium at the correct concentration. Following completion of the treatment protocol as described in section 3.3.1, the medium was drained and the cell monolayer was rinsed with warm sterile PBS. The medium from each well was drained into ten sterile 15 ml Falcon tubes (Greiner Bio One), labelled according to treatment. Cells were trypsinized for approximately 3 minutes or until they detached from the surface of the flask and each cell suspension was added to the appropriate 15 ml Falcon tube and centrifuged for 3 minutes at 1500 rpm. The supernatant was decanted and the pellet resuspended in PBS. 50 µl cell suspension was mixed with 50 µl 0.4% trypan blue and loaded into a haemocytometer for counting. The amount of blue cells and total cells were counted and results were expressed as the percentage (%) of viable cells. A

minimum of three counts per treatment group of at least 3 independent experiments was done. A complete step by step protocol for Trypan blue assay is reproduced in Appendix A (p 107).

3.4.3 Caspase 3/7 activity assay

The Caspase-3/7 activity was measured in MDA-MB231 cells using the Caspase-Glo® 3/7 assay (Promega, Madison, WI, USA). MDA-MB231 cells were randomly divided into groups and seeded in 96-well micro titer plates (Greiner Bio One) at a seeding density of 5 000 cells per well. For the groups that needed transfection, the cells were reverse transfected during plating (Section 3.3.2, p 33). The cells were left to plate and grow in 100 µl growth medium per well and the experimental plan set out in Figure 3.3 was followed. Growth medium for all groups were changed and replaced with fresh growth medium before the indicated treatment (Section 3.3.1, p32) (Figure 3.3, p 34) started. The Caspase-Glo® 3/7 reagent was prepared and equilibrated at room temperature and mixed with the lyophilized substrate before the reconstituted working buffer reagent was stored at -20°C. The working buffer reagent was allowed to equilibrate to room temperature prior to use. The 96-well micro titer plate was also allowed to equilibrate to room temperature 10 minutes prior to the assay. 100 µl of working buffer reagent was then added to each well containing cells where after the plate was incubated in the dark at 22°C for one hour. The content of each well was transferred to a white-walled 96-well plate and the luminescence was measured using a luminometer.

3.4.4 Western blot analysis of Caspase 3 and Cleaved PARP

For Western blotting MDA-MB231 cells were randomly divided into groups and seeded in 6 well plates at a seeding density of 100 000 cells per well. For the groups that needed transfection, the cells were reverse transfected during plating (Section 3.3.2, p33). The cells

were left to plate and grow in 2 ml growth medium per well and the experimental plan set out in Figure 3.3 was followed. Growth medium for all groups were changed and replaced with fresh growth medium before the indicated treatment (Section 3.3.1, p 32) (Figure 3.3, p34) started. The treatment was administered straight into the medium at the correct concentration.

3.4.4.1 Protein extraction and quantification

After treatment of the groups as described in section 3.3.1, cells were drained and placed on ice. Cell monolayers were then rinsed three times with 1 ml cold PBS. Total cell protein was then extracted by incubating the cells for 5 minutes in 200 μ l of a modified radio-immuno precipitation (RIPA) buffer, pH 7.4, containing: 50 mM Tris-HCL, 1 mM EDTA, 1 mM phenylmethylsulfonyl fluoride (PMSF), 1 mM benzamidine, 4 μ g/ml SBTI-1, 1 μ g/ml leupeptin, 1% NP40, and 0.25% Na-deoxycholate. Adherent cells were then harvested from the culture dishes with a cell scraper and transferred to chilled eppendorfs tubes. Whole cell lysates were centrifuged at 4°C and 8000 rpm for 10 minutes. Lysates were then stored at -80°C and had their protein content determined the following day. Protein content was quantified using the Bradford protein determination method (Bradford. 1976), after the preparation of cell lysates. A complete step by step protocol for protein extraction and protein quantification by the Bradford method is included in Appendix A (p 113).

3.4.4.2 Sample preparation

Following protein quantification, aliquots containing 20 μ g of protein were prepared for each sample. Lysates were diluted in Laemmli sample buffer, boiled for 5 minutes and then centrifuged for 5 seconds. Laemmli sample buffer consists of 150 μ l mercaptoethanol and

850 µl of a sample buffer containing: 0.5 M Tris, pH 6.8, 10% SDS, 2.5 ml glycerol, 0.2 ml 0.5% bromophenol blue and distilled water. The prepared samples were stored at -80°C for future analysis by Western blotting. A complete step by step protocol for sample preparation is included in Appendix A.

3.4.4.3 SDS-PAGE and Western blot analysis

The prepared cell lysates were separated on 10% polyacrylamide gels by sodium dodecyl sulphate polyacrylamide gel electrophoresis (SDS-PAGE). For the determination of the molecular weights of specific bands 7.5 µl of a protein marker ladder (peqGold) was loaded in the left most well of each gel. This was also done for orientation purposes. Samples, previously prepared, were boiled for 5 minutes before 20 µg of protein was loaded into each well. Gels ran for an initial 10 minute run at 100 V and 400 mA, followed by 50 minutes at 200 V and 400 mA (Mini Protean System, Bio-Rad, Hercules). Following SDS-PAGE, proteins were transferred to polyvinylidene fluoride (PVDF) membranes (Immoblin-P, Millipore) using a semi-dry electrotransfer system (Bio-Rad, USA) for 60 min at 15 V and 0.5 A. Membranes were blocked in 5% (w/v) fat-free milk in 0.1% Tris Buffered Saline-Tween20 (TBS-T) for 1 hour at room temperature with gentle agitation, in order to prevent non-specific binding. Membranes were then incubated overnight at 4°C with specific primary antibodies against caspase 3 (Cell Signalling, MA, USA) and cleaved PARP (Cell Signalling, MA, USA) (Table 2) diluted in TBS-T (1:1000). On the next day, membranes were washed 3 times in TBS-T with each wash lasting 5 minutes. After washing, membranes were incubated in anti-rabbit horseradish peroxidase-conjugated secondary antibody (Amersham Biosciences, UK, and Dako Cytomation, Denmark) for 1 hour at room temperature with gentle agitation. Following the incubation period, membranes were washed a further three times in TBS-T with each wash lasting 5 minutes. Antibodies were detected using the ECL detection Kit (Bio Vision Inc.) and

bands were exposed to CL-Xposure (Thermo Scientific) X-ray film. Following exposure the membranes were washed 3 times with distilled H₂O and stripped by washing with 0.2 M NaOH followed by another wash with distilled H₂O. Each wash lasted 5 minutes. Stripped membranes were blocked in 5% (w/v) fat-free milk in 0.1% TBS-T for 1 hour at room temperature with gentle agitation, in order to prevent non-specific binding. Membranes were then incubated overnight at 4°C with a specific primary antibody against β -actin (Cell Signalling, MA, USA) diluted in TBS-T (1:1000). On the next day the same procedure for secondary antibody incubation and band exposure was followed as previously mentioned. Exposed bands were quantified by densitometry using the UN-SCAN-IT© densitometry software (Silk Scientific Corporation, Utah, USA). Bands were expressed as optical density readings relative to the untreated control present on the same blot. A complete step by step protocol for SDS-PAGE and Western blot analysis is included in Appendix A (115).

Table 2: Antibodies used in Western blot analysis and the thickness of the polyacrylamide gel that was used.

| Antibody | Size (kD) | Gel thickness |
|--------------|-----------|---------------|
| caspase 3 | 35 kD | 1 mm |
| cleaved PARP | 89 kD | 1 mm |

3.5 Determination of MKP-1 expression

The protocol for the Western blot analysis performed in this section is described in the materials and methods section (section 3.4.4, p 37). 100 000 MDA-MB231 cells were plated into 6-well cell culture plates prior to treatment. For the groups that needed transfection, the cells were reverse transfected during plating (Section 3.3.2, p 33). To determine the level of MKP-1 inhibition and induction, membranes were incubated overnight at 4°C with a specific

primary antibody against MKP-1 (Santa Cruz Biotechnology, CA, USA) (Table 3) diluted in TBS-T (1:1 000).

Table 3: Antibodies used in Western blot analysis and the thickness of the polyacrylamide gel that was used.

| Antibody | Size (kD) | Gel thickness |
|----------|-----------|---------------|
| MKP-1 | 40 kD | 1 mm |

3.6 Determination of autophagic induction

3.6.1 Flow cytometry

This technique was used to analyse the degree of autophagic induction in MDA-MB231 cells by staining with LysoTracker™red (Invitrogen™, USA). MDA-MB231 cells were randomly divided into groups and seeded in 6-well cell culture plates (Greiner Bio One) at a seeding density of 100 000 cells per well. For the groups that needed transfection, the cells were reverse transfected during plating (Section 3.3.2, p 33). The cells were left to plate and grow in 2 ml growth medium per well and the experimental plan set out in Figure 3.3 was followed. Growth medium for all groups were changed and replaced with fresh growth medium before the indicated treatment (Section 3.3.1, p 32) (Figure 3.3, p 34) started. The treatment was administered straight into the medium at the correct concentration. Following completion of the treatment protocol as described in section 3.3.1, the medium was drained and the cell monolayer was rinsed with warm sterile PBS. The medium from each well was drained into ten sterile 15 ml Falcon tubes (Greiner Bio One), labelled according to treatment. Cells were trypsinized for approximately 3 minutes or until they detached from the surface of the flask and each cell suspension was added to the appropriate 15 ml Falcon tube and centrifuged for 3 minutes at 1500 rpm. The supernatant was discarded and each pellet was re-suspended in 0.5 ml LysoTracker™red (Invitrogen™, USA) working solution (final concentration of 100 nmol/L made up in growth medium). The suspension was incubated for 15 minutes at 37°C and gently re-suspended before being filtered through a 50 µm nylon mesh into FACS tubes and analysed immediately on the flow cytometer. Analyses were performed on a FACSAria I flow cytometer (Becton Dickinson Biosciences, San Jose, CA) equipped with a 488 nm Coherent Sapphire solid state laser (13-20 mW), 633 nm JDS Uniphase HeNe air-cooled laser (10-20 mW) and 407 nm Point Source

Violet solid state laser (10-25 mW). For each sample, population information from a minimum of 10 000 events was acquired using FACSDiva Version 6.1 software. Data was expressed in arbitrary values as a percentage relative to the untreated control. A complete step by step protocol for flow cytometry is reproduced in Appendix A (p 110).

3.6.2 LysoTracker™ Stain

LysoTracker™ (Invitrogen™, USA) is a common stain that is used to detect autophagy. It stains autophagic vacuoles – double membrane structures that are produced in the cytoplasm – and on contact with LysoTracker™ it emits a red fluorescence. This method is a way of quantitatively confirming results obtained in flow cytometry with LysoTracker™. MDA-MB231 cells were randomly divided into groups and seeded in 8-well chambers (Greiner Bio One) at a seeding density of 3000 cells per well. For the groups that needed transfection, the cells were reverse transfected during plating (Section 3.3.2, p 33). The cells were left to plate and grow in 200 µl growth medium per well and the experimental plan set out in Figure 3.3 was followed. Growth medium for all groups were changed and replaced with fresh growth medium before the indicated treatment (Section 3.3.1, p 32) (Figure 3.3) started. The treatment was administered straight into the medium at the correct concentration. After treatment of the groups as described in section 3.3.1, the medium was drained and the cell monolayer was washed three times with warm sterile PBS. LysoTracker™ red (1 µl in 2 ml medium) (Invitrogen™, USA) was made up in growth medium and 200 µl growth medium/LysoTracker™ solution was added to each well which covered the entire monolayer. The cells were left to incubate for 5 minutes. Images were acquired directly after the incubation period using an Olympus Cell[^]R system attached to an IX-81 inverted fluorescence microscope equipped with an F-view-II cooled CCD camera (Soft Imaging Systems). Using a Xenon-Arc burner (Olympus Biosystems GMBH) as light source, images were excited with the

572 nm excitation filter. Emission was collected using a UBG triple band pass emission filter cube. Images were processed and background subtracted using the Cell[®] software. Images were taken of a minimum of three randomly chosen fields, of at least three independent experiments per treatment group and the degree of autophagy was detected by means of red stained autophagic vacuoles. A complete step by step protocol for LysoTracker™ staining is reproduced in Appendix A (p 109).

3.6.3 Western blot analysis of LC3 and p62

The protocol for the Western blot analysis performed in this section is described in Section 3.4.4 (p 37) of the Materials and Methods. 100 000 MDA-MB231 cells were plated into 6-well cell culture plates prior to treatment. For the groups that needed transfection, the cells were reverse transfected during plating (Section 3.3.2, p 33). For the determination of autophagic induction, membranes were incubated overnight at 4°C with specific primary antibodies against LC3 (Cell Signalling, MA, USA) and p62 (Cell Signalling, MA, USA) (Table 4) diluted in TBS-T (1:1 000).

Table 4: Antibodies used in Western blot analysis and the thickness of the polyacrylamide gel that was used.

| Antibody | Size (kD) | Gel thickness |
|----------|-----------|---------------|
| LC-3 | 17 kD | 1 mm |
| p62 | 62 kD | 1 mm |

3.7 In-vivo mouse model

3.7.1 Study design

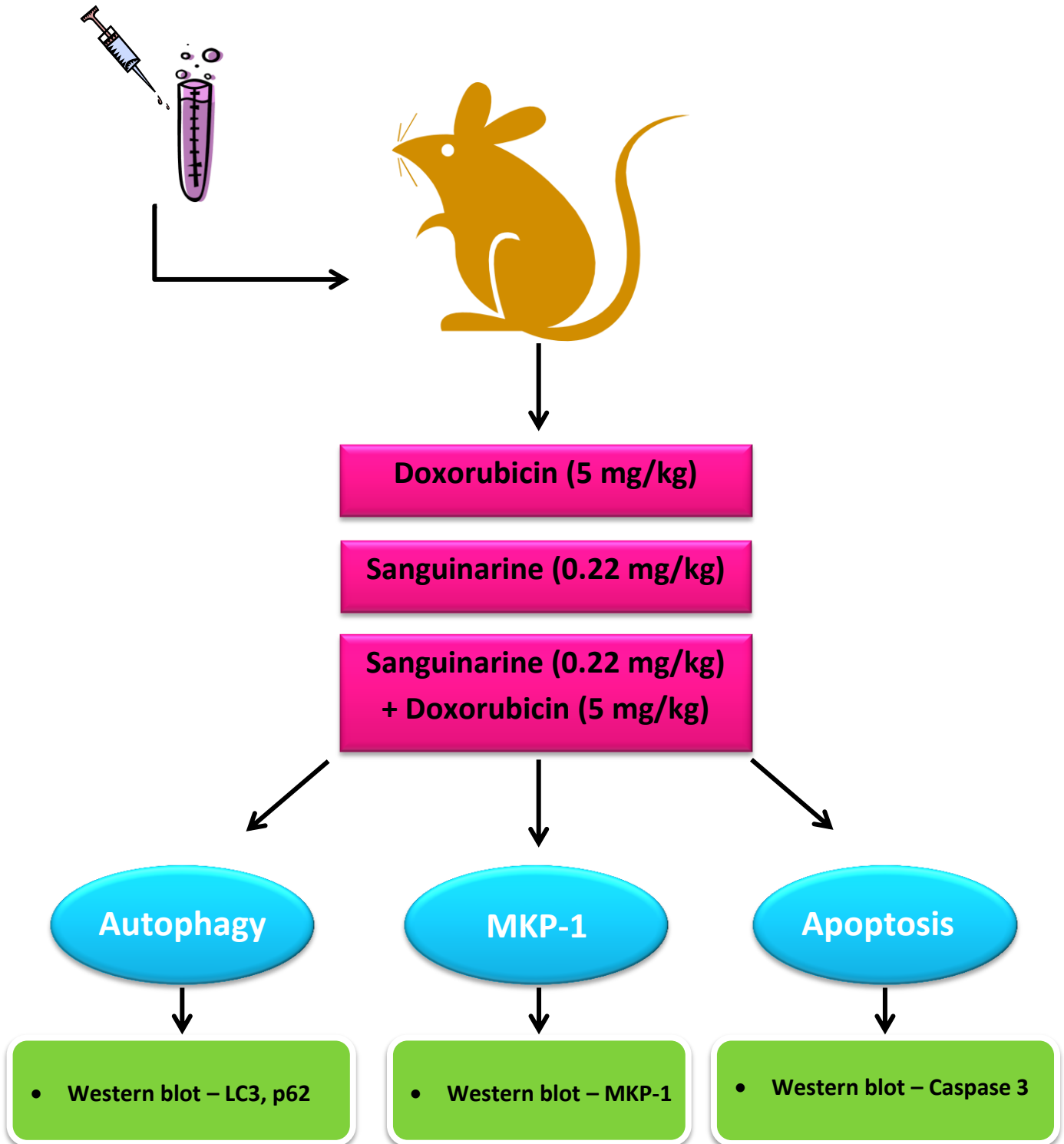


Figure 3.4: Study design: Eight week-old female C57BL6 mice were inoculated with 2.5×10^5 E0771 cells. Tumours were left to grow for 3 weeks before intervention started. Mice were treated with doxorubicin and an MKP-1 inhibitor, sanguinarine. Autophagy and apoptosis was detected by means of western blotting. MKP-1 expression was also detected by western blot.

3.7.2 Experimental protocol

This mouse model was established by a member of our Research group and the protocol was adapted from Ewens *et al.* 2006. The protocols in this study were carried out according to the guidelines for the care and use of laboratory animals implemented at Stellenbosch University. Eight week-old female C57BL6 mice (Stellenbosch University animal facility) were used in this study. Mice were inoculated subcutaneously with 2.5×10^5 E0771 cells suspended in 200 μ l Hanks balanced salt solution (Sigma Chemical Co., St Louis, MO, USA) on the left pad of the fourth mammary gland, using a 23-gauge needle (Figure 3.6). The E0771 cell line is a murine metastatic mammary adenocarcinoma cell line and was generously provided by Fengzhi Li (Roswell Park Cancer Institute, Buffalo, New York, USA). The experimental plan set out in Figure 3.5 was followed.

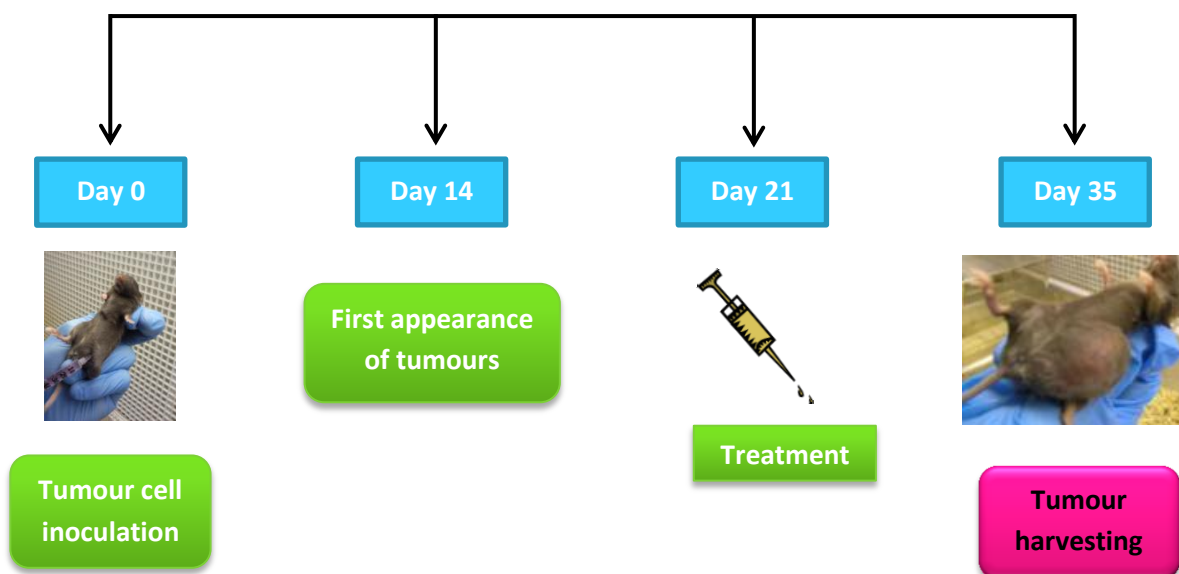


Figure 3.5: Experimental plan for *in vivo* study. Mice were injected with E0771 breast tumour cells on day 0. Tumours started to appear on day 14 after inoculation and doxorubicin and sanguinarine treatment started on day 21. Treatment was given over a course of 14 days after which the mice were sacrificed and the tumours harvested on day 35.

3.7.3 Treatment

Intervention consisted of 4 intraperitoneal injections of doxorubicin (5 mg/kg) and sanguinarine (0.22 mg/kg) dissolved in Hanks balanced salt solution (Sigma Chemical Co., St Louis, MO, USA) given over a course of 14 days. Tumour size was monitored immediately before each treatment injection by making measurements in two perpendicular dimensions parallel with the surface of the mice using digital callipers. The body weight of the mice was monitored at the same time. Mice were sacrificed on day 35 and whole excised tumours were snap-frozen in liquid nitrogen and then stored at -80°C.

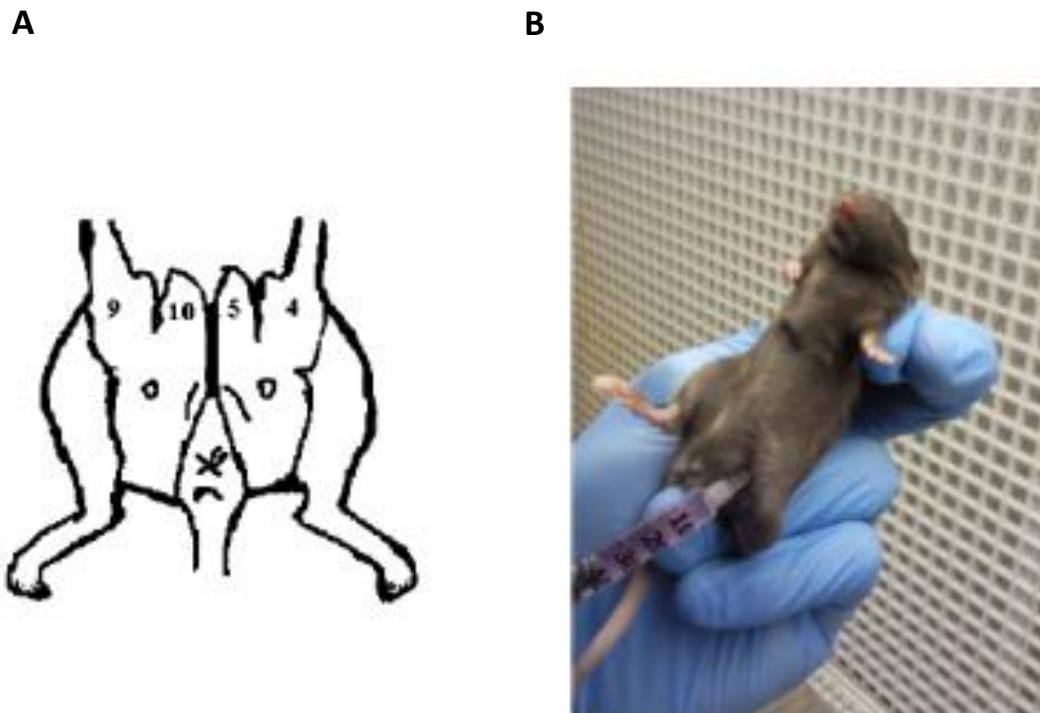


Figure 3.6: 200 μ l E0771 cell suspension was injected subcutaneously into mammary fat pad no.4. (A) Illustration portraying positions of mammary fat pads 4, 5, 10 and 9. (B) Subcutaneous injection with E0771 cell suspension. Protocol adapted from Ewens *et al.* 2006.

3.7.4 Western blot analyses of autophagy, apoptosis and MKP-1

3.7.4.1 Protein extraction and quantification

Frozen samples were allowed to thaw and homogenized in modified RIPA buffer (Appendix A, p 110) on ice before being centrifuged at 4°C and 8 000 rpm for 10 minutes. The protein content was determined using the Bradford protein determination method (Bradford. 1976), after the preparation of lysates. A complete step by step protocol for protein extraction and protein quantification by the Bradford method is included in Appendix A (p 113).

3.7.4.2 Sample preparation

Following protein quantification, aliquots containing 20 µg of protein were prepared for each sample. Lysates were diluted in Laemmli sample buffer, boiled for 5 minutes and then centrifuged for 5 seconds. Laemmli sample buffer consists of 150 µl mercaptoethanol and 850 µl of a sample buffer containing: Tris 0.5 M, pH 6.8, 10% SDS, 2.5 ml glycerol, 0.2 ml 0.5% bromophenol blue and distilled water.

3.7.4.3 SDS-PAGE and Western blot analysis

The protocol for the Western blot analysis set out in section 3.4.4 (p 37) of Materials and Methods was performed and membranes were incubated overnight at 4°C with specific primary antibodies against caspase 3 (Cell Signalling, MA, USA), cleaved PARP (Cell Signalling, MA, USA), MKP-1 (Santa Cruz Biotechnology, CA, USA), LC-3 (Cell Signalling, MA, USA), p62 (Cell Signalling, MA, USA) and β-actin (Cell Signalling, MA, USA) diluted in TBS-T (1:1000).

3.8 Statistical analysis

Controls were normalized and all values were expressed as a percentage of the untreated control. Results are presented as mean \pm Standard Error of the Mean (SEM). Comparisons between different groups were made by one-way analysis of variance (ANOVA), followed by the Bonferroni post-hoc test. Statistical analyses were performed using Graphpad Prism version 5.01 (Graphpad Software, Inc, CA, USA) and a value of $p < 0.05$ was considered statistically significant.

Chapter 4:

Results

4.1 Determination of cell death

The first aim of the research was to determine whether MKP-1 inhibition can sensitise breast cancer cells to doxorubicin treatment. To determine the effect of MKP-1 induction and inhibition in combination with doxorubicin treatment on cell death in MDA-MB231 cells, four techniques were employed. a) Trypan blue assay, b) Caspase-Glo® 3/7 assay, c) Western blots and d) Hoechst 33342 staining technique (Fluorescence microscopy). Three independent experiments were carried out for accuracy and repeatability.

4.1.1 Trypan blue assay

Based on an initial dose response experiment, 5 μ M doxorubicin treatment for 24 hours showed a significant ($p < 0.05$) decrease in cell death compared to the control.

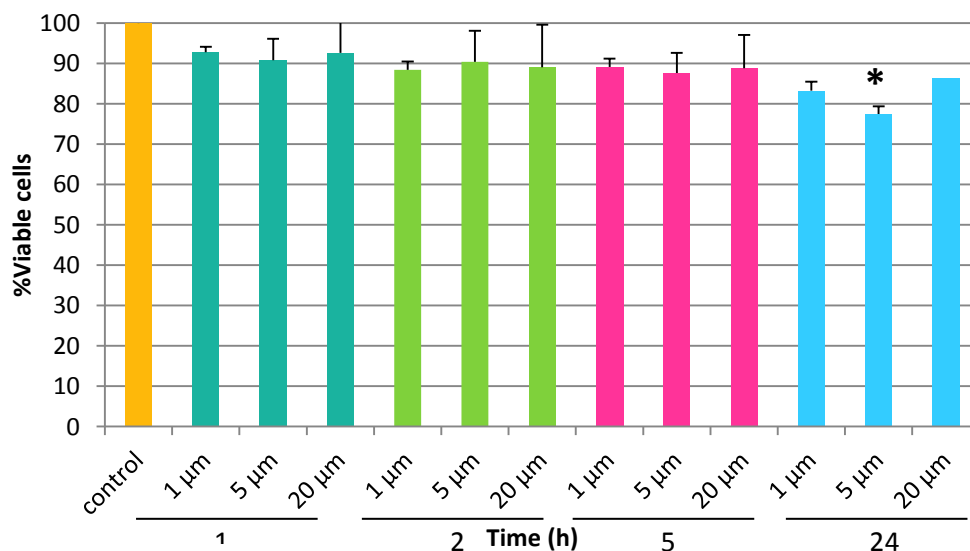


Figure 4.1: The effect of treatment with doxorubicin on cell death induction in MDA-MB231 cells. MDA-MB231 cells were seeded at a high seeding density and treated with doxorubicin at different concentrations over time. Cells were stained with Trypan blue, viable and non-viable cells were counted using a haemocytometer. Results are presented as means \pm SEM (n=3). * $p < 0.05$ vs control

To assess the viability of MDA-MB231 cells after a 24 hour treatment period, the trypan blue exclusion assay was used. The assay is based on the principal that viable cells will be able to exclude the blue dye from entering the cell, whilst non-viable cells are unable to prevent its entrance into the cytoplasm. Doxorubicin treatment showed a highly significant ($p < 0.001$) decrease in cell viability compared to the control group (Figure 4.2). Dexamethasone treatment alone had no effect with no significant decrease in cell viability compared to the control group.

There was a significant ($p < 0.001$) increase in cell viability in the cells treated with dexamethasone in combination with doxorubicin when compared to doxorubicin treatment alone.

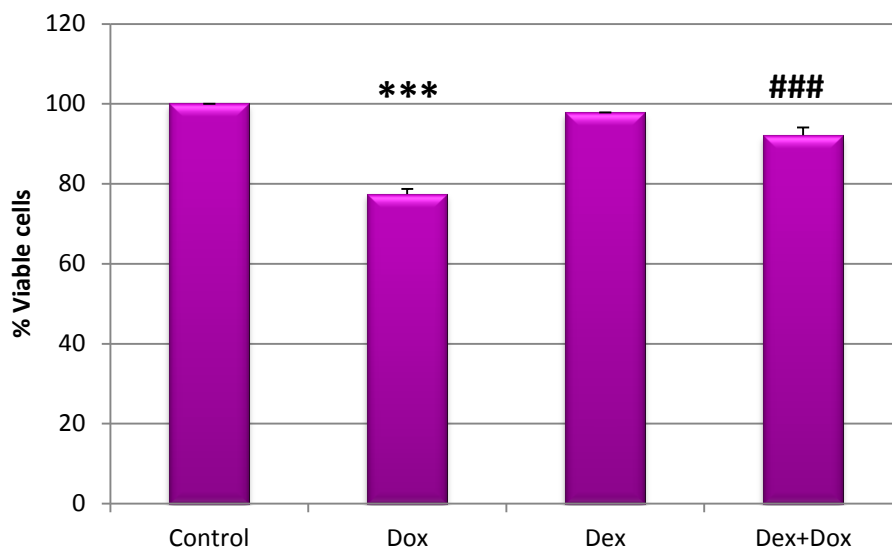


Figure 4.2: The effect of treatment with dexamethasone in conjunction with doxorubicin on cell death induction in MDA-MB231 cells. MDA-MB231 cells were seeded at a high seeding density and treated with dexamethasone (100 nM) and doxorubicin (5 μ M) for 24 hours. Cells were stained with trypan blue, viable and non-viable cells were counted using a haemocytometer. Results are presented as means \pm SEM (n=3). *** $p < 0.001$ vs control, ### $p < 0.001$ vs doxorubicin

Treatment with Doxorubicin alone decreased cell viability significantly ($p < 0.001$) in MDA-MB231 cells. Sanguinarine treatment only showed a small insignificant decrease in cell viability compared to the control group (Figure 4.3). A statistically significant decrease in cell viability was also observed during treatment with Doxorubicin under conditions of MKP-1 inhibition. Here a significant ($p < 0.001$) decrease in cell viability was observed in the group treated with doxorubicin in combination with sanguinarine when compared to doxorubicin treatment alone.

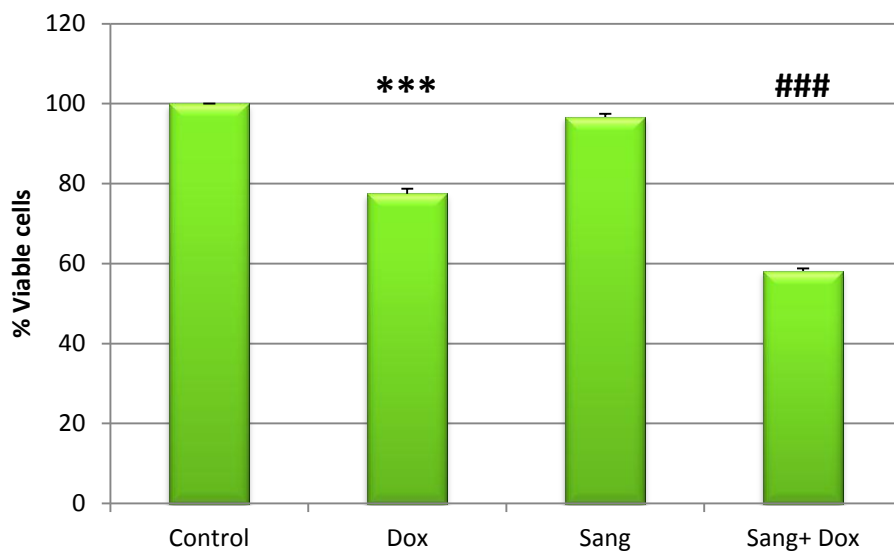


Figure 4.3: The effect of treatment with sanguinarine in conjunction with doxorubicin on cell death induction in MDA-MB231 cells. MDA-MB231 cells were seeded at a high seeding density and treated with sanguinarine (0.5 μM) and doxorubicin (5 μM) for 24 hours. Cells were stained with trypan blue and viable and non-viable cells were counted using a haemocytometer. Results are presented as means \pm SEM ($n=3$). *** $p < 0.001$ vs control, ### $p < 0.001$ vs doxorubicin

5 μM Doxorubicin treatment significantly ($p < 0.001$) reduced cell viability compared to the control. Treatment with MKP-1 siRNA revealed no significant decrease in cell viability when compared to the control (Figure 4.4). A significant ($p < 0.01$) decrease in cell viability was observed with doxorubicin treatment in conjunction with MKP-1 siRNA compared to doxorubicin treatment alone.

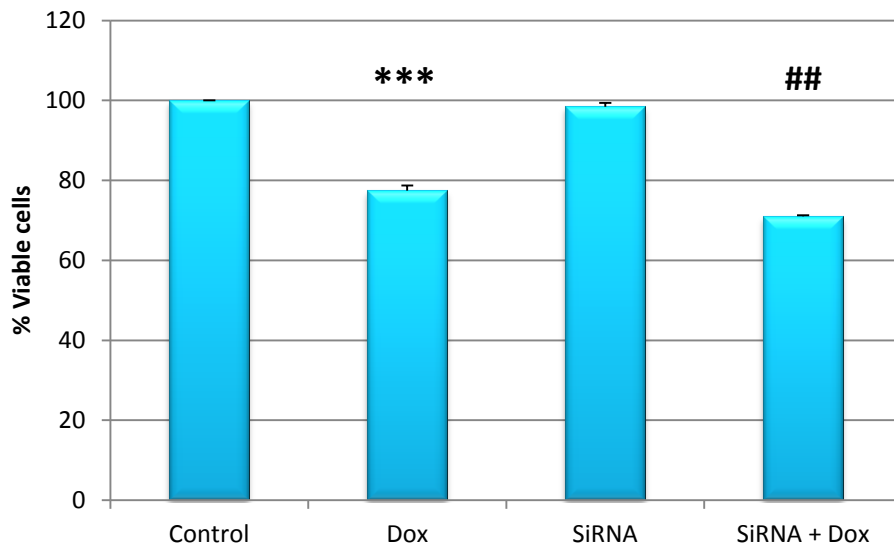


Figure 4.4: The effect of MKP-1 siRNA in conjunction with doxorubicin on cell death induction in MDA-MB231 cells. MDA-MB231 cells were seeded at a high seeding density, MKP-1 was silenced via reverse transcription and cells were treated with doxorubicin (5 μM) for 24 hours. Cells were stained with trypan blue and viable and non-viable cells were counted using a haemocytometer. Results are presented as means \pm SEM (n=3). *** $p < 0.001$ vs control, ## $p < 0.01$ vs doxorubicin

4.1.2 Caspase 3/7 activity assay

The Caspase-Glo® 3/7 assay was used to determine the caspase 3/7 activity in MDA-MB231 cells following treatment. This assay is luminescent assay that provides an extremely sensitive means of monitoring caspase 3/7 activation. Following treatment with 5 µM doxorubicin, a significant ($p < 0.001$) increase in caspase 3/7 cleavage was observed compared to the control (Figure 4.5). Dexamethasone and vehicle treatments had no effect on caspase 3/7 cleavage compared to the control.

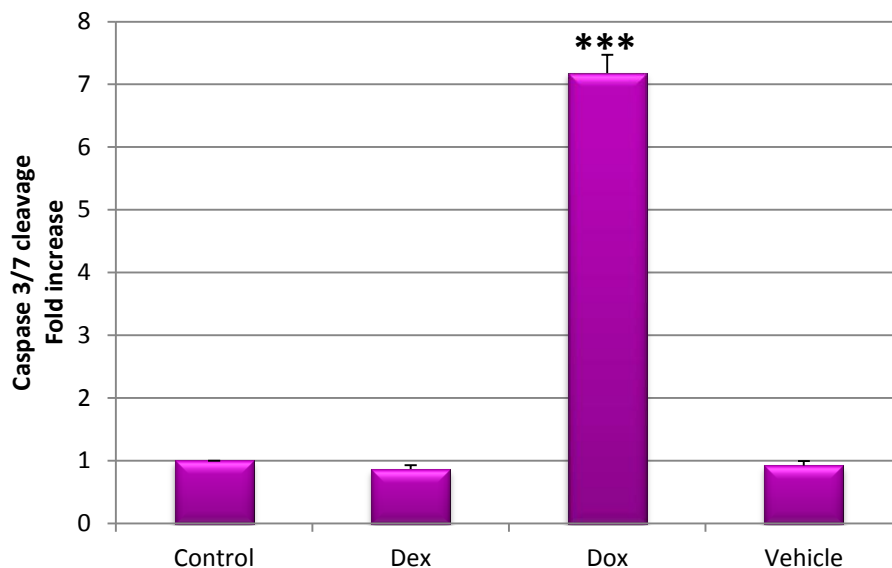


Figure 4.5: The effect of treatment with dexamethasone in conjunction with doxorubicin on caspase 3/7 activity in MDA-MB231 cells. MDA-MB231 cells were seeded at a high seeding density and treated with dexamethasone (100 nM) and doxorubicin (5 µM) for 24 hours. The caspase 3/7 activity was measured using the Caspase-Glo® 3/7 assay. Results are presented as means \pm SEM (n=4). *** $p < 0.001$ vs control

Doxorubicin treatment significantly ($p < 0.001$) increased caspase 3/7 cleavage. Sanguinarine treatment alone had no effect on caspase 3/7 cleavage compared to the control (Figure 4.6). Under conditions of MKP-1 inhibition in combination with doxorubicin treatment there was an increase in caspase 3/7 activity. This was seen in the cells treated with doxorubicin in combination with sanguinarine where a significant ($p < 0.001$) increase in caspase 3/7 cleavage was found compared to doxorubicin treatment alone.

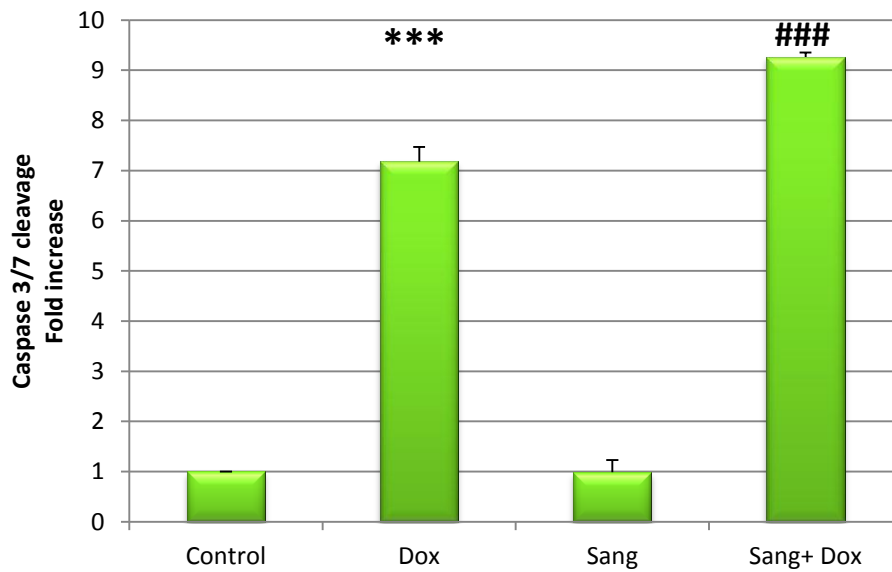


Figure 4.6: The effect of sanguinarine in conjunction with doxorubicin on caspase 3/7 activity in MDA-MB231 cells. MDA-MB231 cells were seeded at a high seeding density and treated with sanguinarine (0.5 μM) and doxorubicin (5 μM) for 24 hours. The caspase-3/7 activity was measured using the Caspase-Glo[®] 3/7 assay. Results are presented as means \pm SEM (n=4). *** $p < 0.001$ vs control, ### $p < 0.001$ vs doxorubicin

MKP-1 siRNA had little effect on caspase 3/7 cleavage with no significant increase compared to the control (Figure 4.7). Negative siRNA had no significant effect on caspase 3/7 cleavage compared to the control.

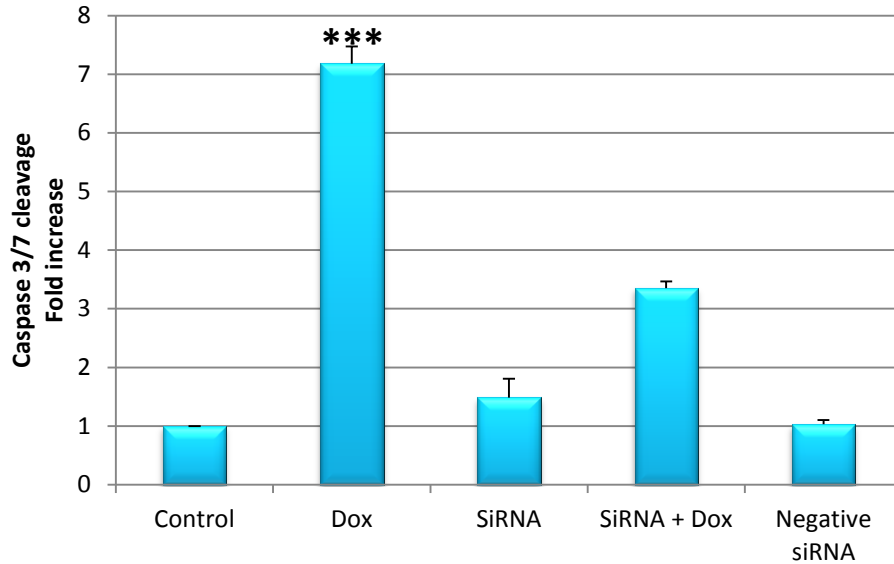


Figure 4.7: The effect of MKP-1 siRNA in conjunction with doxorubicin on the caspase 3/7 activity in MDA-MB231 cells. MDA-MB231 cells were seeded at a high seeding density, MKP-1 was silenced via reverse transcription and cells were treated with doxorubicin (5 μ M) for 24 hours. The caspase-3/7 activity was measured using the Caspase-Glo[®] 3/7 assay. Results are presented as means \pm SEM (n=4). *** p < 0.001 vs control

4.1.3 Western blot analysis

4.1.3.1 Total caspase 3

Caspase-3 is activated by both the intrinsic and extrinsic pathway in an apoptotic cell. Being an executioner caspase, it has no activity until it is cleaved and thereby activated by initiator caspases upon apoptotic signalling. Apoptotic activity was investigated in MDA-MB231 cells using Western blotting and probing for caspase 3.

Doxorubicin treatment presented with a significant ($p < 0.001$) decrease in total caspase 3 levels compared to the control (Figure 4.8). Furthermore, significance was noted under conditions of MKP-1 inhibition in combination with doxorubicin treatment. Here a significant ($p < 0.001$) decrease in total caspase 3 was seen in groups treated with sanguinarine and MKP-1 siRNA in combination with doxorubicin treatment compared to doxorubicin treatment alone.

During dexamethasone treatment in combination with doxorubicin a decrease in caspase 3 was also observed. This decrease was however significantly ($p < 0.01$) higher compared to doxorubicin treatment alone. Dexamethasone ($p < 0.01$) and MKP-1 siRNA ($p < 0.05$) significantly increased caspase 3 expression compared to the control. Sanguinarine treatment showed no significant increase in caspase 3 compared to the control.

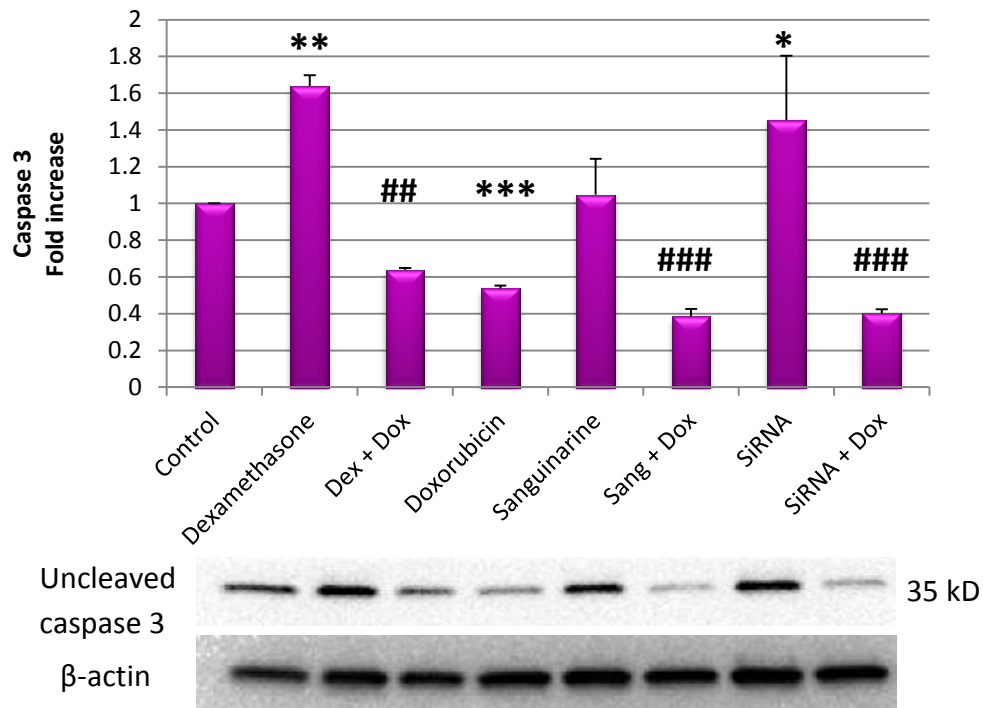


Figure 4.8: The effect of 24 hour doxorubicin treatment together with MKP-1 inhibitors and inducers on caspase 3 expression in MDA-MB231 cells. MDA-MB231 cells were seeded at a high seeding density and treated with dexamethasone (100 nM), doxorubicin (5 μ M) and sanguinarine (0.5 μ M) for 24 hours. MKP-1 was silenced via reverse transfection. Results are presented as means \pm SEM (n=3). * p < 0.05 vs control, ** p < 0.01 vs control, *** p < 0.001 vs control, ## p < 0.01 vs doxorubicin, ### p < 0.001 vs doxorubicin

4.1.3.2 Cleaved PARP

To confirm the results obtained from caspase 3 western blots, the membranes were also probed for cleaved PARP. Following treatment, PARP cleavage increased significantly ($p < 0.001$) in MDA-MB231 cells treated with doxorubicin compared to the control (Figure 4.9). Treatment with doxorubicin in the presence of MKP-1 inhibition showed a substantial increase in PARP cleavage. Here the cells treated with doxorubicin in combination with MKP-1 siRNA revealed a significant ($p < 0.001$) increase in PARP cleavage compared to the control. The combination of MKP-1 induction (dexamethasone) together with doxorubicin treatment also increased PARP cleavage. The increase in PARP cleavage in the cells treated with dexamethasone in conjunction with doxorubicin was however less compared to both doxorubicin treatment and treatment with MKP-1 siRNA in conjunction with doxorubicin treatment.

The combination of sanguinarine and doxorubicin also increased PARP cleavage compared to the control, but PARP cleavage was significantly ($p < 0.05$) reduced compared to doxorubicin treatment. Dexamethasone, sanguinarine, MKP-1 siRNA, negative siRNA and vehicle treated groups had no significant effect on PARP cleavage compared to the control.

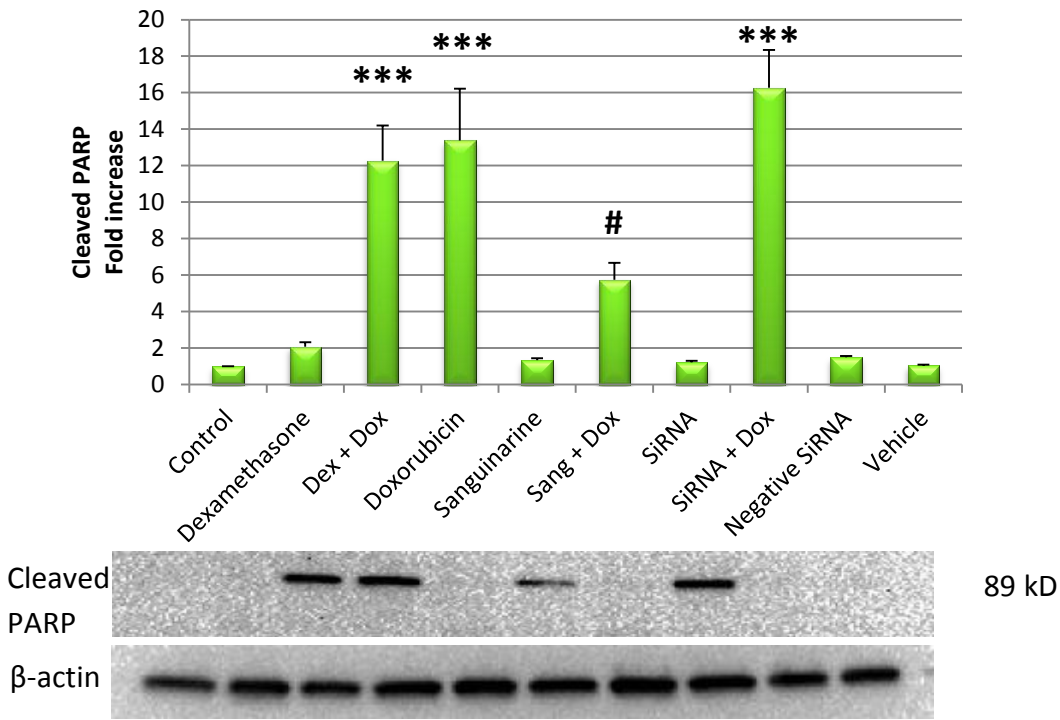
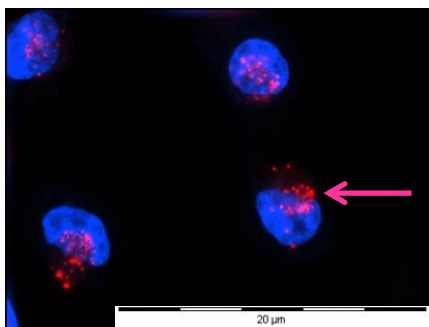


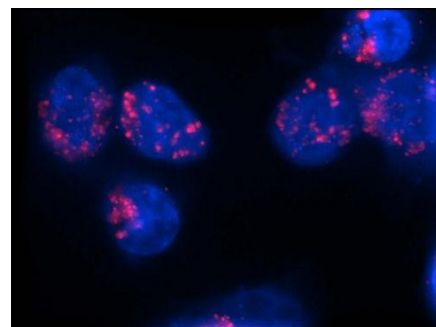
Figure 4.9: The effect of 24 hour doxorubicin treatment together with MKP-1 inhibitors and inducers on cleaved PARP expression in MDA-MB231 cells. MDA-MB231 cells were seeded at a high seeding density and treated with dexamethasone (100 nM), doxorubicin (5 μ M) and sanguinarine (0.5 μ M) for 24 hours. MKP-1 was silenced via reverse transfection. Results are presented as means \pm SEM (n=3). *** p < 0.001 vs control, # p < 0.05 vs doxorubicin

4.2 LysoTracker™ and Hoechst 33342 stain

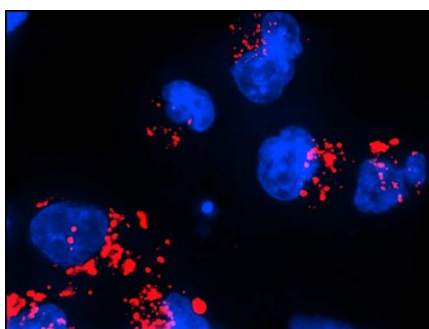
To qualitatively assess the effect of MKP-1 inhibition on the lysosomal compartment and cell death, we investigated morphological changes that signify apoptosis as well as the volume of the acidic compartment by staining MDA-MB231 cells with Hoechst 33342 and LysoTracker™ red respectively. Images taken revealed an increase in the size and number of acidic vesicles in response to sanguinarine or MKP-1 siRNA therapy as well as in cells treated with both sanguinarine and doxorubicin or MKP-1 siRNA and doxorubicin (Figure 4.10). An increase in cell death (pyknosis and apoptotic bodies) was also observed in the groups treated with dexamethasone and doxorubicin or MKP-1 siRNA and doxorubicin and the highest degree of cell death was seen in the cells treated with sanguinarine in combination with doxorubicin.



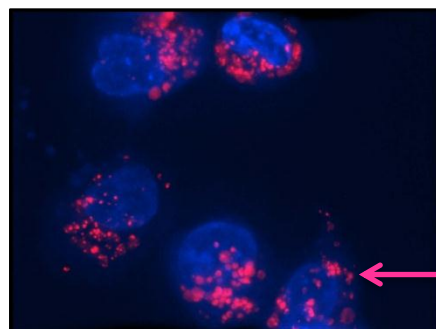
Control



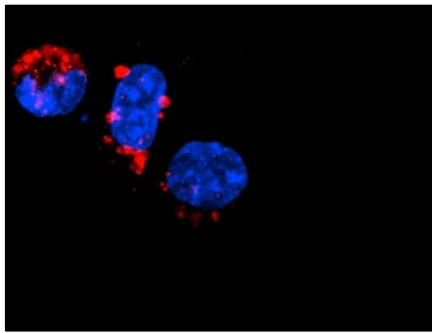
Doxorubicin



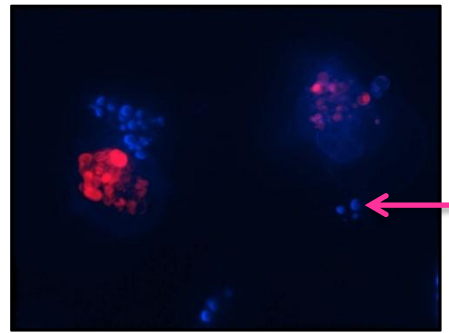
Dexamethasone



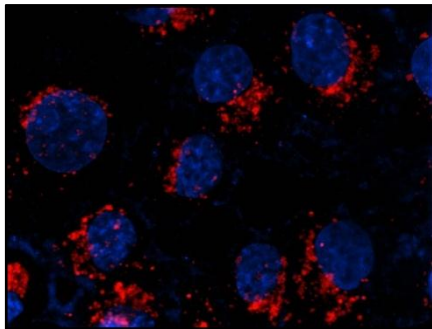
Dexamethasone + Doxorubicin



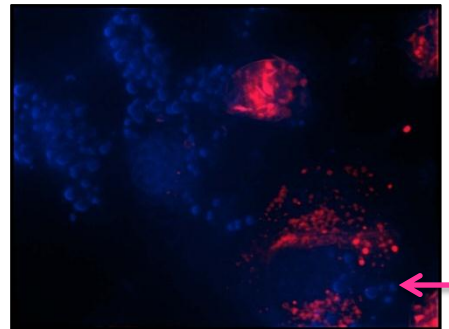
Sanguinarine



Sanguinarine + Doxorubicin



SiRNA



SiRNA + Doxorubicin

Figure 4.10: The effect of 24 hour doxorubicin treatment together with MKP-1 inhibitors and inducers on autophagy and apoptosis in MDA-MB231 cells. MDA-MB231 cells were seeded at a high seeding density and treated with dexamethasone (100 nM), doxorubicin (5 μ M) and sanguinarine (0.5 μ M) for 24 hours. MKP-1 was silenced via reverse transfection. MDA-MB231 cells were stained with Hoechst 33342 (blue) and LysoTracker™ red (red) and apoptosis and autophagy was scrutinized using fluorescence microscopy. The arrow indicates an apoptotic body (blue) and autophagic vacuoles (red).

4.3 MKP-1 expression in MDA-MB231 cells

MKP-1 expression was examined in MDA-MB231 cells by means of western blotting. 100 nM Dexamethasone treatment significantly ($p < 0.01$) increased MKP-1 expression in MDA-MB231 cells compared to the control (Figure 4.11). A significant decrease in MKP-1 expression was observed when MDA-MB231 cells were treated with 0.5 μ M sanguinarine ($p < 0.001$) and MKP-1 siRNA ($p < 0.05$) compared to the control. A significant ($p < 0.001$) decrease in MKP-1 was also observed with combined sanguinarine and doxorubicin treatment when compared to the control.

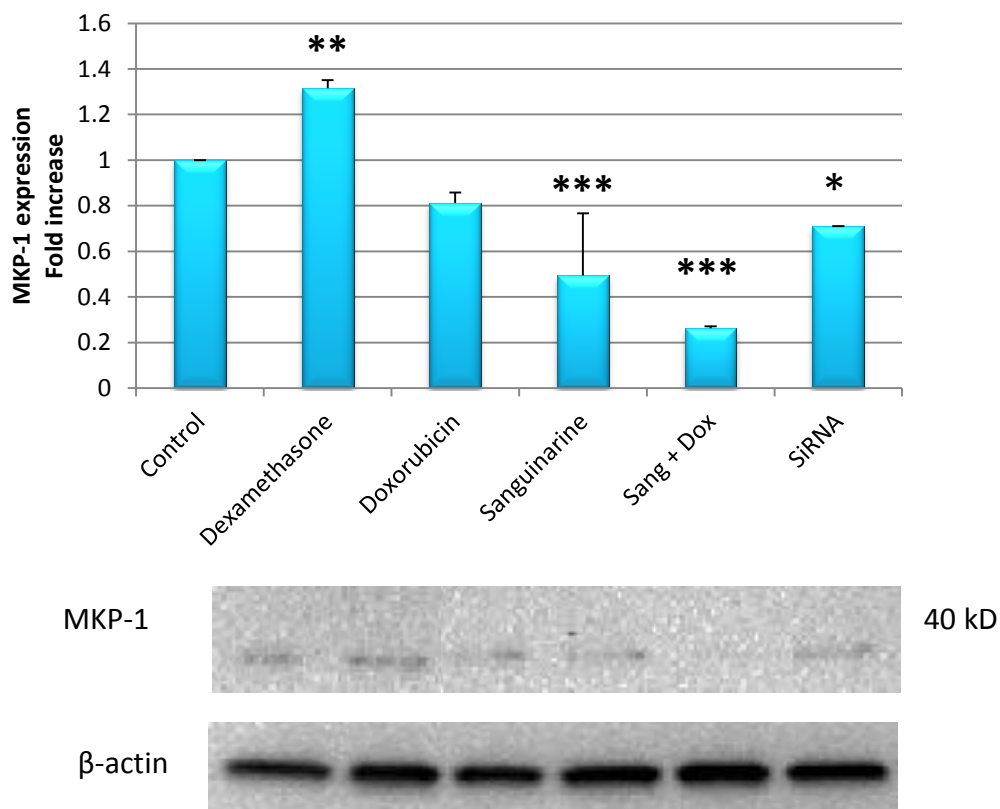


Figure 4.11: The effect of 24 hour doxorubicin treatment together with MKP-1 inhibitors and inducers on MKP-1 expression in MDA-MB231 cells. MDA-MB231 cells were seeded at a high seeding density and treated with dexamethasone (100 nM), doxorubicin (5 μ M) and sanguinarine (0.5 μ M) for 24 hours. MKP-1 was silenced via reverse transfection. Results are presented as means \pm SEM (n=3). * $p < 0.05$ vs control, ** $p < 0.01$ vs control, *** $p < 0.001$ vs control

4.4 Determination of autophagic induction in MDA-MB231 cells

The first aim of this research was to determine whether MKP-1 inhibition can sensitize breast cancer cells to doxorubicin treatment. The second aim was to determine the role of autophagy in this scenario in MDA-MB231 cells. Three techniques were used; flow cytometry, western blotting and LysoTracker™ red staining (fluorescence microscopy). Three independent experiments were conducted for accuracy and reproducibility.

4.4.1 Flow cytometry

To assess the degree of autophagy induction in MDA-MB231 cells following treatment, cells were stained with LysoTracker™ red, and the mean fluorescence intensity was analysed using flow cytometry. Treatment with 5 μ M doxorubicin significantly ($p < 0.05$) increased autophagy compared to the control (Figure 4.12). Dexamethasone treatment, a known MKP-1 inducer, had no effect with a negligible increase in autophagy induction compared to the control. The combination of dexamethasone and doxorubicin also showed a significant ($p < 0.05$) increase in autophagy induction compared to the control; however this had the same effect as doxorubicin treatment alone.

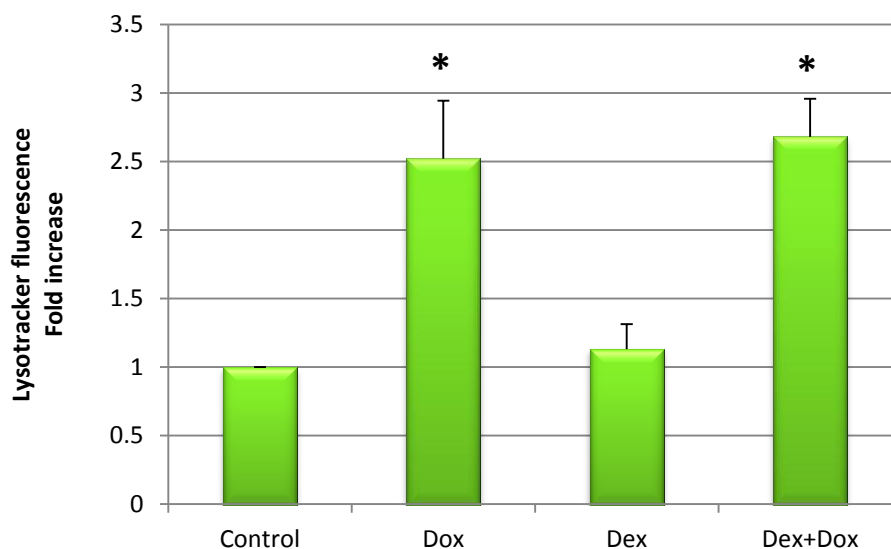


Figure 4.12: The effect of treatment with dexamethasone in conjunction with doxorubicin on the degree of autophagic induction in MDA-MB231 cells. MDA-MB231 cells were seeded at a high seeding density and treated with dexamethasone (100 nM) and doxorubicin (5 μ M) for 24 hours. Cells were stained with LysoTracker™ red, and the mean fluorescence intensity was determined by flow cytometry. Results are presented as means \pm SEM (n=3). * $p < 0.05$ vs control

Treatment with doxorubicin alone significantly ($p < 0.05$) increased autophagic induction in MDA-MB231 cells. Sanguinarine treatment also showed an increase in autophagy but this increase was less compared to doxorubicin therapy alone and not statistically significant (Figure 4.13). An increase in autophagy was also observed during treatment with doxorubicin under conditions of MKP-1 inhibition. The substantial increase in autophagy observed in the group treated with doxorubicin in combination with sanguinarine when compared to both the control and doxorubicin treatment alone was however not statistically significant.

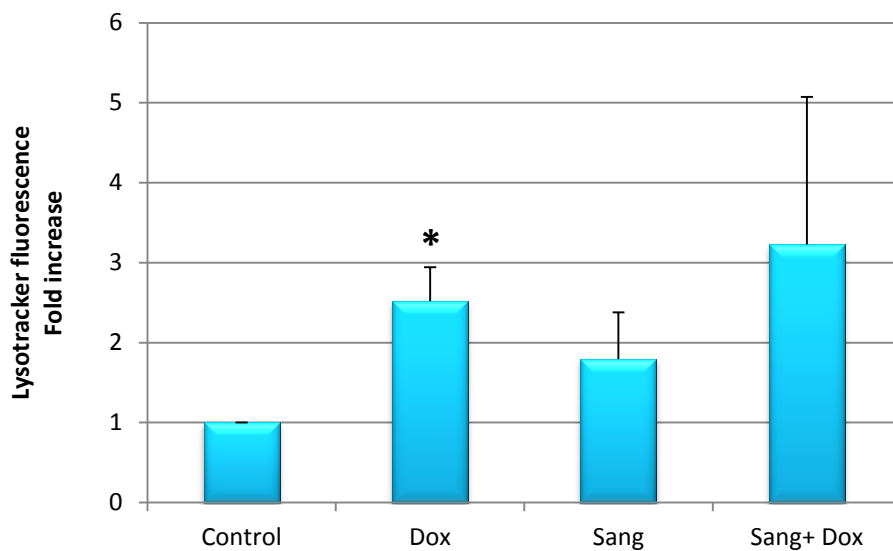


Figure 4.13: The effect of sanguinarine in conjunction with doxorubicin on the degree of autophagic induction in MDA-MB231 cells. MDA-MB231 cells were seeded at a high seeding density and treated with sanguinarine (0.5 μM) and doxorubicin (5 μM) for 24 hours. Cells were stained with LysoTracker™red and the mean fluorescence intensity was determined by flow cytometry. Results are presented as means \pm SEM ($n=3$). * $p < 0.05$ vs control

Treatment with MKP-1 siRNA showed no significant increase in autophagy induction compared to the control (Figure 4.14). A significant ($p < 0.05$) increase in autophagic induction was observed with doxorubicin treatment in conjunction with MKP-1 siRNA, however, this effect was similar as with doxorubicin treatment alone.

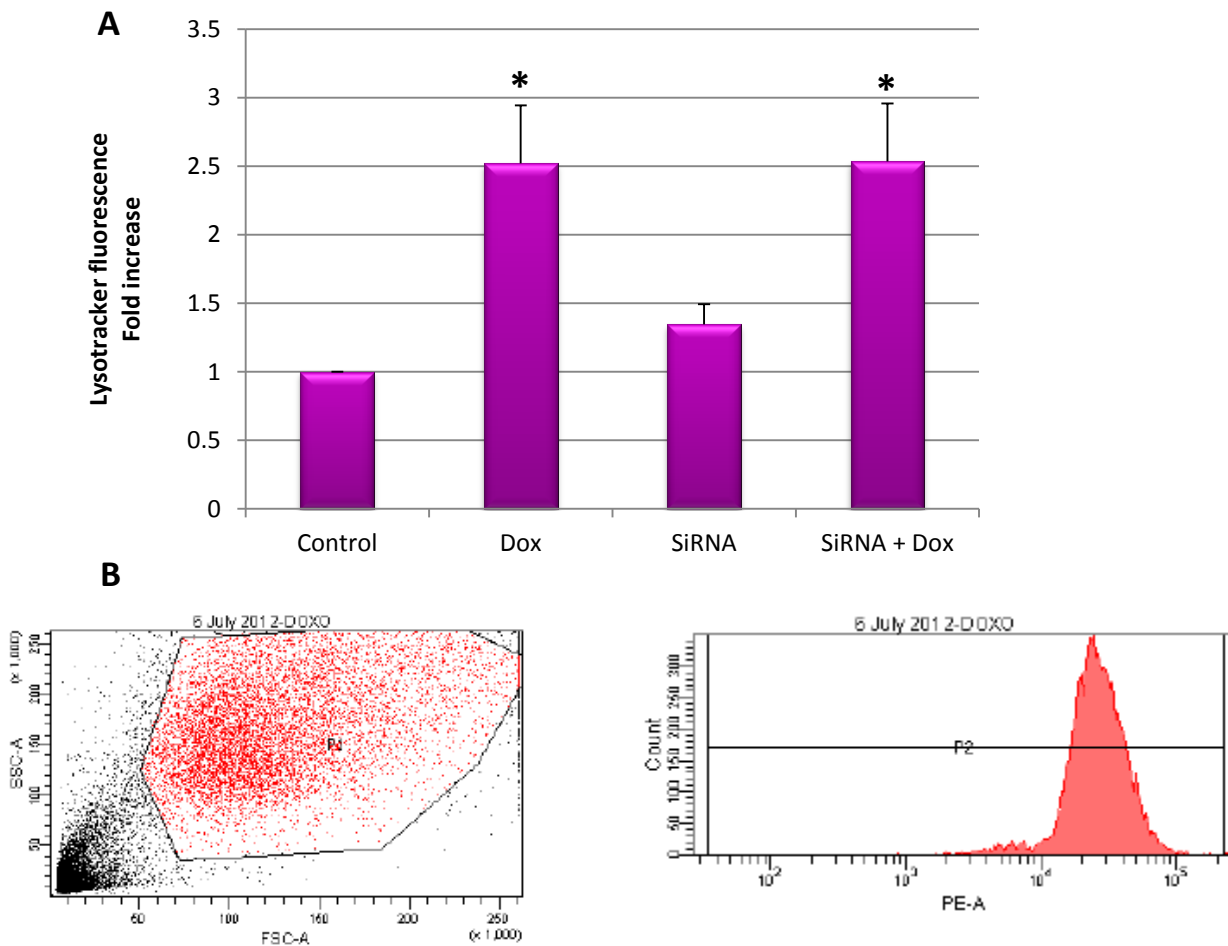


Figure 4.14: The effect MKP-1 siRNA in conjunction with doxorubicin on the degree of autophagic induction in MDA-MB231 cells. A) MDA-MB231 cells were seeded at a high seeding density, MKP-1 was silenced via reverse transcription and cells were treated with doxorubicin (5 μ M) for 24 hours. Cells were stained with LysoTracker™red and the mean fluorescence intensity was determined by flow cytometry. B) The scatterplot indicates how the gating was done and P2 shows the shift in doxorubicin treated cells. Results are presented as means \pm SEM (n=3). * $p < 0.05$ vs control

4.4.2 Western blot analysis

4.4.2.1 LC3

LC3 is used as one of the most common markers of autophagy. The conversion of LC3 I to LC3 II indicates increased autophagy activity in a cell.

Following treatment, elevated LC3 II expression was an indicator of increased autophagy in MDA-MB231 cells. LC3 II expression increased in all the treatment groups, except for siRNA and vehicle, when compared to the control (Figure 4.15). A significant ($p < 0.01$) increase in LC3 II expression was observed under conditions of MKP-1 inhibition where the cells were treated with doxorubicin in combination with sanguinarine.

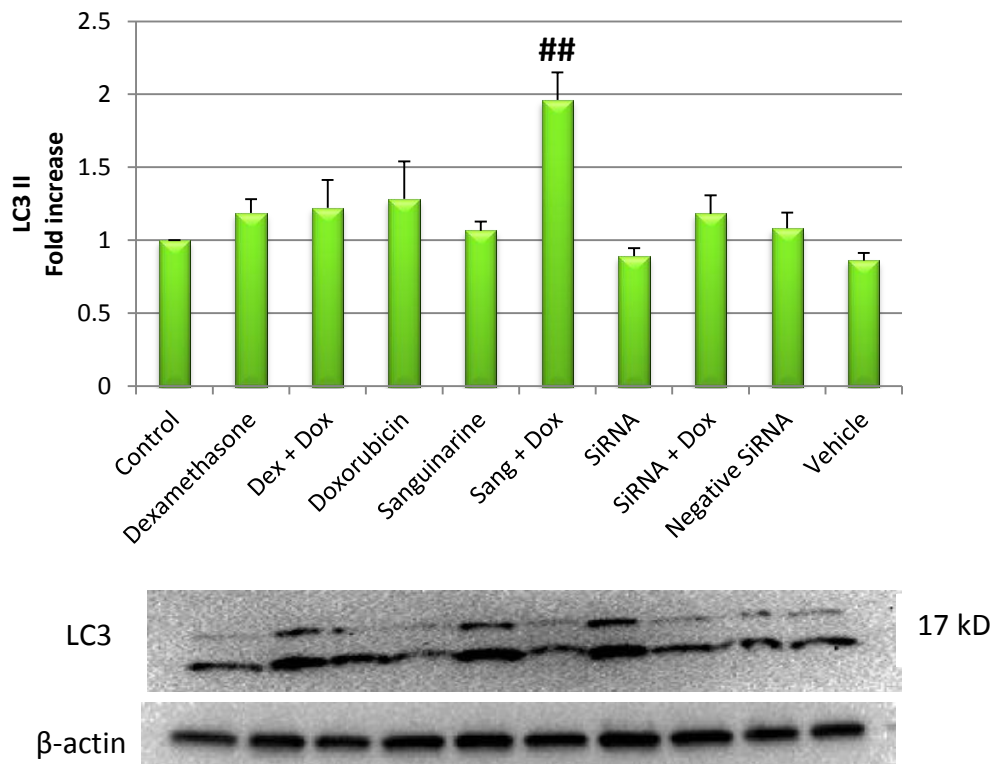


Figure 4.15: The effect of 24 hour doxorubicin treatment together with MKP-1 inhibitors and inducers on LC3 II expression in MDA-MB231 cells. MDA-MB231 cells were seeded at a high seeding density and treated with dexamethasone (100 nM), doxorubicin (5 μ M) and sanguinarine (0.5 μ M) for 24 hours. MKP-1 was silenced via reverse transfection. Results are presented as their means \pm SEM (n=3). ^{##} $p < 0.01$ vs doxorubicin.

4.4.2.2 p62

Another common marker of autophagy, p62, was used to confirm the results obtained from LC3 western blots. p62 is present in the autophagolysosome and its expression is decreased during high autophagic activity due to recycling.

Following treatment, decreased p62 expression was evident of increased autophagy in MDA-MB231 cells. Doxorubicin therapy decreased p62 expression compared to the control (Figure 4.16). Also, p62 expression was even further decreased under conditions of MKP-1 inhibition in combination with doxorubicin treatment. This was evident in the groups treated with sanguinarine in conjunction with doxorubicin and siRNA in conjunction with doxorubicin. The lowest p62 expression was observed in the cells treated with sanguinarine in combination with doxorubicin when compared to doxorubicin treatment alone. Although a trend was noticed these findings was not significant.

p62 was significantly increased in dexamethasone ($p < 0.001$) and sanguinarine ($p < 0.01$) treated groups compared to the control. MKP-1 siRNA treatment showed no significant changes compared to the control. Under conditions of MKP-1 induction in combination with doxorubicin treatment there was also an increase in p62 expression. This was evident in the cells treated with dexamethasone in combination with doxorubicin and the increase was larger compared to doxorubicin treatment alone, however it was not significant.

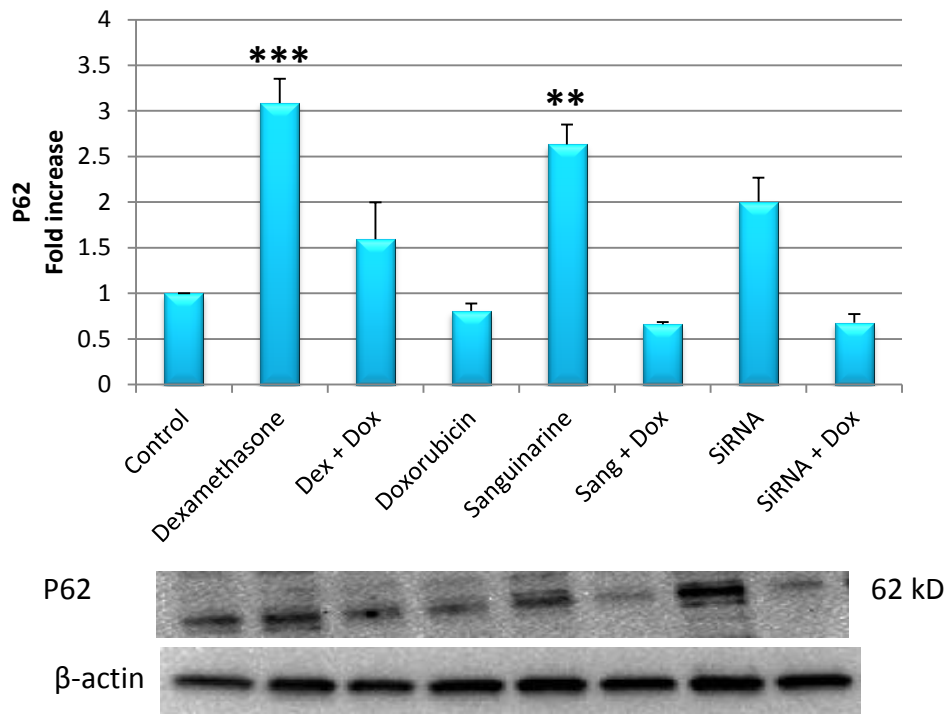


Figure 4.16: The effect of 24 hour doxorubicin treatment together with MKP-1 inhibitors and inducers on p62 expression in MDA-MB231 cells. MDA-MB231 cells were seeded at a high seeding density and treated with dexamethasone (100 nM), doxorubicin (5 μ M) and sanguinarine (0.5 μ M) for 24 hours. MKP-1 was silenced *via* reverse transfection. Results are presented as means \pm SEM (n=3). ** p < 0.01 vs control, *** p < 0.001 vs control

4.5 *In-vivo* Study

4.5.1 Tumour growth

Tumour volume increased over time for all treatment groups.

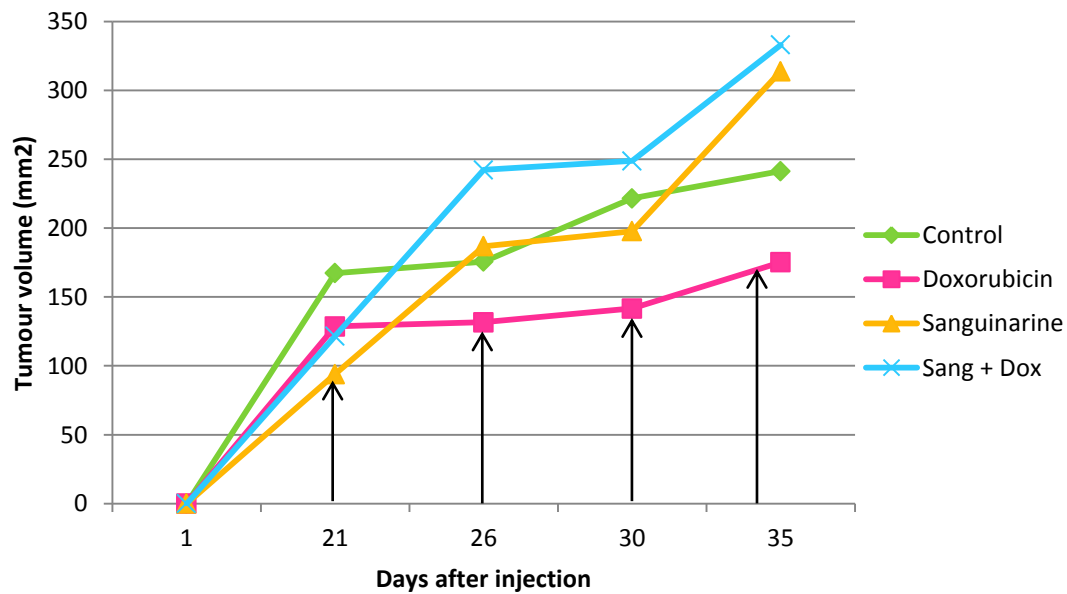


Figure 4.17: Change in tumour volume of C57BL6 mice injected with E0771 murine mammary cancer cells at day 0 (n=4). Arrows indicate days when animals were treated.

4.5.2 Western blot analysis

4.5.2.1 Total Caspase 3

Total caspase 3 levels decreased in the tumours of mice treated with doxorubicin in combination with sanguinarine ($p < 0.05$) compared to the control (Figure 4.18). This echoed previous findings (Section 2.3.1) where caspase 3 was found to be decreased in MDA-MB231 cells when treated with doxorubicin under conditions of MKP-1 inhibition.

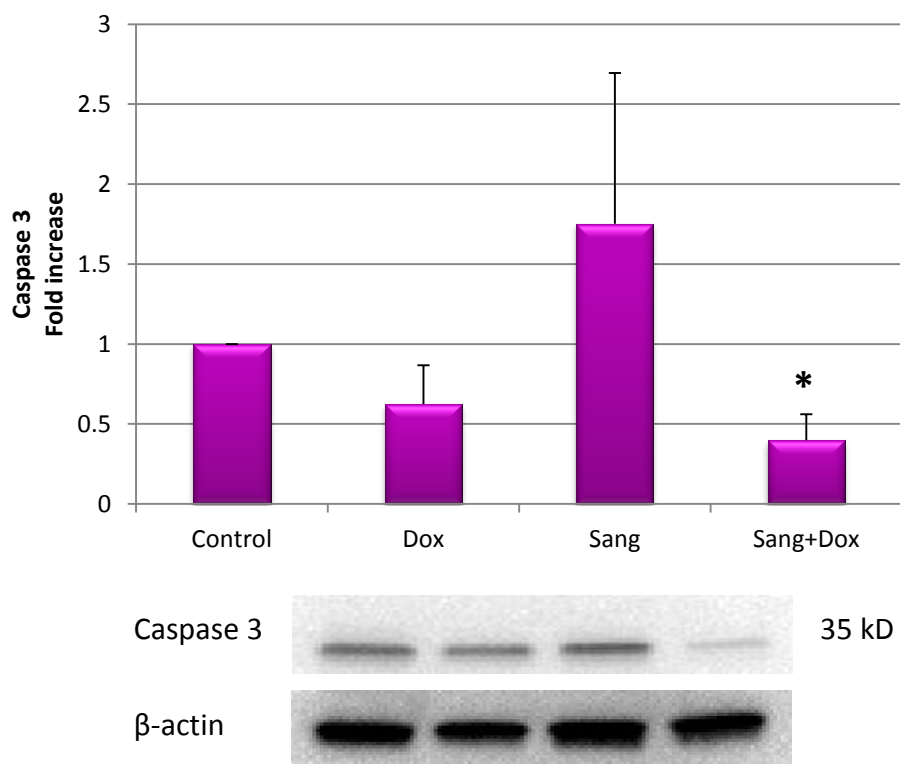


Figure 4.18: The effect of doxorubicin treatment together with MKP-1 inhibitor, sanguinarine, on caspase 3 expression in tumour bearing mice. Mice were inoculated with doxorubicin (5 mg/kg) and sanguinarine (0.22 mg/kg). Results are presented as means \pm SEM (n=3). * $p < 0.05$ vs control

4.5.2.2 MKP-1

MKP-1 expression was significantly ($p < 0.001$) decreased in all treated groups compared to the control (Figure 4.19). These findings correlate, once again with the findings from the *in-vitro* study.

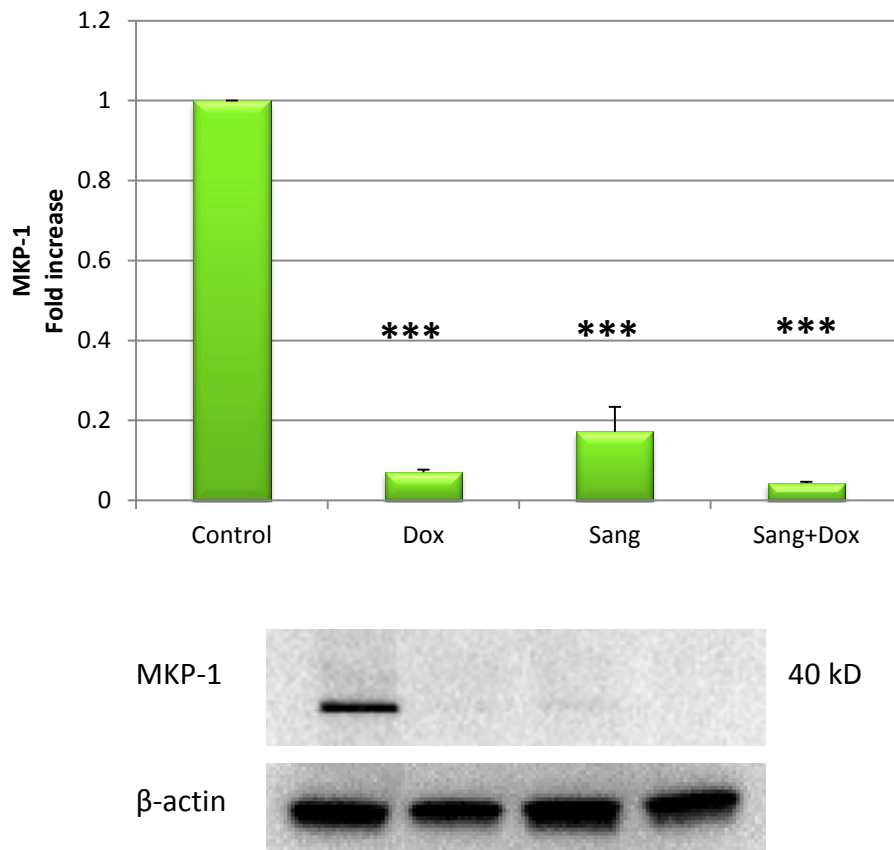


Figure 4.19: The effect of doxorubicin treatment together with MKP-1 inhibitor, sanguinarine, on MKP-1 expression in tumour bearing mice. Mice were inoculated with doxorubicin (5 mg/kg) and sanguinarine (0.22 mg/kg). Results are presented as means \pm SEM (n=2). *** $p < 0.001$ vs control

4.5.2.3 LC3 II

Treatment with doxorubicin combined with sanguinarine showed a significant ($p < 0.05$) increase in LC3 II expression in tumour bearing mice compared to doxorubicin treatment alone (Figure 4.20). This correlates with the increase in LC3 II expression in MDA-MB231 cells following treatment with doxorubicin in combination with MKP-1 inhibition. Sanguinarine treatment alone presented with a decrease in LC3 II whereas no significant differences were observed in LC3II with doxorubicin treatment alone compared to the control.

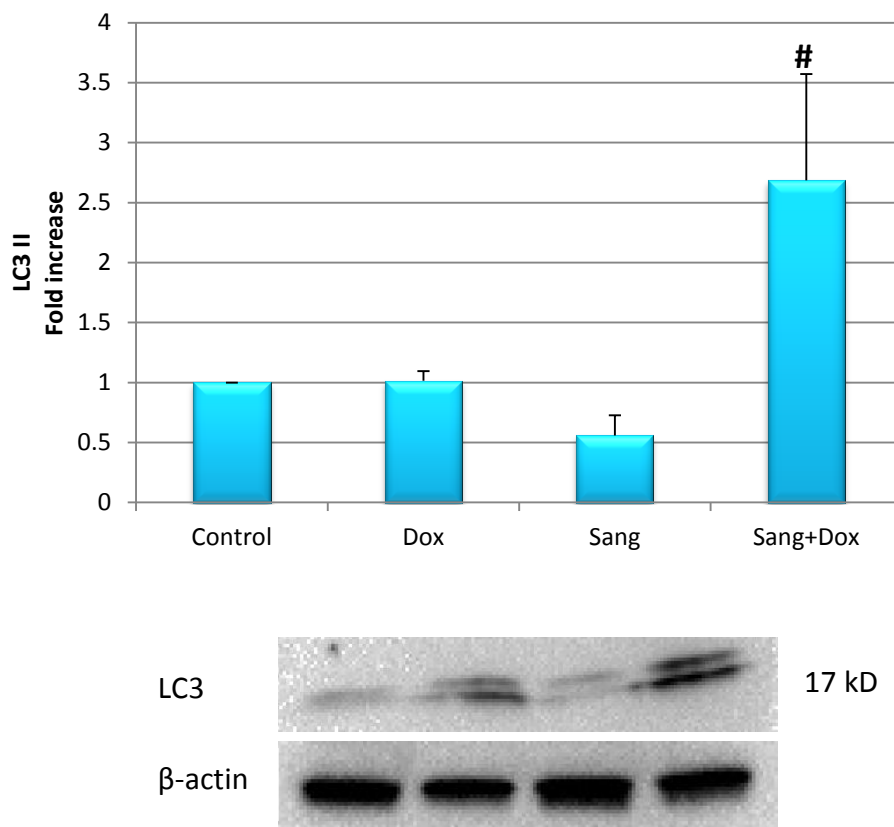


Figure 4.20: The effect of doxorubicin treatment together with MKP-1 inhibitor, sanguinarine, on LC3 II expression in tumour bearing mice. Mice were inoculated with doxorubicin (5 mg/kg) and sanguinarine (0.22 mg/kg). Results are presented as means \pm SEM (n=3). [#] $p < 0.05$ vs doxorubicin

4.5.2.4 p62

P62 expression was non-significantly decreased in tumours treated with doxorubicin, and doxorubicin combined with sanguinarine compared to the control (Figure 4.21). The lowest p62 expression was seen in the tumours treated with doxorubicin in combination with MKP-1 inhibition. Sanguinarine treatment showed a non-significant increase in p62.

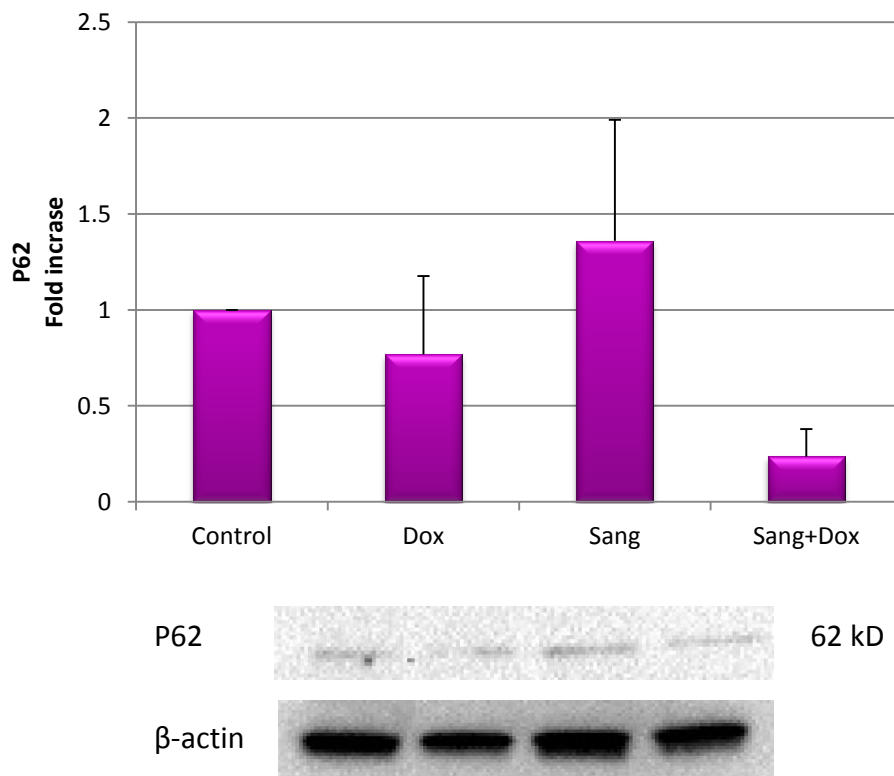


Figure 4.21: The effect of doxorubicin treatment together with MKP-1 inhibitor, sanguinarine, on p62 expression in tumour bearing mice. Mice were inoculated with doxorubicin (5 mg/kg) and sanguinarine (0.22 mg/kg). Results are presented as means \pm SEM (n=3).

Chapter 5: Discussion

Cancer is an emerging health problem in South Africa, and with breast cancer being one of the leading causes of death in woman world wide, the need for novel effective therapeutic targets is evident. Chemotherapeutic agents can be limited in their ability to induce cell death in certain instances due to chemoresistance. It is therefore essential to find therapeutic targets that can assist anticancer agents in eliciting the desired response. In this study we evaluated the effect of MKP-1 inhibition on MDA-MB231 cells as well as in an *in vivo* mouse tumour model to investigate whether its inhibition together with doxorubicin treatment has an influence on autophagy levels and cell death in breast carcinoma cells.

5.1 *In vitro* study

5.1.1 Role of MKP-1 inhibition on cell viability

The Trypan blue exclusion assay was used to assess the viability of MDA-MB231 cells following a 24 hour treatment period. Cell viability was investigated in MDA-MB231 breast cancer cells treated with doxorubicin, a MKP-1 inducer (dexamethasone), and MKP-1 inhibitors – sanguinarine and MKP-1 siRNA – as well as combinations of these compounds.

In MDA-MB231 cells, 5 μ M doxorubicin treatment significantly decreased cell viability after 24 hour treatment (Figure 4.2). This was in line with previous observations where doxorubicin caused DNA damage following addition to cancer cells (Eom *et al.* 2005).

No significant difference in cell viability was detected when cells were treated with dexamethasone alone compared to the control. This is in agreement with previous studies where it was shown that glucocorticoids protect mammary gland epithelial cells and hepatocytes as well as ovarian follicular cells against cell death signals (Redondo *et al.* 2007).

Dexamethasone induces MKP-1 via dimerization of the glucocorticoid receptor (Vandevyver *et al.* 2012). Interestingly, when the MDA-MB231 cells were treated with dexamethasone in conjunction with doxorubicin treatment, a significant increase in viability was observed compared to doxorubicin treatment alone (Figure 4.2).

Pre-treatment with sanguinarine followed by doxorubicin caused a significant decrease in cell viability in MDA-MB231 cells when compared to the group treated with doxorubicin alone (Figure 4.3). This is a novel finding which can be supported by studies showing that MKP-1 inhibition induced apoptosis in Caski-1, KU 20-01 cells (Mizuno *et al.* 2004) and rat mesangial cells (Xu *et al.* 2004). This finding suggests that sanguinarine therapy sensitized the MDA-MB231 cells to doxorubicin-induced-cell death. This is encouraging since this could be used in future studies looking to overcome doxorubicin resistance in breast cancer cells.

Treatment with MKP-1 siRNA had no effect on cell viability (Figure 4.4). The addition of MKP-1 siRNA with doxorubicin decreased cell viability significantly compared to doxorubicin therapy alone (Figure 4.4). This suggests that inhibiting MKP-1 together with doxorubicin therapy have a synergistic effect on decreasing cell viability in MDA-MB231 cells.

5.1.2 The role of MKP-1 on apoptosis in MDA-MB231 cells

To further substantiate the results obtained from the viability assay and to confirm the role of apoptosis in our cell model, the Caspase-Glo[®] 3/7 assay was done. This assay measures caspase 3/7 activity. Doxorubicin treatment caused a significant increase in caspase 3/7 activity in MDA-MB231 cells (Figure 4.5). This is in agreement with results which have shown that doxorubicin induces apoptosis via the activation of caspases and the disruption of the mitochondrial membrane potential (Gamen *et al.* 2000). Dexamethasone treatment alone

had no effect on caspase 3/7 activity, which correlated with results from the Trypan blue assay (Figure 4.2).

Sanguinarine treatment alone had no effect on caspase activity; however with the addition of doxorubicin to sanguinarine a significant increase in caspase 3/7 activity was observed compared to doxorubicin treatment alone (Figure 4.6). Pre-treatment with sanguinarine followed by doxorubicin had a more pronounced effect on caspase 3/7 activity compared to MKP-1 siRNA and doxorubicin treatment. This finding correlates with data from the Trypan blue assay and even further substantiates the proposition that under conditions of MKP-1 inhibition with sanguinarine, MDA-MB231 cells become sensitized to doxorubicin-induced apoptosis.

MKP-1 siRNA alone had no effect on caspase 3/7 activity. MKP-1 siRNA in combination with doxorubicin also did not have an additive effect compared to doxorubicin treatment alone (Figure 4.7). This is in contrast with a study done in 2007 where MKP-1 siRNA together with cisplatin treatment increased cell death in OV433 ovarian cancer cells (Wang *et al.* 2007). This finding does not correlate with results obtained from the Trypan blue assay or the western blotting results where caspase 3 cleavage and PARP was measured.

Western blot analysis indicated a significant decrease in uncleaved caspase 3 (Figure 4.8) with a subsequent significant increase in cleaved PARP (Figure 4.9) in MDA-MB231 cells treated with 5 μ M doxorubicin. This finding confirmed the work of Gamen and co-workers who showed that doxorubicin-induced apoptosis in human T-cell leukaemia is mediated by caspase-3 activation (Gamen *et al.* 1997). Furthermore, in Jurkat cells, the doxorubicin induced caspase 3 activation was followed by PARP cleavage (Ferrari *et al.* 1998). Treatment with dexamethasone in combination with doxorubicin also showed a significant decrease in caspase 3 (Figure 4.8) followed by an increase in cleaved PARP (Figure 4.9). Interestingly,

uncleaved caspase 3 levels was significantly higher compared to the control group which confirmed the work of Redondo and co-workers who have demonstrated that glucocorticoids protect cancer cells against apoptosis (Redondo *et al.* 2007).

Uncleaved caspase 3 was significantly decreased in MDA-MB231 cells treated with sanguinarine in combination with doxorubicin when compared to doxorubicin treatment alone. Interestingly, this was not mirrored in PARP cleavage where the addition of sanguinarine to doxorubicin caused an attenuation of PARP cleavage. This finding was unexpected and does not correlate with any previously mentioned findings. It is also in contrast with findings in human cervical cells (Ding *et al.* 2002), primary effusion lymphoma cells (Hussain *et al.* 2007) human leukaemia U937 cells (Han *et al.* 2008) and human colon cancer cells (Matkar *et al.* 2008) where sanguinarine-induced activation of caspase 3 was followed by PARP cleavage. An explanation for this might be the fact that PARP cleavage is a downstream event of caspase 3 cleavage. An increase might have been observed if the treatment period was extended. Furthermore, the above mentioned studies all used a high concentration (5 μ M) of sanguinarine that had the ability to induce apoptosis on its own in various cell models; in our study sanguinarine was used as an MKP-1 inhibitor and 0.5 μ M sanguinarine could inhibit MKP-1 without causing apoptosis on its own. MKP-1 siRNA combined with doxorubicin treatment also showed a significant decrease in uncleaved caspase 3 and increase in cleaved PARP. Our results corroborated that by Wang *et al.* (2007) who showed that the inhibition of MKP-1, using MKP-1 siRNA, enhanced cisplatin-induced caspase 3 and PARP cleavage in OV433 ovarian cancer cells (Wang *et al.* 2007).

Morphological changes, which are commonly associated with the progression of apoptosis, such as chromatin condensation and the formation of apoptotic bodies, were investigated in MDA-MB231 cells following the indicated treatment as previously described. Images taken

confirmed the results from the various cell death assays as an increase in cell death (pyknosis and apoptotic bodies) was observed in doxorubicin treated groups (Figure 4.10). The highest degree of cell death was observed in the cells pre-treated with sanguinarine followed by doxorubicin treatment. This further substantiates the notion that under conditions of MKP-1 inhibition, MDA-MB231 cells are sensitized to doxorubicin-induced apoptosis.

5.1.3 MKP-1 expression in MDA-MB231 cells

MKP-1 is a dual specificity phosphatase that is commonly associated with cancer progression and the resistance of cancer cells to chemotherapy. Hence, MKP-1 expression was investigated in MDA-MB231 breast cancer cells treated with doxorubicin, as well as with MKP-1 inducer (dexamethasone), and the MKP-1 inhibitors - sanguinarine and MKP-1 siRNA. Inducing MKP-1, using 100 nM dexamethasone, significantly increased MKP-1 expression in the MDA-MB231 cells (Figure 4.11). Several studies (Chen *et al.* 2002; Clark. 2003; Kassel *et al.* 2002; Lasa *et al.* 2002) demonstrated MKP-1 induction following dexamethasone treatment.

Dexamethasone, a synthetic glucocorticoid, has significantly increased MKP-1 induction in our cell model compared with the control group. This is in agreement with the work of Lasa *et al* who has shown that MKP-1 expression is induced in HeLa cells following treatment with dexamethasone (Lasa *et al.* 2002). This increase in MKP-1 expression is mediated by the deactivation of p38 MAPK (Huang *et al.* 2011).

MKP-1 was significantly inhibited following treatment with 0.5 μ M sanguinarine and MKP-1 siRNA. Moreover, MKP-1 siRNA was also shown to successfully inhibit MKP-1 expression in

MDA-MB231 cells (Wu *et al.* 2004). Sanguinarine is a bioactive plant extract that has been shown to effectively inhibit MKP-1 expression in PANC-1 and HeLa cells (Vogt *et al.* 2005).

Doxorubicin treatment tended to decrease MKP-1 expression (Figure 4.11). Furthermore, MKP-1 expression was significantly reduced with sanguinarine pre-treatment in doxorubicin treated cells compared to the control. It has been reported that doxorubicin can deplete MKP-1 activity in rat pinealocytes (Price *et al.* 2007) as well as in A1N4-myc human mammary and BT-474 breast carcinoma cells, where the decrease in MKP-1 triggered enhanced JNK activation (Small *et al.* 2003).

It has been suggested that the overexpression of MKP-1 in breast cancer inhibits the ability of alkylating agents, anthracyclines and taxanes to induce apoptosis in these cells. This overexpression is associated with decreased JNK activation (Small *et al.* 2007). Furthermore, when MKP-1 was suppressed with siRNA, or targeted deletion, enhanced chemo sensitivity and increased JNK activity was observed (Small *et al.* 2007).

5.1.4 The relation of MKP-1 with autophagy in MDA-MB231 cells

Little is known about the role of MKP-1 in autophagy. We aimed to investigate whether MKP-1 inhibition might sensitize doxorubicin treated breast cancer cells to apoptosis through a mechanism involving autophagy. We therefore treated MDA-MB231 cells as previously described and evaluated autophagy levels with flow cytometry and western blotting.

Results from both flow cytometry and western blots indicated an increase in autophagy with doxorubicin treatment. This was evident with a significant increase in LysoTracker™ fluorescence as well as a non-significant increase in LC3 II and decrease in p62 compared to the control (Figures 4.12 - 4.16). This can be supported by the fact that doxorubicin is known

to induce an autophagic response in cancer cells following treatment (Lambert *et al.* 2008; Manov *et al.* 2011). As expected, dexamethasone treatment had little effect on autophagy as evident in results from flow cytometry and both LC3 II and p62 western blots. LysoTracker™ fluorescence and LC3 II expression was slightly increased compared to the control. Although a significant increase in p62 was observed; it can be attributed to the fact that p62 is accumulating in the autophagolysosome and not being recycled due to a low autophagy flux.

This finding does however not coincide with the literature where it has been shown that dexamethasone induced an autophagic response in lymphoid leukaemia cells (Laane *et al.* 2009) and multiple myeloma cells (Grandér *et al.* 2009). Once again, discrepancies might be attributed to the concentration of dexamethasone used in these studies, as a concentration of 1 µM was used vs 100 nM used in our study.

Inhibiting MKP-1 using sanguinarine and MKP-1 siRNA did not increase autophagy in MDA-MB231 cells. This is evident from both flow cytometry (Figure 4.13 - 4.14) and western blot (Figure 4.15 – 4.16) results showing almost no change in LC3 II compared to the control and an increase in p62 following treatment. However, when MDA-MB231 cells were treated with doxorubicin in combination with MKP-1 inhibition, an increase in autophagy was observed. Sanguinarine pre-treatment showed the highest LysoTracker™ fluorescence compared to both dexamethasone and MKP-1 siRNA. This was however not significant, but it can be attributed to the large standard deviation between samples due to the flow cytometer being serviced between the initial and final experiment.

The increase in autophagy in the cells treated with sanguinarine in combination with doxorubicin was also evident in the significant increase in LC3 II and decrease in p62 expression. This novel finding demonstrates that the inhibition of MKP-1 together with doxorubicin treatment activate autophagy in our cell model. In contrast to our findings,

recent literature indicated that autophagy induction was associated with MKP-1 activation in oral cancer cells (Lu *et al.* 2010) as opposed to MKP-1 inhibition. Although no significance was evident in some of the results obtained from LC3 II and p62 western blots, clear difference was apparent in the blots, but due to a small sample size and large standard deviation these effects were blunted.

Studies on the effect of MKP-1 inhibition in autophagy are limited and leave one to speculate whether JNK and p38 MAPK's are involved in this scenario. A study done by Li *et al.* (2009) showed that JNK activation in human cancer cell lines, CNE2 and Hep3B, mediated Beclin 1 expression which induced autophagy and subsequently resulted in cell death (Li *et al.* 2009).

5.2 *In vivo* study

5.2.1 The effect of MKP-1 inhibition on autophagy and apoptosis in tumour bearing mice

In order to further substantiate the results obtained from the *in vitro* study an *in vivo* study was conducted. C57BL6 mice were inoculated with E0771 breast cancer cells and tumours were left to grow for 21 days before intervention started. Intervention consisted of four 5 mg/kg doxorubicin or 0.22 mg/kg sanguinarine intraperitoneal injections or a combination of the two given over a course of 14 days after which the tumours were excised and frozen at -80 °C. Western blotting was used to determine protein expression.

Although no changes were observed in tumour growth between the different groups during the course of treatment, molecular events did occur. The reason being, that too much time has passed before the intervention started, and thus the tumours have already reached a large volume. The MKP-1 expression, as evaluated by western blotting, was significantly

inhibited in all treated groups when compared to the control (Figure 4.19). Treatment with sanguinarine in combination with doxorubicin induced the highest degree of apoptosis in these tumours (Figure 4.18). This was evident from a significant decrease in caspase 3 expression in excised tumours. This echoed the results obtained from the *in vitro* study and can be supported by the fact that doxorubicin induces cell death in cancer cells (Gamen *et al.* 2000).

Following doxorubicin treatment LC3 II expression was not changed compared to control (Figure 4.20); however a decrease in p62 was evident indicating an increase in autophagy activity following doxorubicin treatment (Figure 4.21). This finding was expected as it had been proven that doxorubicin induced an autophagic response in cancer (Lambert *et al.* 2008; Manov *et al.* 2011). Autophagy was also upregulated in these tumours as can be seen from the significant increase in LC3 II (Figure 4.20) expression and subsequent decrease in p62 (Figure 4.21) in mice treated with sanguinarine in combination with doxorubicin. The highest degree of autophagy was observed in the tumours treated with sanguinarine in combination with doxorubicin. This once again echoed the results obtained from the *in vitro* study for autophagy induction.

5.3 Conclusions

Collectively the results from both the *in vitro* and *in vivo* study indicate that sanguinarine therapy in conjunction with doxorubicin results in a higher degree of apoptosis when compared to other treatment groups and the highest level of autophagy was also observed for combined sanguinarine and doxorubicin therapy. This correlation indicate that the inhibition of MKP-1 together with doxorubicin treatment might act synergistically in inducing autophagy and apoptosis in MDA-MB231 and E0771 breast cancer cells. There is overlap between the two pathways and both doxorubicin and MKP-1 have been associated with

apoptosis, where doxorubicin induces apoptosis and MKP-1 expression inhibited apoptosis in cancer cells.

Doxorubicin has also been shown to induce autophagy in cancer cells; however the effect of MKP-1 expression on autophagy in breast cancer cells is unknown. To establish if the observed correlation between autophagy and apoptosis has a causal link to MKP-1 expression, autophagy and apoptosis were analysed during conditions of MKP-1 induction and MKP-1 inhibition. Results showed that by inducing MKP-1 with dexamethasone during doxorubicin treatment a significant decrease in apoptosis compared to doxorubicin treatment alone was observed. This finding could have far reaching implication in patients receiving glucocorticoid- and chemotherapy. It was also observed that when MKP-1 was inhibited with MKP-1 siRNA during doxorubicin treatment, it resulted in an increased degree of apoptosis compared to doxorubicin treatment alone. Combination therapy with sanguinarine and doxorubicin showed similar trends to combined MKP-1 siRNA and doxorubicin treatment, except that sanguinarine and doxorubicin together induced even greater levels of apoptosis.

An increase in autophagy was observed under conditions of MKP-1 inhibition with sanguinarine and doxorubicin therapy compared to doxorubicin treatment alone. This indicates that the observed correlation between autophagy and apoptosis is linked to MKP-1 expression as it was shown that by inhibiting MKP-1, the degree of autophagy and cell death increased.

Levels of apoptosis and autophagy increased with the inhibition of MKP-1 in MDA-MB231 cells and in E0771 cell tumours. Also, inhibiting MKP-1 with doxorubicin does act synergistically in inducing autophagy and apoptosis. These findings suggest that inhibiting MKP-1 with sanguinarine sensitized the MDA-MB231 cells and E0771 cell tumours to

doxorubicin-induced-apoptosis through a mechanism involving autophagy. This is an encouraging finding that could hopefully be used in future studies looking to overcome doxorubicin-resistance in breast cancer cells overexpressing MKP-1.

5.4 Limitations and future studies

It would be of great importance to further confirm our findings in an *in vivo* setting by increasing the sample size for better statistical power. Continuation of the research should investigate the mechanism involved in the up-regulation of autophagy in this scenario. JNK and p38 MAPK activation and expression was not quantified in this study.

It would also be relevant to see if the effect that sanguinarine has, is blunted under conditions of autophagy inhibition. It would be of great benefit to investigate and identify the exact mechanism whereby MKP-1 inhibition results in autophagic induction in breast cancer cells. If there is indeed a direct link, it could be manipulated during the clinical setting to improve therapeutic options for breast cancer patients.

Bibliography

Aburai N, Yoshida M, Ohnishi M and Kimura K. Sanguinarine as a potent and specific inhibitor of protein phosphatase 2C in vitro and induces apoptosis via phosphorylation of p38 in HL60 cells.

Biosci.Biotechnol.Biochem. 74: 3: 548-552, 2010.

Adhami VM, Aziz MH, Reagan-Shaw SR, Nihal M, Mukhtar H and Ahmad N. Sanguinarine causes cell cycle blockade and apoptosis of human prostate carcinoma cells via modulation of cyclin kinase

inhibitor-cyclin-cyclin-dependent kinase machinery. *Molecular Cancer Therapeutics* 3: 8: 933-940, 2004.

Ahmad N, Gupta S, Husain MM, Heiskanen KM and Mukhtar H. Differential antiproliferative and apoptotic response of sanguinarine for cancer cells versus normal cells. *Clin.Cancer Res.* 6: 4: 1524-1528, 2000.

Ahsan H, Reagan-Shaw S, Breur J and Ahmad N. Sanguinarine induces apoptosis of human pancreatic carcinoma AsPC-1 and BxPC-3 cells via modulations in Bcl-2 family proteins. *Cancer Lett.* 249: 2: 198-208, 2007.

Arends MJ and Wyllie AH. Apoptosis: mechanisms and roles in pathology. *Int.Rev.Exp.Pathol.* 32: 223-254, 1991.

Bailly-Maitre B, De Sousa G, Boulukos K, Gugenheim J and Rahmani R. Dexamethasone inhibits spontaneous apoptosis in primary cultures of human and rat hepatocytes via Bcl-2 and Bcl-xL induction. *Cell Death Differ.* 8: 3: 279-288, 2001.

Bang Y-, Kwon JH, Kang SH, Kim JW and Yang YC. Increased MAPK activity and MKP-1 overexpression in human gastric adenocarcinoma. *Biochem.Biophys.Res.Commun.* 250: 1: 43-47, 1998.

Beltman J, McCormick F and Cook SJ. The selective protein kinase C inhibitor, Ro-31-8220, inhibits mitogen-activated protein kinase phosphatase-1 (MKP-1) expression, induces c-Jun expression, and activates Jun N-terminal kinase. *J.Biol.Chem.* 271: 43: 27018-27024, 1996.

Boutros T, Chevet E and Metrakos P. Mitogen-activated protein (MAP) kinase/MAP kinase phosphatase regulation: roles in cell growth, death, and cancer. *Pharmacol.Rev.* 60: 3: 261-310, 2008.

Bradford MM. A rapid and sensitive method for the quantitation of microgram quantities of protein utilizing the principle of protein dye binding. *Anal.Biochem.* 72: 1-2: 248-254, 1976.

Brown M and Wilson G. Apoptosis genes and resistance to cancer therapy: What do the experimental and clinical data tell us? *Cancer Biology and Therapy* 2: 5: 477-490, 2003.

Chang L and Karin M. Mammalian MAP kinase signalling cascades. *Nature* 410: 6824: 37-40, 2001.

Chen P, Li J, Barnes J, Kokkonen GC, Lee JC and Liu Y. Restraint of proinflammatory cytokine biosynthesis by mitogen-activated protein kinase phosphatase-1 in lipopolysaccharide-stimulated macrophages. *J.Immunol.* 169: 11: 6408-6416, 2002.

Chu Y, Solski PA, Khosravi-Far R, Der CJ and Kelly K. The mitogen-activated protein kinase phosphatases PAC1, MKP-1, and MKP-2 have unique substrate specificities and reduced activity in vivo toward the ERK2 sevenmaker mutation. *J.Biol.Chem.* 271: 11: 6497-6501, 1996.

Clark AR. MAP kinase phosphatase 1: A novel mediator of biological effects of glucocorticoids? *J.Endocrinol.* 178: 1: 5-12, 2003.

Cohen GM. Caspases: the executioners of apoptosis. *Biochem.J.* 326 (Pt 1): Pt 1: 1-16, 1997.

Cory S and Adams JM. The BCL2 family: Regulators of the cellular life-or-death switch. *Nature Reviews Cancer* 2: 9: 647-656, 2002.

Coughlin SS and Ekwueme DU. Breast cancer as a global health concern. *Cancer Epidemiology* 33: 5: 315-318, 2009.

Cowling V and Downward J. Caspase-6 is the direct activator of caspase-8 in the cytochrome c-induced apoptosis pathway: Absolute requirement for removal of caspase-6 prodomain. *Cell Death Differ.* 9: 10: 1046-1056, 2002.

Cuervo AM. Autophagy: in sickness and in health. *Trends Cell Biol.* 14: 2: 70-77, 2004.

Cuvillier O, Nava VE, Murthy SK, Edsall LC, Levade T, Milstien S and Spiegel S. Sphingosine generation, cytochrome c release, and activation of caspase-7 in doxorubicin-induced apoptosis of MCF7 breast adenocarcinoma cells. *Cell Death Differ.* 8: 2: 162-171, 2001.

Das A, Mukherjee A and Chakrabarti J. Sanguinarine: An evaluation of in vivo cytogenetic activity. *Mutation Research - Genetic Toxicology and Environmental Mutagenesis* 563: 1: 81-87, 2004.

de Bruin EC and Medema JP. Apoptosis and non-apoptotic deaths in cancer development and treatment response. *Cancer Treat.Rev.* 34: 8: 737-749, 2008.

Degtarev A, Boyce M and Yuan J. A decade of caspases. *Oncogene* 22: 53: 8543-8567, 2003.

Ding Z, Tang S-, Weerasinghe P, Yang X, Pater A and Liepins A. The alkaloid sanguinarine is effective against multidrug resistance in human cervical cells via bimodal cell death. *Biochem.Pharmacol.* 63: 8: 1415-1421, 2002.

Eisenberg-Lerner A and Kimchi A. The paradox of autophagy and its implication in cancer etiology and therapy. *Apoptosis* 14: 4: 376-391, 2009.

Engelbrecht Y, De Wet H, Horsch K, Langeveldt CR, Hough FS and Hulley PA. Glucocorticoids induce rapid up-regulation of mitogen-activated protein kinase phosphatase-1 and dephosphorylation of

extracellular signal-regulated kinase and impair proliferation in human and mouse osteoblast cell lines. *Endocrinology* 144: 2: 412-422, 2003.

Eom Y-, Kim MA, Park SS, Goo MJ, Kwon HJ, Sohn S, Kim W-, Yoon G and Choi KS. Two distinct modes of cell death induced by doxorubicin: Apoptosis and cell death through mitotic catastrophe accompanied by senescence-like phenotype. *Oncogene* 24: 30: 4765-4777, 2005.

Ewens A, Luo L, Berleth E, Alderfer J, Wollman R, Hafeez BB, Kanter P, Mihich E and Ehrke MJ. Doxorubicin plus interleukin-2 chemoimmunotherapy against breast cancer in mice. *Cancer Res.* 66: 10: 5419-5426, 2006.

Fan W, Sui M and Huang Y. Glucocorticoids selectively inhibit paclitaxel-induced apoptosis: Mechanisms and its clinical impact. *Curr.Med.Chem.* 11: 4: 403-411, 2004.

Ferrari D, Stepczynska A, Los M, Wesselborg S and Schulze-Osthoff K. Differential regulation and ATP requirement for caspase-8 and caspase-3 activation during CD95- and anticancer drug-induced apoptosis. *J.Exp.Med.* 188: 5: 979-984, 1998.

Finn NA, Findley HW and Kemp ML. A switching mechanism in doxorubicin bioactivation can be exploited to control doxorubicin toxicity. *PLoS Computational Biology* 7: 9: 2011.

Folkman J. Angiogenesis. *Annu.Rev.Med.* 57: 1-18, 2006.

Franklin CC, Srikanth S and Kraft AS. Conditional expression of mitogen-activated protein kinase phosphatase-1, MKP-1, is cytoprotective against UV-induced apoptosis. *Proc.Natl.Acad.Sci.U.S.A.* 95: 6: 3014-3019, 1998.

Fulda S and Debatin K-. Extrinsic versus intrinsic apoptosis pathways in anticancer chemotherapy. *Oncogene* 25: 34: 4798-4811, 2006.

Gamen S, Anel A, Lasierra P, Alava MA, Martinez-Lorenzo MJ, Piñeiro A and Naval J. Doxorubicin-induced apoptosis in human T-cell leukemia is mediated by caspase-3 activation in a Fas-independent way. *FEBS Lett.* 417: 3: 360-364, 1997.

Gamen S, Anel A, Perez-Galan P, Lasierra P, Johnson D, Pineiro A and Naval J. Doxorubicin treatment activates a Z-VAD-sensitive caspase, which causes deltapسيم loss, caspase-9 activity, and apoptosis in Jurkat cells. *Exp.Cell Res.* 258: 1: 223-235, 2000.

Garcia M, Jemal A, Ward E, Center M, Hao Y, Siegel R and Thun M. *Global Cancer Facts & Figures 2007* Atlanta, GA: American Cancer Society, 2007.

Gerl R and Vaux DL. Apoptosis in the development and treatment of cancer. *Carcinogenesis* 26: 2: 263-270, 2005.

Ghobrial IM, Witzig TE and Adjei AA. Targeting apoptosis pathways in cancer therapy. *CA Cancer.J.Clin.* 55: 3: 178-194, 2005.

Grandér D, Kharaziha P, Laane E, Pokrovskaja K and Panaretakis T. Autophagy as the main means of cytotoxicity by glucocorticoids in hematological malignancies. *Autophagy* 5: 8: 1198-1200, 2009.

Groom LA, Sneddon AA, Alessi DR, Dowd S and Keyse SM. Differential regulation of the MAP, SAP and RK/p38 kinases by Pyst1, a novel cytosolic dual-specificity phosphatase. *EMBO J.* 15: 14: 3621-3632, 1996.

Haagenson ,Kelly and Wu ,Gen. The role of MAP kinases and MAP kinase phosphatase-1 in resistance to breast cancer treatment. *Cancer Metastasis Rev.* 1: 143-149, 2010.

Hamdi M, Kool J, Cornelissen-Steijger P, Carlotti F, Popeijus HE, Van Der Burgt C, Janssen JM, Yasui A, Hoeben RC, Terleth C, Mullenders LH and Van Dam H. DNA damage in transcribed genes induces apoptosis via the JNK pathway and the JNK-phosphatase MKP-1. *Oncogene* 24: 48: 7135-7144, 2005.

Han MH, Kim SO, Kim GY, Kwon TK, Choi BT, Lee WH and Choi YH. Induction of apoptosis by sanguinarine in C6 rat glioblastoma cells is associated with the modulation of the Bcl-2 family and activation of caspases through downregulation of extracellular signal-regulated kinase and Akt. *Anticancer Drugs* 18: 8: 913-921, 2007.

Han MH, Yoo YH and Choi YH. Sanguinarine-induced apoptosis in human leukemia U937 cells via Bcl-2 downregulation and caspase-3 activation. *Chemotherapy* 54: 3: 157-165, 2008.

Hanahan D and Weinberg RA. The hallmarks of cancer. *Cell* 100: 1: 57-70, 2000.

Hanahan D and Weinberg R. Hallmarks of Cancer: The Next Generation. *Cell* 144: 5: 646-674, 2011.

Hengartner MO. The biochemistry of apoptosis. *Nature* 407: 6805: 770-776, 2000.

Herr I, Ucur E, Herzer K, Okouoyo S, Ridder R, Krammer PH, Von Knebel Doeberitz M and Debatin K. Glucocorticoid cotreatment induces apoptosis resistance toward cancer therapy in carcinomas. *Cancer Res.* 63: 12: 3112-3120, 2003.

Hicks C, Pannuti A and Miele L. Associating GWAS information with the Notch signaling pathway using transcription profiling. *Cancer Informatics* 10: 93-108, 2011.

Hortobagyi GN. Anthracyclines in the treatment of cancer. An overview. *Drugs* 54 Suppl 4: 1-7, 1997.

Hoyer-Hansen M and Jaattela M. Autophagy: an emerging target for cancer therapy. *Autophagy* 4: 5: 574-580, 2008.

Hsieh Y-, Athar M and Chaudry IH. When apoptosis meets autophagy: deciding cell fate after trauma and sepsis. *Trends Mol.Med.* 15: 3: 129-138, 2009.

Huang J, Wang H, Song Z, Lin X and Zhang C. Involvement of MAPK phosphatase-1 in dexamethasone-induced chemoresistance in lung cancer. *J.Chemother.* 23: 4: 221-226, 2011.

Hussain AR, Al-Jomah NA, Siraj AK, Manogaran P, Al-Hussein K, Abubaker J, Plataniias LC, Al-Kuraya KS and Uddin S. Sanguinarine-dependent induction of apoptosis in primary effusion lymphoma cells. *Cancer Res.* 67: 8: 3888-3897, 2007.

Igney FH and Krammer PH. Death and anti-death: Tumour resistance to apoptosis. *Nature Reviews Cancer* 2: 4: 277-288, 2002.

Jang BC, Park JG, Song DK, Baek WK, Yoo SK, Jung KH, Park GY, Lee TY and Suh SI. Sanguinarine induces apoptosis in A549 human lung cancer cells primarily via cellular glutathione depletion. *Toxicology in Vitro* 23: 2: 281-287, 2009.

Jemal A, Bray F, Center MM, Ferlay J, Ward E and Forman D. Global cancer statistics. *CA Cancer Journal for Clinicians* 61: 2: 69-90, 2011.

Jin S and White E. Tumor suppression by autophagy through the management of metabolic stress. *Autophagy* 4: 5: 563-566, 2008.

Jordan MA and Wilson L. Microtubules as a target for anticancer drugs. *Nat.Rev.Cancer.* 4: 4: 253-265, 2004.

Kanzawa T, Kondo Y, Ito H, Kondo S and Germano I. Induction of autophagic cell death in malignant glioma cells by arsenic trioxide. *Cancer Res.* 63: 9: 2103-2108, 2003.

Kassel O, Sancono A, Krätzschar J, Kreft B, Stassen M and Cato ACB. Glucocorticoids inhibit MAP kinase via increased expression and decreased degradation of MKP-1. *EMBO J.* 20: 24: 7108-7116, 2002.

Kennedy NJ and Davis RJ. Role of JNK in tumor development. *Cell.Cycle* 2: 3: 199-201, 2003.

Kerr JF, Wyllie AH and Currie AR. Apoptosis: a basic biological phenomenon with wide-ranging implications in tissue kinetics. *Br.J.Cancer* 26: 4: 239-257, 1972.

Kim S, Lee T, Leem J, Kyeong SC, Park J and Taeg KK. Sanguinarine-induced apoptosis: Generation of ROS, down-regulation of Bcl-2, c-FLIP, and synergy with TRAIL. *J.Cell.Biochem.* 104: 3: 895-907, 2008.

King KL and Cidlowski JA. Cell cycle regulation and apoptosis. *Annu.Rev.Physiol.* 60: 601-617, 1998.

Kitakaze M, Fong M, Yoshitake M, Minamino T, Node K, Okuyama Y, et al. Vesnarinone inhibits adenosine uptake in endothelial cells, smooth muscle cells and myocytes, and mediates cytoprotection. *J Mol Cell Cardiol.* 29: 12: 3413-3417, 1997.

Kundu M and Thompson CB. Autophagy: Basic principles and relevance to disease. *Annual Review of Pathology: Mechanisms of Disease* 3: 427-455, 2008.

Laane E, Tamm KP, Buentke E, Ito K, Khahariza P, Oscarsson J, Corcoran M, Björklund A-, Hultenby K, Lundin J, Heyman M, Söderhäll S, Mazur J, Porwit A, Pandolfi PP, Zhivotovsky B, Panaretakis T and Grandér D. Cell death induced by dexamethasone in lymphoid leukemia is mediated through initiation of autophagy. *Cell Death Differ.* 16: 7: 1018-1029, 2009.

Lambert LA, Qiao N, Hunt KK, Lambert DH, Mills GB, Meijer L and Keyomarsi K. Autophagy: A novel mechanism of synergistic cytotoxicity between doxorubicin and roscovitine in a sarcoma model. *Cancer Res.* 68: 19: 7966-7974, 2008.

Lasa M, Abraham SM, Boucheron C, Saklatvala J and Clark AR. Dexamethasone causes sustained expression of mitogen-activated protein kinase (MAPK) phosphatase 1 and phosphatase-mediated inhibition of MAPK p38. *Mol.Cell.Biol.* 22: 22: 7802-7811, 2002.

Lazo JS, Nunes R, Skoko JJ, de Oliveira PEQ, Vogt A and Wipf P. Novel benzofuran inhibitors of human mitogen-activated protein kinase phosphatase-1. *Bioorganic and Medicinal Chemistry* 14: 16: 5643-5650, 2006.

Leist M, Single B, Naumann H, Fava E, Simon B, Kühnle S and Nicotera P. Inhibition of mitochondrial ATP generation by nitric oxide switches apoptosis to necrosis. *Exp.Cell Res.* 249: 2: 396-403, 1999.

Levine B. Cell biology: autophagy and cancer. *Nature* 446: 7137: 745-747, 2007.

Levine B and Yuan J. Autophagy in cell death: An innocent convict? *J.Clin.Invest.* 115: 10: 2679-2688, 2005.

Li DD, Wang LL, Deng R, Tang J, Shen Y, Guo JF, Wang Y, Xia LP, Feng GK, Liu QQ, Huang WL, Zeng YX and Zhu XF. The pivotal role of c-Jun NH2-terminal kinase-mediated Beclin 1 expression during anticancer agents-induced autophagy in cancer cells. *Oncogene* 28: 6: 886-898, 2009.

Liang XH, Jackson S, Seaman M, Brown K, Kempkes B, Hibshoosh H and Levine B. Induction of autophagy and inhibition of tumorigenesis by beclin 1. *Nature* 402: 6762: 672-676, 1999.

Liao Q, Guo J, Kleeff J, Zimmermann A, Büchler MW, Korc M and Friess H. Down-regulation of the dual-specificity phosphatase MKP-1 suppresses tumorigenicity of pancreatic cancer cells. *Gastroenterology* 124: 7: 1830-1845, 2003.

Liu Y, Gorospe M, Yang C and Holbrook NJ. Role of mitogen-activated protein kinase phosphatase during the cellular response to genotoxic stress: Inhibition of c-Jun N-terminal kinase activity and AP-1-dependent gene activation. *J.Biol.Chem.* 270: 15: 8377-8380, 1995.

Lockshin RA and Williams CM. Programmed cell death-IV. The influence of drugs on the breakdown of the intersegmental muscles of silkworms. *J.Insect Physiol.* 11: 6: 803-809, 1965.

Lockshin RA and Zakeri Z. Apoptosis, autophagy, and more. *Int.J.Biochem.Cell Biol.* 36: 12: 2405-2419, 2004.

Loos B and Engelbrecht AM. Cell death: A dynamic response concept. *Autophagy* 5: 5: 590-603, 2009.

Lowe SW, Cepero E and Evan G. Intrinsic tumour suppression. *Nature* 432: 7015: 307-315, 2004.

Lu H-, Kao S-, Liu T-, Liu S-, Huang W-, Chang K- and Lin S-. Areca nut extract induced oxidative stress and upregulated hypoxia inducing factor leading to autophagy in oral cancer cells. *Autophagy* 6: 6: 725-737, 2010.

Mackraj I, Govender T and Gathiram P. Sanguinarine. *Cardiovasc.Ther.* 26: 1: 75-83, 2008.

Maiuri MC, Zalckvar E, Kimchi A and Kroemer G. Self-eating and self-killing: Crosstalk between autophagy and apoptosis. *Nature Reviews Molecular Cell Biology* 8: 9: 741-752, 2007.

Manov I, Pollak Y, Broneshter R and Iancu TC. Inhibition of doxorubicin-induced autophagy in hepatocellular carcinoma Hep3B cells by sorafenib - The role of extracellular signal-regulated kinase counteraction. *FEBS Journal* 278: 18: 3494-3507, 2011.

Matkar SS, Wrischnik LA and Hellmann-Blumberg U. Sanguinarine causes DNA damage and p53-independent cell death in human colon cancer cell lines. *Chem.Biol.Interact.* 172: 1: 63-71, 2008.

Meijer AJ and Codogno P. Regulation and role of autophagy in mammalian cells. *Int.J.Biochem.Cell Biol.* 36: 12: 2445-2462, 2004.

Mizuno R, Oya M, Shiomi T, Marumo K, Okada Y and Murai M. Inhibition of MKP-1 expression potentiates JNK related apoptosis in renal cancer cells. *J.Urol.* 172: 2: 723-727, 2004.

Moscat J and Diaz-Meco MT. p62 at the Crossroads of Autophagy, Apoptosis, and Cancer. *Cell* 137: 6: 1001-1004, 2009.

Nagata S. Apoptotic DNA fragmentation. *Exp.Cell Res.* 256: 1: 12-18, 2000.

Park H, Bergeron E, Senta H, Guillemette K, Beauvais S, Blouin R, Sirois J and Fauchoux N. Sanguinarine induces apoptosis of human osteosarcoma cells through the extrinsic and intrinsic pathways. *Biochem.Biophys.Res.Commun.* 399: 3: 446-451, 2010.

Pattingre S and Levine B. Bcl-2 inhibition of autophagy: a new route to cancer? *Cancer Res.* 66: 6: 2885-2888, 2006.

Pearson G, Robinson F, Beers Gibson T, Xu BE, Karandikar M, Berman K and Cobb MH. Mitogen-activated protein (MAP) kinase pathways: regulation and physiological functions. *Endocr.Rev.* 22: 2: 153-183, 2001.

Price DM, Wloka MT, Chik CL and Ho AK. Mitogen-activated protein kinase phosphatase-1 (MKP-1) preferentially dephosphorylates p42/44MAPK but not p38MAPK in rat pinealocytes. *J.Neurochem.* 101: 6: 1685-1693, 2007.

Redondo M, Téllez T, Roldan MJ, Serrano A, García-Aranda M, Gleave ME, Hortas ML and Morell M. Anticlustarin treatment of breast cancer cells increases the sensitivities of chemotherapy and tamoxifen and counteracts the inhibitory action of dexamethasone on chemotherapy-induced cytotoxicity. *Breast cancer research : BCR* 9: 6: 2007.

Riedl SJ and Salvesen GS. The apoptosome: signalling platform of cell death. *Nat.Rev.Mol.Cell Biol.* 8: 5: 405-413, 2007.

Rojo F, González-Navarrete I, Bragado R, Dalmases A, Menéndez S, Cortes-Sempere M, Suárez C, Oliva C, Servitja S, Rodríguez-Fanjul V, Sánchez-Pérez I, Campas C, Corominas JM, Tusquets I, Bellosillo B, Serrano S, Perona R, Rovira A and Albanell J. Mitogen-activated protein kinase phosphatase-1 in human breast cancer independently predicts prognosis and is repressed by doxorubicin. *Clinical Cancer Research* 15: 10: 3530-3539, 2009.

Roninson IB, Broude EV and Chang BD. If not apoptosis, then what? Treatment-induced senescence and mitotic catastrophe in tumor cells. *Drug Resist Updat* 4: 5: 303-313, 2001.

Salazar M, Carracedo A, Salanueva ÍJ, Hernández-Tiedra S, Lorente M, Egia A, Vázquez P, Blázquez C, Torres S, García S, Nowak J, Fimia GM, Piacentini M, Cecconi F, Pandolfi PP, González-Feria L,

Iovanna JL, Guzmán M, Boya P and Velasco G. Cannabinoid action induces autophagy-mediated cell death through stimulation of ER stress in human glioma cells. *J.Clin.Invest.* 119: 5: 1359-1372, 2009.

Sanchez-Perez I, Martinez-Gomariz M, Williams D, Keyse SM and Perona R. CL100/MKP-1 modulates JNK activation and apoptosis in response to cisplatin. *Oncogene* 19: 45: 5142-5152, 2000.

Serafim TL, Matos JAC, Sardão VA, Pereira GC, Branco AF, Pereira SL, Parke D, Perkins EL, Moreno AJM, Holy J and Oliveira PJ. Sanguinarine cytotoxicity on mouse melanoma K1735-M2 cells-Nuclear vs. mitochondrial effects. *Biochem.Pharmacol.* 76: 11: 1459-1475, 2008.

Shimgu T, Fujiwara K, Bogler O, Akiyama Y, Meritake K, Shinojima N, Tamacla Y, Yokoyama T and Kondo S. Inhibition of autophagy at a late stage enhances imatinib-induced cytotoxicity In human malignant glioma cells. *International Journal of Cancer* 124: 5: 1060-1071, 2009.

Shimizu S, Kanaseki T, Mizushima N, Mizuta T, Arakawa-Kobayashi S, Thompson CB and Tsujimoto Y. Role of Bcl-2 family proteins in a non-apoptotic programmed cell death dependent on autophagy genes. *Nat.Cell Biol.* 6: 12: 1221-1228, 2004.

Small GW, Shi YY, Higgins LS and Orlowski RZ. Mitogen-activated protein kinase phosphatase-1 is a mediator of breast cancer chemoresistance. *Cancer Res.* 67: 9: 4459-4466, 2007.

Small GW, Somasundaram S, Moore DT, Shi YY and Orlowski RZ. Repression of mitogen-activated protein kinase (MAPK) phosphatase-1 by anthracyclines contributes to their antiapoptotic activation of p44/42-MAPK. *J.Pharmacol.Exp.Ther.* 307: 3: 861-869, 2003.

Smith L, Watson MB, O'Kane SL, Drew PJ, Lind MJ and Cawkwell L. The analysis of doxorubicin resistance in human breast cancer cells using antibody microarrays. *Mol.Cancer.Ther.* 5: 8: 2115-2120, 2006.

Song JJ and Lee YJ. Differential cleavage of Mst1 by caspase-7/-3 is responsible for TRAIL-induced activation of the MAPK superfamily. *Cell.Signal.* 20: 5: 892-906, 2008.

Staples CJ, Owens DM, Maier JV, Cato ACB and Keyse SM. Cross-talk between the p38 α and JNK MAPK pathways mediated by MAP kinase phosphatase-1 determines cellular sensitivity to UV radiation. *J.Biol.Chem.* 285: 34: 25928-25940, 2010.

Stromhaug PE and Klionsky DJ. Approaching the molecular mechanism of autophagy. *Traffic* 2: 8: 524-531, 2001.

Tasdemir E, Maiuri MC, Morselli E, Criollo A, D'Amelio M, Djavaheri-Mergny M, Cecconi F, Tavernarakis N and Kroemer G. A dual role of p53 in the control of autophagy. *Autophagy* 4: 6: 810-814, 2008.

Tsujimoto Y and Shimizu S. Another way to die: Autophagic programmed cell death. *Cell Death Differ.* 12: SUPPL. 2: 1528-1534, 2005.

United Nations. *United Nations World Population Prospects: The 2008 Revision* 2008.

Vandevyver S, Dejager L, Van Bogaert T, Kleyman A, Liu Y, Tuckermann J and Libert C. Glucocorticoid receptor dimerization induces MKP1 to protect against TNF-induced inflammation. *J.Clin.Invest.* 122: 6: 2130-2140, 2012.

Vicent S, Garayoa M, López-Picazo JM, Lozano MD, Toledo G, Thunnissen FBJM, Manzano RG and Montuenga LM. Mitogen-activated protein kinase phosphatase-1 is overexpressed in non-small cell lung cancer and is an independent predictor of outcome in patients. *Clinical Cancer Research* 10: 11: 3639-3649, 2004.

Vogelstein B and Kinzler KW. Cancer genes and the pathways they control. *Nat.Med.* 10: 8: 789-799, 2004.

Vogt A, Tamewitz A, Skoko J, Sikorski RP, Giuliano KA and Lazo JS. The benzo[c]phenanthridine alkaloid, sanguinarine, is a selective, cell-active inhibitor of mitogen-activated protein kinase phosphatase-1. *J.Biol.Chem.* 280: 19: 19078-19086, 2005.

Vorobiof DA, Sitas F and Vorobiof G. Breast cancer incidence in South Africa. *Journal of Clinical Oncology* 19: 18 SUPPL.: 125s-127s, 2001.

Vrba J, Doležel P, Vičar J and Ulrichová J. Cytotoxic activity of sanguinarine and dihydrosanguinarine in human promyelocytic leukemia HL-60 cells. *Toxicology in Vitro* 23: 4: 580-588, 2009.

Walczak H and Krammer PH. The CD95 (APO-1/Fas) and the TRAIL (APO-2L) apoptosis systems. *Exp.Cell Res.* 256: 1: 58-66, 2000.

Wang H-, Cheng Z and Malbon CC. Overexpression of mitogen-activated protein kinase phosphatases MKP1, MKP2 in human breast cancer. *Cancer Lett.* 191: 2: 229-237, 2003.

Wang J, Zhou J- and Gen SW. ERK-dependent MKP-1-mediated cisplatin resistance in human ovarian cancer cells. *Cancer Res.* 67: 24: 11933-11941, 2007.

Wang S, Konorev EA, Kotamraju S, Joseph J, Kalivendi S and Kalyanaraman B. Doxorubicin induces apoptosis in normal and tumor cells via distinctly different mechanisms: Intermediacy of H₂O₂- and p53-dependent pathways. *J.Biol.Chem.* 279: 24: 25535-25543, 2004.

Wang Z, Xu J, Zhou J-, Liu Y and Wu GS. Mitogen-activated protein kinase phosphatase-1 is required for cisplatin resistance. *Cancer Res.* 66: 17: 8870-8877, 2006.

WHO/ICO. *Human Papillomavirus and related cancers* 2010

Wu GS. Role of mitogen-activated protein kinase phosphatases (MKPs) in cancer. *Cancer Metastasis Rev.* 26: 3-4: 579-585, 2007.

Wu GS. The functional interactions between the p53 and MAPK signaling pathways. *Cancer.Biol.Ther.* 3: 2: 156-161, 2004.

Wu JJ and Bennett AM. Essential role for mitogen-activated protein (MAP) kinase phosphatase-1 in stress-responsive MAP kinase and cell survival signaling. *J.Biol.Chem.* 280: 16: 16461-16466, 2005.

Wu W, Chaudhuri S, Brickley DR, Pang D, Karrison T and Conzen SD. Microarray Analysis Reveals Glucocorticoid-Regulated Survival Genes That Are Associated with Inhibition of Apoptosis in Breast Epithelial Cells. *Cancer Res.* 64: 5: 1757-1764, 2004.

Wu W, Pew T, Zou M, Pang D and Conzen SD. Glucocorticoid receptor-induced MAPK phosphatase-1 (MPK-1) expression inhibits paclitaxel-associated MAPK activation and contributes to breast cancer cell survival. *J.Biol.Chem.* 280: 6: 4117-4124, 2005.

Xu Q, Konta T, Nakayama K, Furusu A, Moreno-Manzano V, Lucio-Cazana J, Ishikawa Y, Fine LG, Yao J and Kitamura M. Cellular defense against H₂O₂-induced apoptosis via MAP kinase–MKP-1 pathway. *Free Radical Biology and Medicine* 36: 8: 985-993, 2004.

Yang C, Kaushal V, Shah SV and Kaushal GP. Autophagy is associated with apoptosis in cisplatin injury to renal tubular epithelial cells. *American Journal of Physiology - Renal Physiology* 294: 4: F777-F787, 2008.

Yang H and Wu GS. p53 transactivates the phosphatase MKP1 through both intronic and exonic p53 responsive elements. *Cancer Biology and Therapy* 3: 12: 1277-1282, 2004.

Yousefi S and Simon HU. Autophagy in cancer and chemotherapy. *Results Probl.Cell Differ.* 49: 183-190, 2009.

Zhang HH, Kumar S, Barnett AH and Eggo MC. Dexamethasone inhibits tumor necrosis factor- α -induced apoptosis and interleukin-1 β release in human subcutaneous adipocytes and preadipocytes. *J.Clin.Endocrinol.Metab.* 86: 6: 2817-2825, 2001.

Zhou JY, Liu Y and Wu GS. The role of mitogen-activated protein kinase phosphatase-1 in oxidative damage-induced cell death. *Cancer Res.* 66: 9: 4888-4894, 2006.

Zhuang W, Qin Z and Liang Z. The role of autophagy in sensitizing malignant glioma cells to radiation therapy. *Acta Biochim.Biophys.Sin.(Shanghai)* 41: 5: 341-351, 2009.

Zong WX and Thompson CB. Necrotic death as a cell fate. *Genes Dev.* 20: 1: 1-15, 2006.

Appendix A

Protocol 1 – Cell Culture

Breast carcinoma cells – MDA-MB231 cells

Making up Growth medium

| Component | Final percentage % |
|--------------------|--------------------|
| DMEM 500 ml | |
| PenStrep 5.5 ml | 1% |
| Fetal Bovine Serum | 10% |
| Glutamine 20 ml | |

Medium constituents must be thawed in a water bath at 37 °C and the volumes as specified above are added together under sterile conditions.

Cracking a vile

1. Remove a vial of MDA-MB231 cells from the liquid N₂ tank and warm in the water bath at 37 °C until there is a small floating block of frozen cells. (*be careful not to wet the lid of the cryovial*)
 2. Remove cells from cryovile and grow in 5 ml growth medium in a T₂₅ flask at 37 °C and 5% CO₂.
 3. Wash cells in warm PBS and replace the medium every day until the cells reach ± 70% confluence
 4. When 70% confluence is reached cells are ready to be split.
-

Splitting and seeding of cells

1. Split cells when a confluency of ~80% is reached. Confluency is determined by viewing cells under 20x objective
2. Warm growth medium, trypsin and PBS in the waterbath until a temperature of 37°C is reached
3. Decanted medium and rinse the monolayer once with PBS
4. Decant PBS and add 4ml trypsin (T₇₅) and place in the shaker incubator for ~ 4min. Check under the microscope to verify that cells are loose
5. Now add double the amount of warm medium (8 ml in T₇₅) and transfer to a falcon tube before centrifuging at 1500 rpm for 3 minutes.
6. Decant the supernatant leaving just the pellet
7. Add 5ml warm medium and gently re-suspend the pellet (*use 1000 µl pipette*)
8. Count re-suspended cells using a haemocytometer and seed at following densities:
 - A. 100 000 cells per well for 6 well plates
 - B. 5000 cells per well for 96 well plates
 - C. 300 000 cells per T₇₅ flask

After splitting and re-seeding, leave cells to plate for 48 hours before changing the medium in order to maintain healthy culture conditions. Once 70% confluent, cells are ready to be split. Cell maintenance should remain consistent at all times

Cell Freezing

1. Use cells that are ~80% confluent
2. Discard old medium using sterile pipette
3. Rinse monolayer with warm sterile PBS
4. Decant PBS and add 4 ml Trypsin (T₇₅) and place in the shaker incubator for ~4min at 37°C
5. Now add double the amount of warm medium (8 ml in T₇₅) and transfer to a falcon tube before centrifuging at 1500 rpm for 3 minutes.

6. Decant the supernatant leaving just the pellet
 7. Resuspended pellet in FCS at a concentration of $1-2 \times 10^6$ cells/ml
 8. Make up Freezing medium (10% DMSO) and add cells
 9. Transfer cells to -80°C for 24h and then into liquid nitrogen
-

Protocol 2 – Reverse transfection

For each petri dish to be transfected, prepare RNAi duplex-Lipofectamine RNAiMAX complexes in the following way:

1. Prepare mastermix by diluting 20 pmol of duplex into 250 ul of transfection medium (medium containing no antibiotics or serum).
2. Mix lipofectamine RNAiMAX gently and add 2 ul per 250 ul of mix.
3. Resuspend and add 250 ul to each petri dish.
4. Allow to incubate for 20 minutes.
5. Split and dilute cells in growth medium (must contain no antibiotics) to have a final volume of 2 ml in each petri.
6. Add 1.5 ml of diluted cell suspension to each well containing the RNAi duplex-Lipofectamine RNAiMAX complexes.
7. Mix gently
8. Allow to incubate until cells are ready to treat (24-48 hours later).

Protocol 3 - Trypan Blue exclusion technique

Trypan blue stock solution (0.4%) was prepared with PBS and stored in the dark at 4 °C

Method

1. Medium was removed from cells, washed with warm PBS and trypsinized as previously described (Protocol 1)
2. Cell solution containing trypsin was neutralized using warm growth medium and centrifuged at 1300-1500 rpm for 3 minutes
3. The resulting pellet was resuspended in 200 μ l warm PBS
4. 50 μ l suspension was added to 50 μ l 0.4 % trypan blue solution and allowed to stand for 2-5 minutes prior to counting
5. 40 μ l of the resuspended solution was placed into the haemocytometer and counted

Protocol 4 – Caspase-Glo® 3/7 assay

Preparation of working reagent solution and storage:

1. Mix the Caspase-Glo® 3/7 buffer reagent gently and allow to equilibrate at room temperature.
2. Transfer the lyophilized substrate to the buffer and mix by swirling
3. Store at -20°C. (Note that reconstituted reagent that is freeze thawed will display diminished signal over time – approximately 60% compared to freshly prepared reagent after 4 weeks according to the manufacturer. However, little reduction in signal intensity was noticed over longer time periods of freeze thawing in our experiments.)

Assay protocol:

1. Allow the working buffer reagent to equilibrate at room temperature for at least 30 minutes.
2. Remove plates containing cells from 37°C growing conditions to allow them to equilibrate at room temperature. (At least 10 minutes).
3. Transfer 50 µl (1:1) of working reagent to each well containing cells.
4. Mix plates on a shaker for 30 seconds.
5. Incubate plates in the dark for 1 hour at *constant* room temperature. (Can incubate for up to 3 hours).
6. Measure the luminescence in a luminometer.

Protocol 5 – Immunofluorescence microscopy

LysoTracker™ and Hoechst staining

1. Remove DMEM and wash cells with cold sterile PBS (3X)
2. Add 1 μ l LysoTracker™ per 2 ml of fresh medium
3. Add 10mg/ml in a 1:200 dilution of Hoechst to the same medium
4. Add this medium to the cells and allow to sit at room temperature for 5 min
5. Do imaging

Protocol 6 – Flow cytometry

Lysis of cells from monolayer

1. Following completion of the treatment protocol, remove culture media and wash cells in 2 ml PBS.
2. Add 2 ml Trypsin/EDTA (0.25%) to each well and place on the cell shaker for 5 min or until the cells have detached from the surface of the well.
3. Add 1 ml of appropriate culture medium to each well.
4. Transfer each resulting cell suspension to a separate, sterile 15 ml falcon tube.
5. Centrifuge at 1500 rpm for 3 min.
6. Pour off the media-trypsin.

Preparation of Samples for Analysis

1. Re-suspend each cell pellet in 0.5 ml LysoTracker™ red (Invitrogen/Molecular Probes) working solution (final concentration of 100 nmol/L).
2. Incubate the suspension for 15 min at 37°C
3. Gently re-suspend cell suspension directly before filtering through into FACS tube
4. Analyse on the flow cytometer (BD FACSAria I) immediately
5. Collect a minimum of 5000 events using 488 nm laser and 610LP, 616/23BP emission filters.

Protocol 7 - Protein extraction and centrifuging

PBS:

20 mM Tris HCL pH 7.4

137 mM NaCl

1 mM CaCl₂

1 mM MgCl₂

0.1 Sodium Orthovanadate

RIPA Buffer:

50 mM Tris-HCL

1 mM EDTA

1 mM phenylmethylsulfonyl fluoride (PMSF)

1 mM benzamidine

4 µg/ml SBTI-1

1 µg/ml leupeptin

1% NP40

0.25% Na-deoxycholate.

Protein extraction:

1. Discard medium from wells and place immediately on ice.
2. Rinse cell monolayer's three times with PBS

3. Incubate for 5min in 250 ul RIPA
 4. Scrape cells from wells/flasks using a rubber policeman and transfer to 1.5 ml microcentrifuge tubes.
-

Centrifuging and storage

1. Centrifuge microcentrifuge tubes at 8000 rpm for 10min at 4°C
 2. Label new microcentrifuge tubes and place on ice
 3. Decant into new correctly labelled microcentrifuge tubes
 4. Store tubes at -80°C overnight
-

Protocol 8 – Western blotting

Bradford Reagent: (5x concentrated)

Dilute 500 mg of Coomassie Brilliant Blue G in 250 ml 95% ethanol

Add 500 ml of Phosphoric acid and mix thoroughly

Make up to 1 L with dH₂O

Filter and store at 4°C

Bradford Working Solution

Dilute stock in 1:5 ratio with dH₂O

Filter using 2 filter papers at the same time

Solution should be a light brown colour

Bradford quantification

1. Thaw a 1 mg/ml BSA stock solution
2. Thaw protein samples if in -80°C freezer – Keep on ice at all times
3. Make up a working solution of 100 µl BSA: 400 µl dH₂O. Vortex mixture
4. Mark 7 eppendorf tubes for the standards as well as tubes for the samples to be tested
5. Now add BSA and water to marked Eppendorf tubes as follows:

| Blank | 0 μ l BSA | | 100 μ l dH ₂ O |
|--------------------|-----------------|-----------------------------|-------------------------------|
| 2 μ g protein | 10 μ l BSA | | 90 μ l dH ₂ O |
| 4 μ g protein | 20 μ l BSA | | 80 μ l dH ₂ O |
| 8 μ g protein | 40 μ l BSA | | 60 μ l dH ₂ O |
| 12 μ g protein | 60 μ l BSA | | 40 μ l dH ₂ O |
| 16 μ g protein | 80 μ l BSA | | 20 μ l dH ₂ O |
| 20 μ g protein | 100 μ l BSA | | 0 μ l dH ₂ O |
| Each sample | 0 μ l BSA | 95 μ l H ₂ O | 5 μ l of sample protein |

6. Vortex all tubes briefly
7. Now add 900 μ l of Bradford reagent to each Eppendorf tube. Vortex again.
8. Incubate at room temperature
9. Read absorbencies, twice each, at 595 nm.
10. Make use of excel to draw a linear plot of absorbencies vs protein concentration and then calculate the amount of each sample to be added to aliquots.

SDS-PAGE and western blotting

1. Clean pairs of large and small glass plates with methanol and a paper towel.
2. Place the small glass plate onto the large plate and slide these into the green assembly.
3. Tighten the assembly by pushing the green clips outward.
4. Place the assembly on the rubber, pushing down gently.
5. Get two small beakers, two Pasteur pipettes and a small stirring bar.
6. Fill one beaker with H₂O and get isobutanol ready.
7. Separating gel recipe for 10% 1 mm gels:

| | |
|--------|----------------------|
| 4 ml | dH ₂ O |
| 2.5 ml | 1.5M Tris-HCL pH 8.8 |
| 0.1 ml | 10% SDS (stock) |
| 0.1 ml | 10% APS (0.1 g/ml) |
| 3.3 ml | Acrylamide 40% |
| 4 µl | Temed |

8. Add everything except for the APS and Temed and let the mixture stand for a few minutes so to allow it to degas.
9. Add the APS first and stir briefly (~30 seconds)
10. Add Temed and mix the solution momentarily
11. Quickly pour the mixture between the glass plates using a Pasteur pipette leaving enough space for the stacking gel.
12. Add a layer of isobutanol using a fresh Pasteur pipette.
13. Allow to set for 1 hour. Prepare running buffer and TBS-T in 1:10 dilutions.
14. After 45 minutes has passed begin to prepare the stacking gel (4% recipe):
15. Once the gels are set (after 1 hour), wash off the isobutanol and make sure that the plates are dry.
16. Add Temed to the stacking solution, mix quickly and add stack between the plates.

17. Gently push combs (of the correct width) into the stacking gel.
18. Leave to set for 30 minutes
19. At this stage, retrieve the standard marker from the freezer and allow it to warm to room temperature
20. Switch on the heating block (it must reach a temperature of 95 °C).
21. Retrieve prepared samples for the -80 °C freezer and allow them to thaw.
22. Ready the electrophoresis apparatus for use.
23. Once thawed, vortex each sample briefly before denaturing in the heating block for 5 minutes.
24. In the meantime, carefully remove the combs and wash the gels gently with H₂O being careful not to damage the wells.
25. Vortex each sample briefly before centrifuging by pulsing for a few seconds.
26. Take the gel plates out of the assembly stand and place them into the U-shaped adaptor cassette. The small plates must be facing inwards.
27. Place the U-shaped adaptor into the loading system and push the latches closed, away from you.
28. Carefully pour prepared running buffer into the middle compartment between the gel plates, allowing the buffer to flow over in the wells.
29. Add 7.5µl of molecular weight marker into the first well on the left of each gel. Remember that the left of the far gel will be on your right hand side.
30. Add your samples into each well using a micropipette and loading tips.
31. Place the system into the outer running chamber, and add running buffer to approximately 1cm below the wells.
32. Place the green lid onto the system making sure to attach the correct electrodes (red to red and black to black)
33. Perform an initial ten minute run at 100 V (constant) and 400 mA.
34. Thereafter, perform a longer run (usually ~50 minutes) at 200 V (constant)

35. Turn off the power and disconnect the electrodes before removing the gel plates from the system. Proteins will slowly dissolve from the gel, so do not let the gels stand at this point. Move directly onto the transfer step.
36. Electrotransfer can now be performed on the semi-dry apparatus.
37. Cut 8 Whatman 3mm filter papers and one PVDF membrane per gel.
38. For every membrane soak three papers in anode buffer 1 (0.3 M Tris-base, pH 10.4, 20% methanol)
39. Soak one paper in anode buffer 2 (25mM Tris-base, pH 10.4, 2% methanol)
40. Place these papers – first those from anode buffer 1 then from anode buffer 2 – onto the anode plate. Roll them flat with a test tube to remove air bubbles.
41. Soak one PVDF membrane in methanol for 15 seconds and then rinse with water before soaking it in anode buffer 2. Place the membrane onto the anode buffer 2 papers already on the anode plate. Role again to remove any bubbles.
42. Carefully remove gels from their respective plates – make sure that the gels do not tear in the process – and place them onto the membranes. Role with a wet tube to remove any bubbles that may have formed.
43. Soak four papers in cathode buffer (25 mM Tris-base, 40 mM ϵ -aminohexanoic acid, pH 9.4, 20% methanol), and place these onto the gel.
44. Close the system and run at limit 0.5A and 15V for one hour.
45. Wash the membranes in copious amounts of prepared TBS-Tween (allow foam to develop. Wash three times for five minutes.
46. Block the membranes in non-fat milk (5 g/100ml TBS-T) for two hours on the belly dancer.
47. Make up the primary antibody (5 μ l in 5 ml TBS-T).
48. Mix in the walk in freezer overnight.
49. Wash membranes in TBS-T with agitation. Three times for five minutes.
50. Place the membranes in the HRP-conjugated secondary antibody (1.25 μ l in 5 ml TBS-T). Incubate with agitation for one hour.

51. To expose, use the ECL detection kit.
52. Add 500 μ l of each of the ECL cocktail kit to a foil covered falcon tube and vortex briefly.
53. Cover the area of the membrane known to have the bands that you are looking for, for one minute.
54. Expose membranes in the dark room.

Protocol 9 - Cancer cell injection

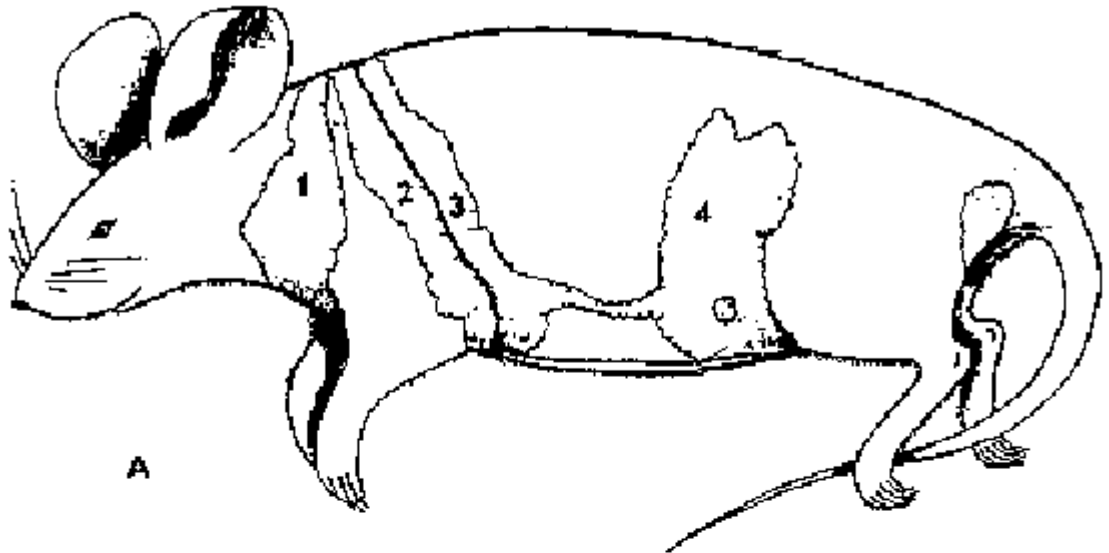
Adapted from Ewans *et al.* 2006 (Doxorubicin plus Interleukin-2 Chemoimmunotherapy against Breast Cancer in Mice).

1. Culture E0771 cells until 80% confluent.
 2. Digest cultured E0771 cells using trypsin (0.05% trypsin-EDTA) for 5 minutes at 37°C.
 3. Centrifuge at 1500 rpm for 3 minutes.
 4. Wash cells once with sterile PBS.
 5. Count cells and dilute with Hanks Balanced Salt solution to a concentration of 1250 cells/ μ l (2.5x10⁵ cells in 200 μ l)
 6. Inject the cell suspension s.c. in the lower abdomen of each mouse, in or near the no. 4 mammary fat pad (Day 0)
-

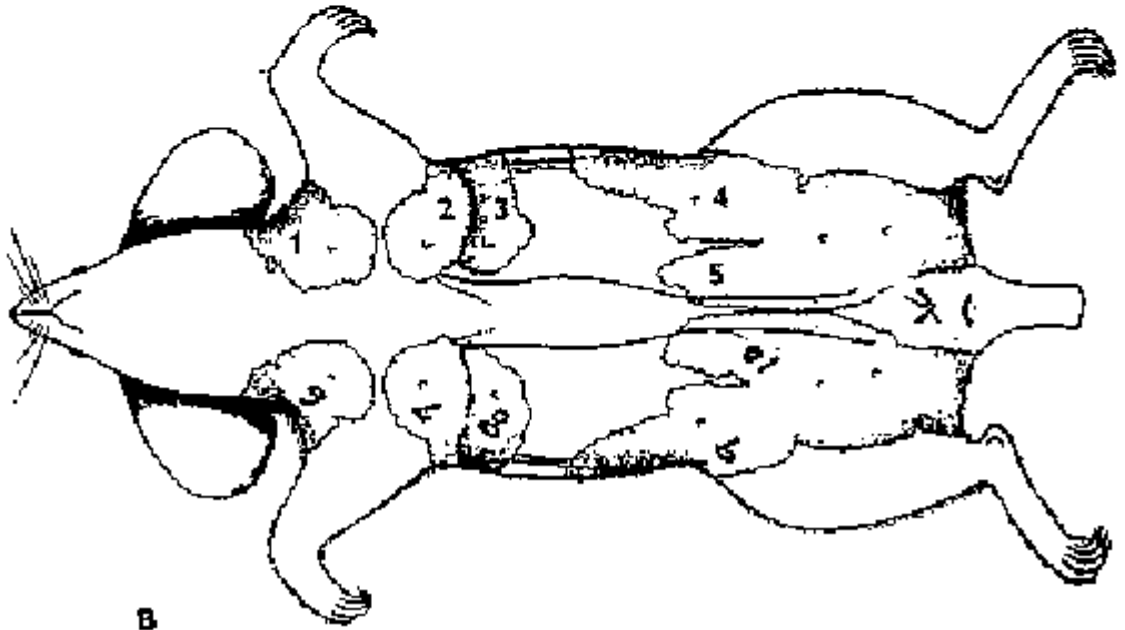
MICE Subcutaneous injection:

Adapted from **Guidelines for Handling, Restraint, Injections and Blood Collection from Small Laboratory animals** (<http://campusvet.wsu.edu/infofac/handling.htm>).

SC injections can be administered easily to mice. The needle is inserted between the folds of skin into the base of the triangle that is formed when traction is applied to the skin overlying the animal's scruff. The syringe's plunger should be retracted to verify that a vacuum is created and no blood or tissue fluid can be aspirated. Subsequently, the plunger is depressed releasing the material. In general no greater than 1 ml should be injected per SC injection site in adult mice (> 25 grams). Several sites over the animal's back should be used if larger volumes must be administered. In general, needles should be 0.5 - 1 long and 23 ga or larger gauge.



A



B

Reagents

X1 Phosphate Buffer Saline (PBS)-2L

Dissolve the following in 1 L of water

- 16 g NaCl
- 0.4 g KCl
- 2.88 g Na₂HPO₄ (di Sodium hydrogen phosphate)
- 0.48 g KH₂PO₄ (potassium dihydrogen phosphate)
- Adjust pH to 7.4, fill up to the 2 L mark with distilled water and sterilize by autoclaving

Trypan Blue dye

- Weigh out 40 g trypan blue dye and dissolve this in 100 ml PBS
- Store away at 4 °C

BSA (Bovine serum albumin 1mg/ml)

- For 1 ml BSA, weight out 1 mg BSA and add 1000 µl distilled water.
- For use during Western blotting, this BSA needs to be diluted. Pipette 100 µl from 1 mg/ml BSA in new eppendorf tube and add 400 µl distilled water
- Mix well

Bradford Reagent (1L)

- Weigh out 500 mg Coomassie Brilliant Blue G and add it to 25 ml 95% ethanol
- Add 500 ml phosphoric acid and mix well
- Fill up to 1 L with distilled water and store at 4 °C
- Filter twice and make 1:5 dilution for Western blotting

3X Sample buffer

- Measure 33.3 ml stacking Tris (0.5 M) and place in a beaker
- Weigh out 8.8 g SDS and 20 g glycerol and place in the beaker
- Add a pinch of Bromo-phenol blue to the mixture
- Add and make up to 75.47 ml with distilled water

1.5 M Tris pH 8.8 (500ml)

- Weigh out 68.1 g Tris (1.124 M) and 1.5 g SDS (0.3 %) and place in a beaker.
- Add 400 ml distilled water, stir and then adjust pH using HCL
- Add 100 ml distilled water to make the final volume to 500 ml

1.5 M Tris pH 6.8 (500ml)

- Weigh out 30.3 g Tris (0.5 M) and 2 g SDS (0.4 %) and place in a beaker.
- Add 400 ml distilled water, stir and then adjust pH using HCL
- Add 100 ml distilled water to make the final volume to 500 ml

10% Sodium dodecyl sulphate (SDS 500ml)

- Weigh out 50 g SDS and dissolve it in 500 ml distilled water using a volumetric flask

10% Ammonium persulphate (1000 µl)

- Weigh out 0.1 g APS into an eppendorf tube and add 1000 µl distilled water

Running buffer (1L)

- Weigh out 3.03 g Tris, 1.44 g Glycine and 1 g SDS into a 1 L beaker. Add 500 ml distilled water and stir until dissolved.
- Fill up to 1 L with distilled water

10X TBS (5L)

- Weigh out 121 g Tris and 80 g NaCl into a 5 L beaker. Add 2.5 L distilled water and stir until dissolved.
- Adjust pH to 7.6 using HCl and then fill up to 5 L with distilled water
- For use in Western blotting, take a 1 L measuring cylinder and add 100 ml 10X TBS and dilute with 900 ml distilled water
- To make **TBST**, add 1 ml tween to 1 L diluted solution of TBS

Milk blocking solution (100ml)

- Weigh out 5 g non-fat dry instant milk powder into a beaker. Add 100 ml TBST and mix well

Primary (1°) antibody

- Pipette 5 μ l 1° antibody and 5 ml TBST in a 50 ml falcon tube. This concentration is suitable for most 1° antibodies but others require a higher concentration

Secondary (2°) antibody

- Pipette 2.5 μ l 2° antibody and 5 ml TBS-Tween20 in a 50ml falcon tube